

## **Chapter 4**

### **Data Processing and Results**

#### **4.1 Introduction**

This chapter describes the step of data manipulation which is used to present and analyze its valuable for the mineral exploration. Field data which are recorded in a receiver's memory will be printed out or dumped into a desktop computer for further processing purposes. Data dumping facility of geophysical computer program is introduced to load out raw data from resident memory of the Scintrex IPR-11 receiver. Thereafter, raw field data were converted to be raw data file by a conversion module, to perform a standard format file for further processing. Then data reduction module is used to calculate all parameters contained in data file in order to make the illustration. After that, each set of data will be re-arranged in a suitable form for illustrations. Data processing flow chart and its presentation are shown in Figure 4.1

Different data acquisitions were applied in three different kinds of deposit. First area is Mae Chong sulphide deposit, data was acquired with pole-dipole array of 50 meter dipole separation. Second area is Khao Khi Nok graphite deposit, data was acquired with several array configurations and with several dipole separations. Third area is Pong Nok Gaew clay deposit, data was acquired with a parameter similar to the later one.

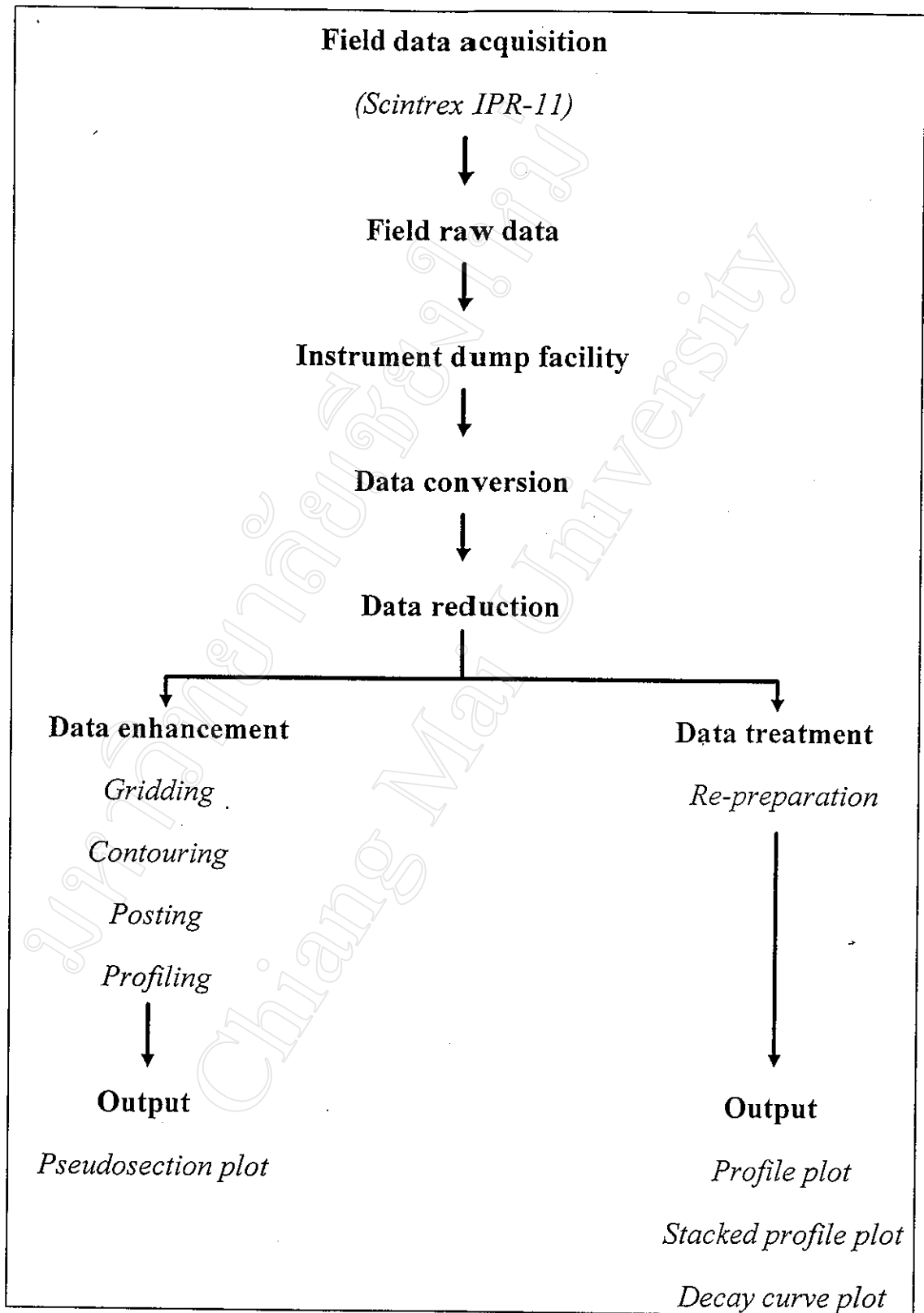


Figure 4.1 Flowchart of data preparation, processing, and presentation.

In the first stage of data processing, pole-dipole array with 50 meters dipole separation of Mae Chong area, 10 meters of Khao Khi Nok and Pong Nok Gaew areas are selected to process and compare for the results. Thereafter, decay curve of each deposit will be presented to observe its characteristics. Next, different of array configuration and different of dipole separations will be selected to compare in order to analyze in detail of somewhat affect on induced polarization response of the ground.

#### **4.2 Data processing**

The data reduction was applied to calculate the parameters which contain in raw data. From filed data, it composes of location of current and potential electrodes, potential and current values for calculating apparent resistivity, self potential, decay voltage of ten slices. After the application of data reduction, raw data file will be decomposed into seventeen files. There are apparent resistivity file, average apparent chargeability file, self potential file, metal factor file, computed chargeability file, frequency dependent file, time constant file, and ten files of each slices of apparent chargeability.

The seventeen processed data files can be divided into two groups, conventional and complex resistivity parameters, as shown in Table 4.1.

#### **4.3 Data analysis**

Data of Mae Chong area is selected from pole-dipole array of 50 meters dipole separation. This array configuration is selected in order to investigate the deeper and, moreover, this configuration is less effect

Table 4.1 Summary of various processed data from data reduction.

Parameter	Quantity (file)
<b>Conventional:</b>	
- Self potential	1
- Apparent resistivity	1
- Apparent chargeability	11
- Metal factor	1
<b>Complex resistivity:</b>	
- Chargeability	1
- Frequency dependent	1
- Time constant	1

Table 4.2 Summary of data files used in data analysis.

Parameter	Profile	Stacked profile	Pseudosection
<b>Conventional:</b>			
- Self potential	n	n	n
- Apparent resistivity	y	y	y
- Metal factor	y	y	y
<b>Complex resistivity:</b>			
- Chargeability	y	y	y
- Frequency dependent	y	y	y
- Time constant	y	y	y

y = use, n = not use

from topographic effect (*Techawan, 1995*). Khao Khi Nok area data is selected from dipole-dipole array of 10 meters dipole separation. Data of Pong Nok Gaew area is selected from dipole-dipole array of 10 meters dipole separation. Data from Khao Khi Nok and Pong Nok Gaew are selected of 10 meters dipole separation in order to reduce the influence of electromagnetic coupling which occurs during the surveys with large dipole separation. Whole data sets are surveyed with 2 seconds transmitting time. The effect of dipole separation will be presented in the later topic of analysis.

The data obtained from data reduction process will be presented in various kinds of illustration. First, whole data files will be used to construct a pseudosection plot. Second, the reduced data will be furnished for profile plot. There are two types of profile plot, single profile and stacked profiles. Table 4.2 shows the detail of data presentation. Third, decay curve will be redrawn from raw data file at the location which is interesting. Finally, the decay curve will be analyzed with an effect of changing parameters such as; array configuration, dipole separation, and transmitting time duration.

#### **4.4 Results of Mae Chong sulphide deposit**

Induced polarization survey was acquired with pole-dipole array configuration of 50 meters dipole separation. Transmitting time of transmitter TSQ-3 is 2 seconds. Traverse line is allocated from station -50 to station 2750 with the separation 50 meters, total length of 2,800 meters. Survey line is laid in approximate east-west direction.

#### 4.4.1 Conventional parameters

Apparent resistivity profiles are shown in Figure 4.2, for  $n=1$  to  $n=6$  pseudo-depth. For  $n=1$ , apparent resistivity is lowest at about station 1200 with magnitude about 2 ohm-meter, this zone is defined as anomalous zone. While pseudodepth increases from  $n=3$  to  $n=6$ , anomalous zone splits out into two zones, the first zone is located near station 1050 and the second is at station 1350. Stacked profile of apparent resistivity is shown in Figure 4.3, which indicates four low resistivity zones. The first zone is occupied between station 350 down to station -50. The second zone is located at station 1050. The third zone is located about station 1400. The fourth zone is located about station 2500 but this zone has higher apparent resistivity than the others. From stacked profiles, it should be noted that apparent resistivity of earth layers increases with depth because porosity in rock will be reduced by mass of the overlaying layers, apparent resistivity of non-mineralized rock depends on its porosity and resistivity of connate water. But for mineralized rock, apparent resistivity changes very little because apparent resistivity depends mostly on the characteristics of mineral rather than the porosity and connate water. Pseudosection plot of apparent resistivity is shown in Figure 4.4(a). From pseudosection, low resistivity zones represent by blue color appear first at left portion and second at center portion of the pseudosection.

Apparent chargeability profiles are plotted in Figure 4.5. From  $n=1$  pseudodepth, anomalous zone is located at the center portion of survey line down to pseudodepth of  $n=6$  which the anomaly peak

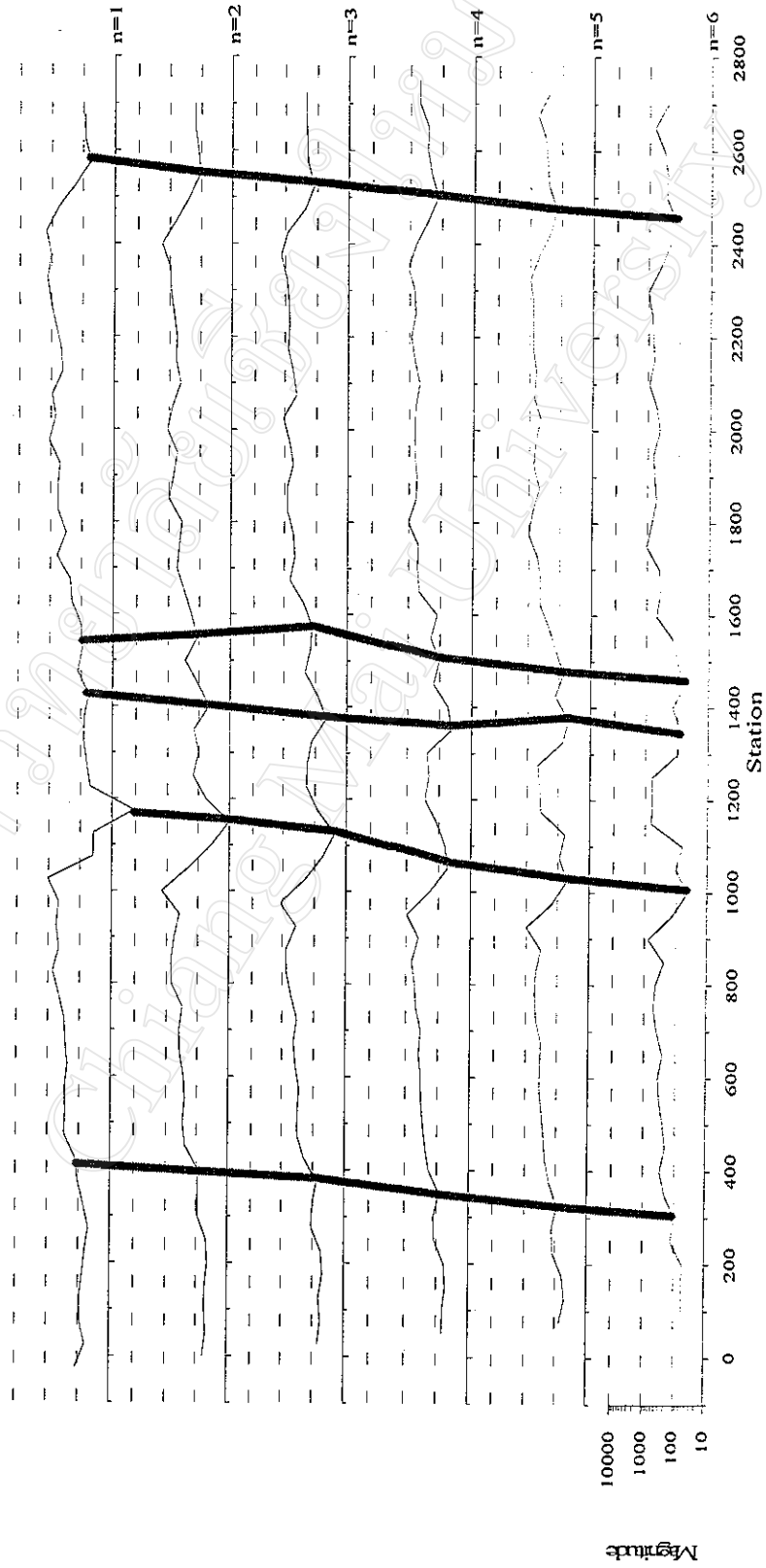


Figure 4.2 Profile plot of apparent resistivity of Mae Chong sulphide deposit.  
Pole-dipole array of 10 meter dipole separation. Solid lines are the trend of low apparent resistivity.

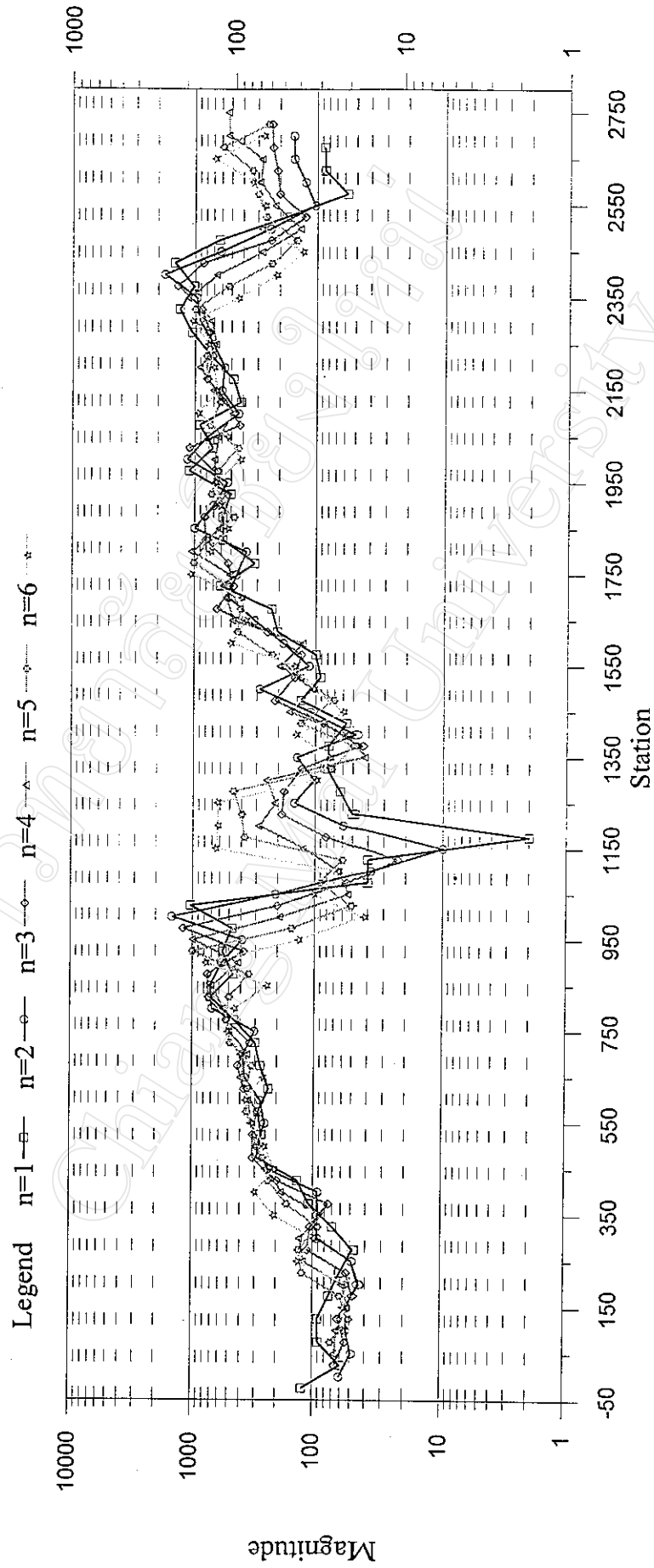
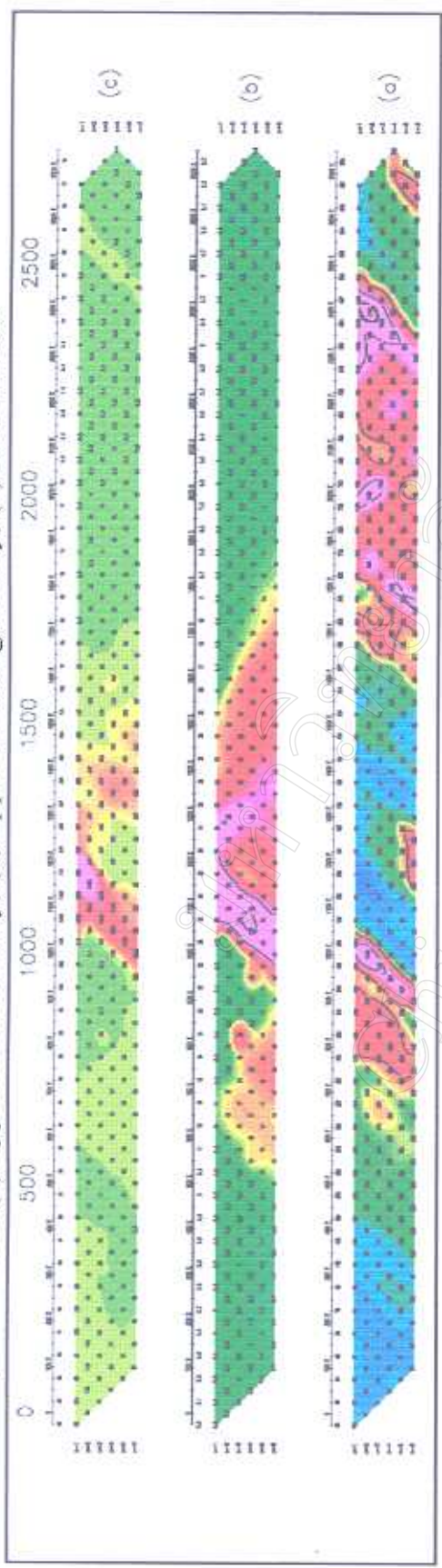


Figure 4.3 Stacked profile plot of apparent resistivity of Mae Chong sulphide deposit. Pole-dipole array of 10 meter dipole separation.

Conventional parameters; (a) apparent resistivity, (b) apparent chargeability, (c) metal factor



Complex resistivity parameters; (d) chargeability, (e) frequency dependent, (f) time constant

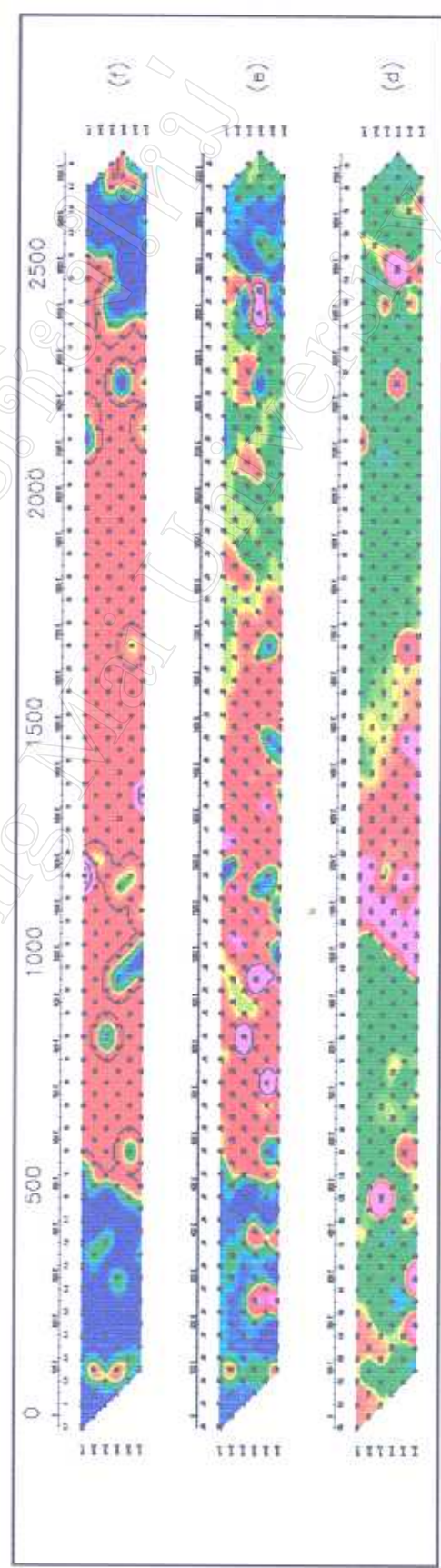


Figure 4.4 Conventional and complex resistivity pseudosections plot of Mae Chong sulphide deposit.

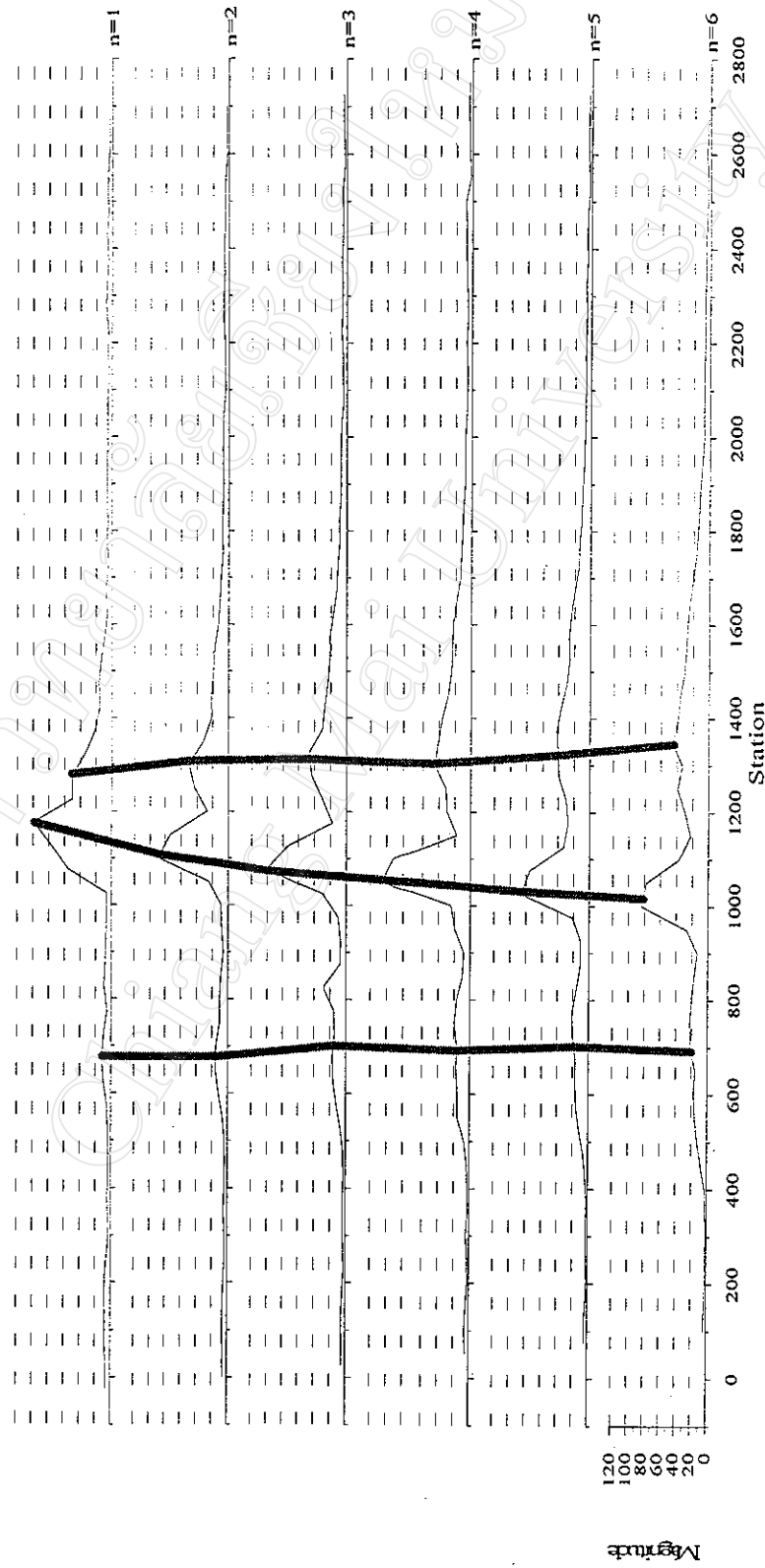


Figure 4.5 Profile plot of apparent chargeability of Mae Chong sulphide deposit.  
Pole-dipole array of 10 meter dipole separation. Solid lines are the trend of high apparent chargeability.

slightly shift to the left. These zones are tracked by the thick solid lines overlaid on the figure. Stacked profile plot of apparent resistivity is shown in Figure 4.6, anomalous zone can be classified into three types. The first is the very high magnitude of apparent chargeability located at the center of the survey line closed to station 1100. The second is the high magnitude located beside the first zone at the right portion but its magnitude decrease to background level at station 2000. The third is moderately high magnitude locate at the left portion of the first zone from station 850 down to station 500. The background value of this area is about 5 to 7 millivolt/volt, not exceed 10 millivolt/volt. Pseudosection plot of apparent chargeability is shown in Figure 4.4(b) which indicate these three anomalous zone, pink color represents very high anomalous zone, red color represents high anomalous zone, yellow color represents moderately high anomalous zone, and green color represents background value of this study area.

Theoretically, metal factor is a parameter of the apparent chargeability that normalized with the apparent resistivity value. While the apparent resistivity is increased, the metal factor will be decreased. On contrary, if the apparent chargeability is increased, the metal factor will be going up also. This parameter will be rising to very high magnitude in case of the anomalous body has very low resistivity and that body give high chargeability value.

Metal factor profile plots of pseudodepth  $n=1$  to  $n=6$  are shown in Figure 4.7. The high magnitude is located about station 1100 except for  $n=1$  and  $n=2$  which have very high magnitude. Figure 4.8 shows a

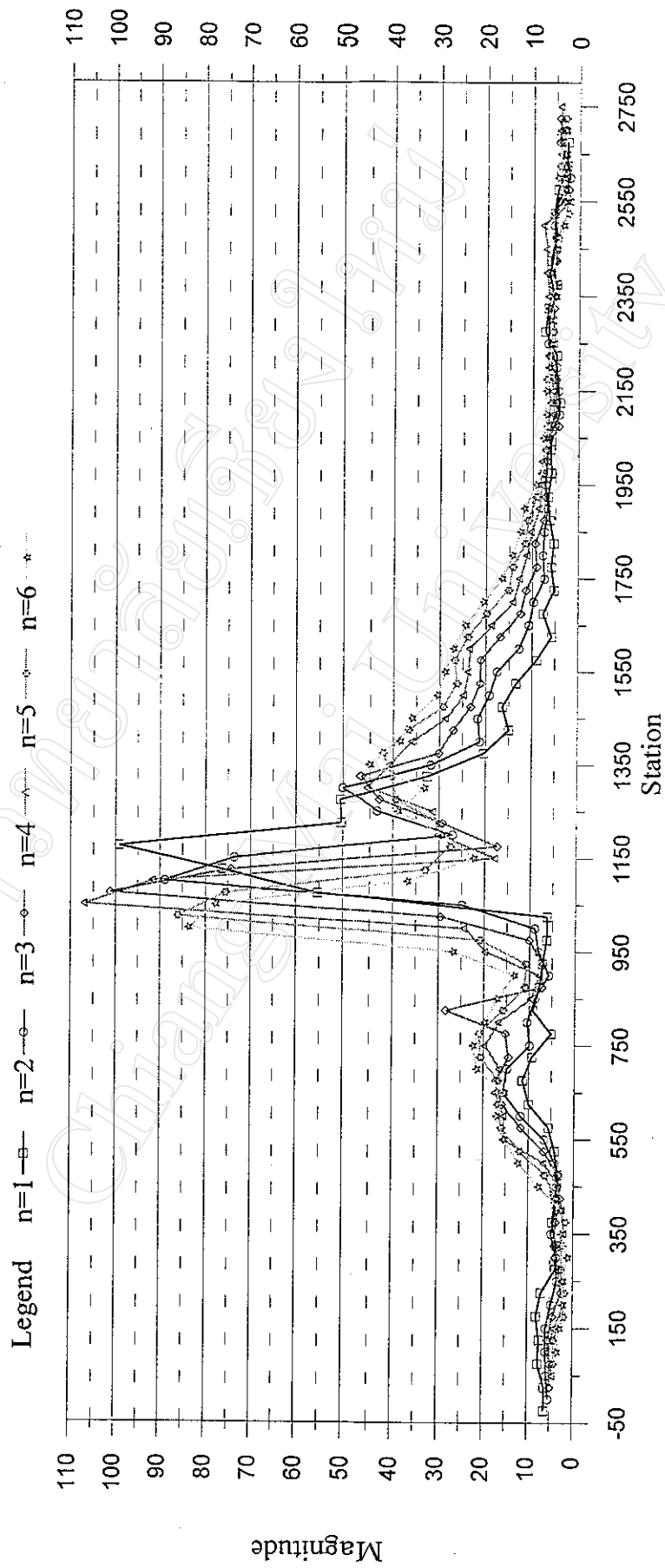


Figure 4.6 Stacked profile plot of apparent chargeability of Mae Chong sulphide graphite deposit.  
Pole-dipole array of 10 meter dipole separation.

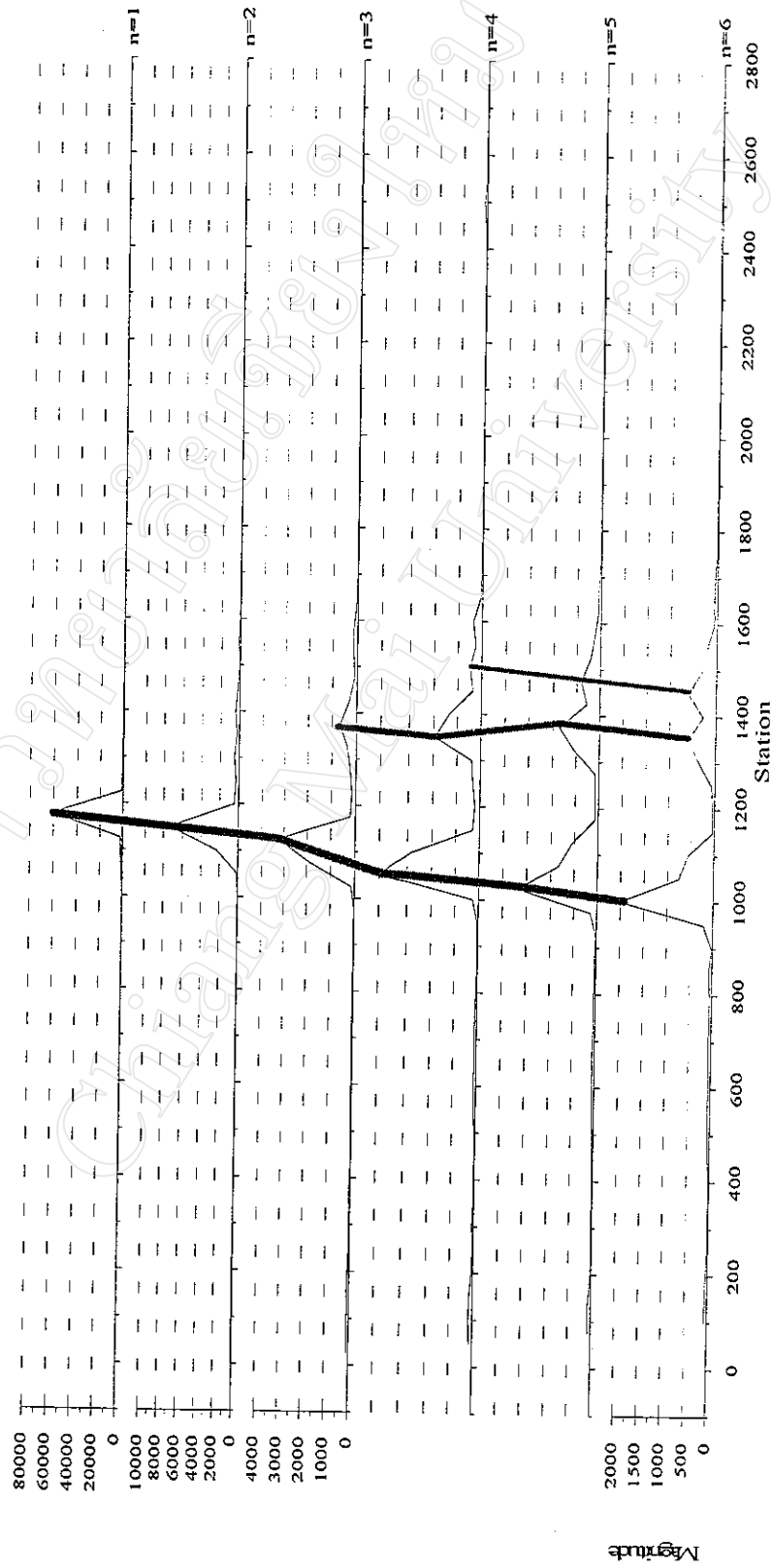


Figure 4.7 Profile plot of metal factor of Mae Chong sulphide deposit.  
Pole-dipole array of 10 meter dipole separation. Solid lines are the trend of high metal factor.

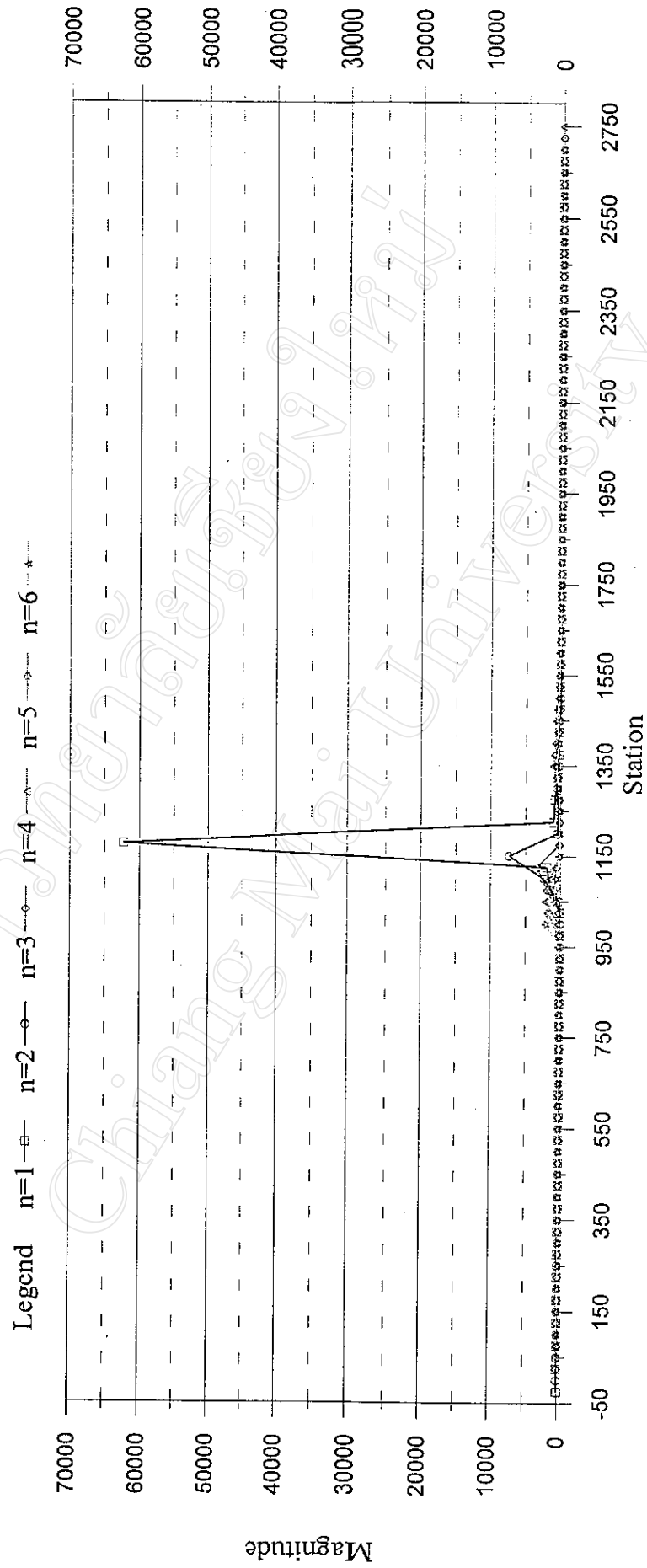


Figure 4.8 Stacked profile plot of metal factor of Mae Chong sulphide deposit.  
Pole-dipole array of 10 meter dipole separation.

stacked profile of metal factor, anomalous zone locate at center of survey line about station 1100. Pseudosection plot is shown in Figure 4.4(c), anomalous zone represents by red to pink color. This parameter shows good correlation of its value with apparent resistivity and apparent chargeability.

#### 4.4.2 Complex resistivity parameters

Chargeability is one of three parameters calculated by computer software. Refer to Cole-Cole relaxation model, relevant parameter consists of chargeability ( $m$ ), frequency dependent ( $c$ ), and time constant ( $\tau$ ). These parameters represent the behavior of the ground under an impressed external force.

Profiles plot of chargeability are shown in Figure 4.9. It continuously shows good relationship with anomalous zone at the center portion while out of this zone has not related to other pseudodepth. Figure 4.10 shows stacked profile plot of chargeability, it has anomalous zone locate at center portion of survey line while beside that is not meaningful. The computer software is applied to enhance the data quality and plotted in pseudosection form that the anomalous zone can be continuously observed at the center portion and will be represented by pink to red color as shown in Figure 4.4(d).

Profiles plot of the frequency dependent are shown in Figure 4.11. This parameter has not distinctive value in order to identify anomalous zone. Stacked profile plot of the frequency dependent is shown in Figure 4.12, frequency dependent in anomalous zone is about 0.4 and about 0.25 for background value. Very high magnitude represents strong

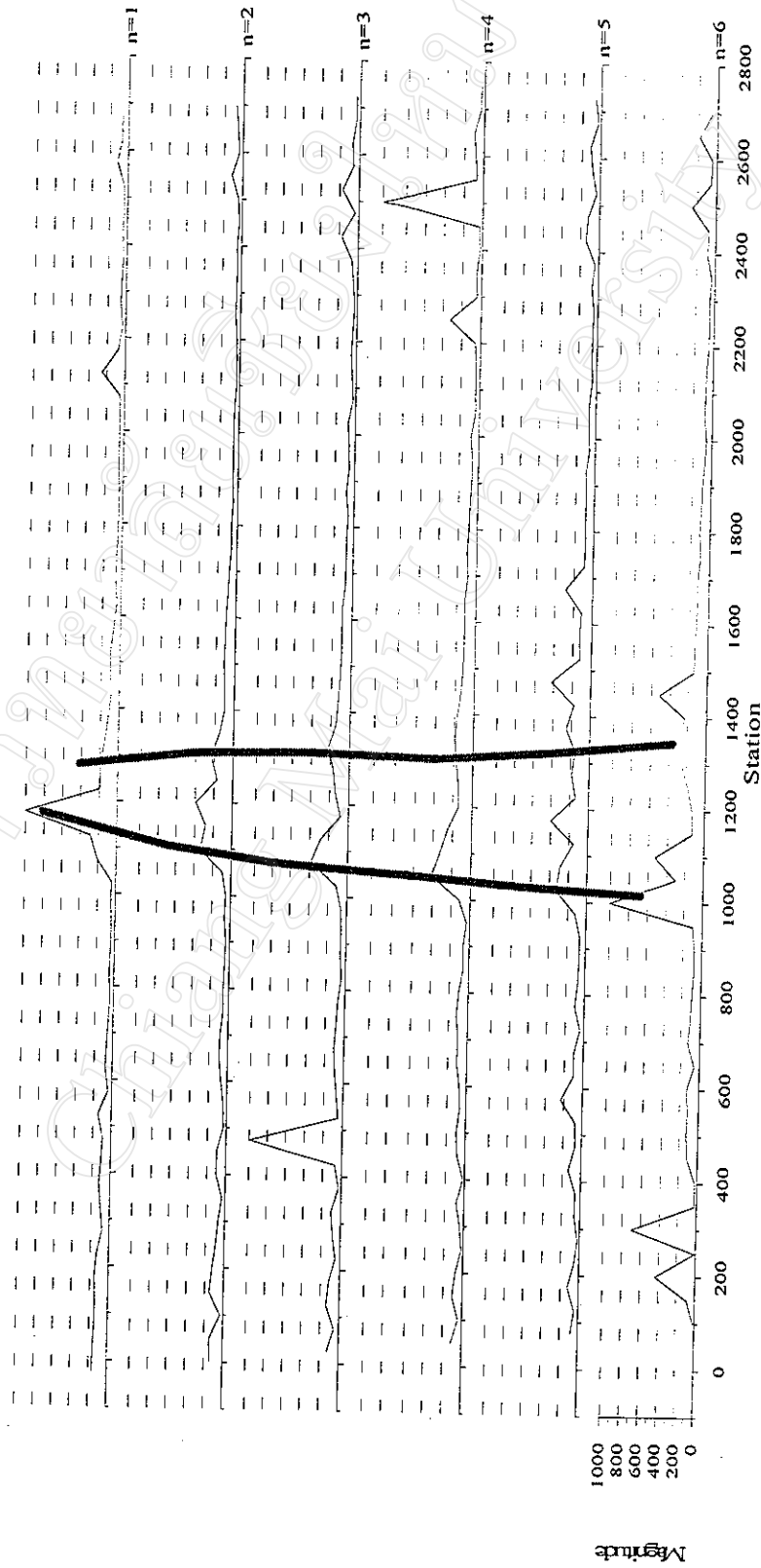


Figure 4.9 Profile plot of chargeability of Mae Chong sulphide deposit.  
Pole-dipole array of 10 meter dipole separation. Solid lines are the trend of high chargeability.

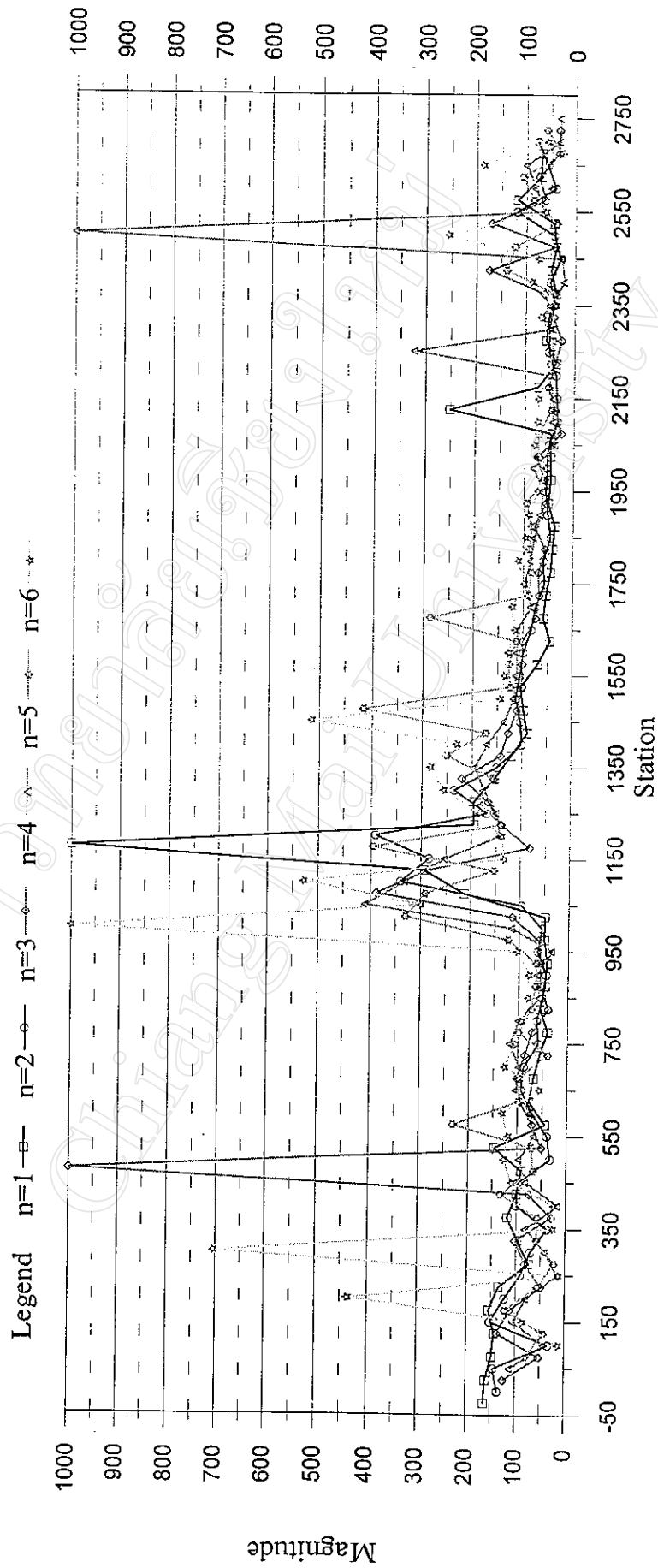


Figure 4.10 Stacked profile plot of chargeability of Mae Chong sulphide deposit.  
Pole-dipole array of 10 meter dipole separation.

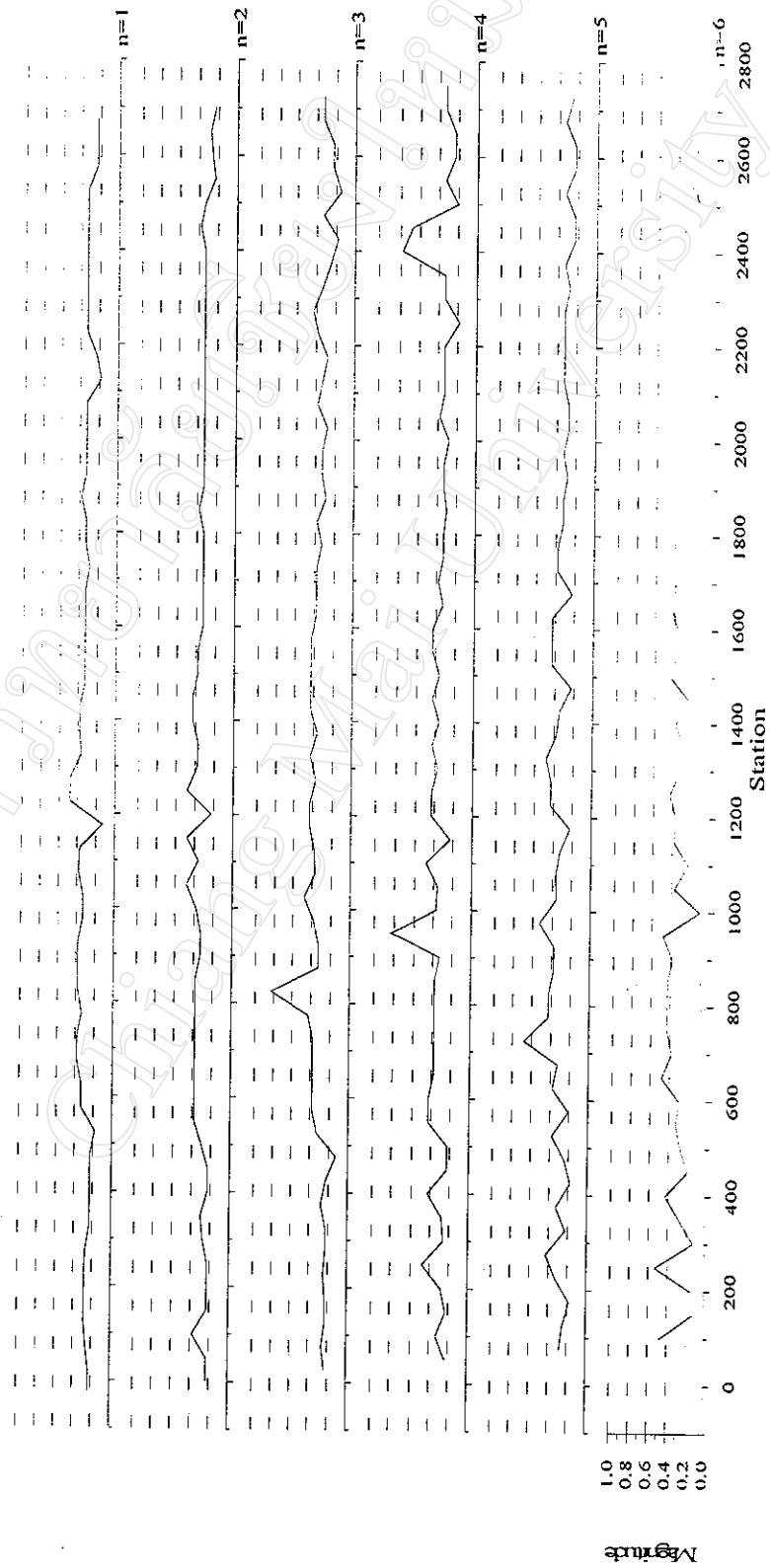


Figure 4.11 Profile plot of frequency dependent of Mae Chong sulphide deposit.  
Pole-dipole array of 10 meter dipole separation.

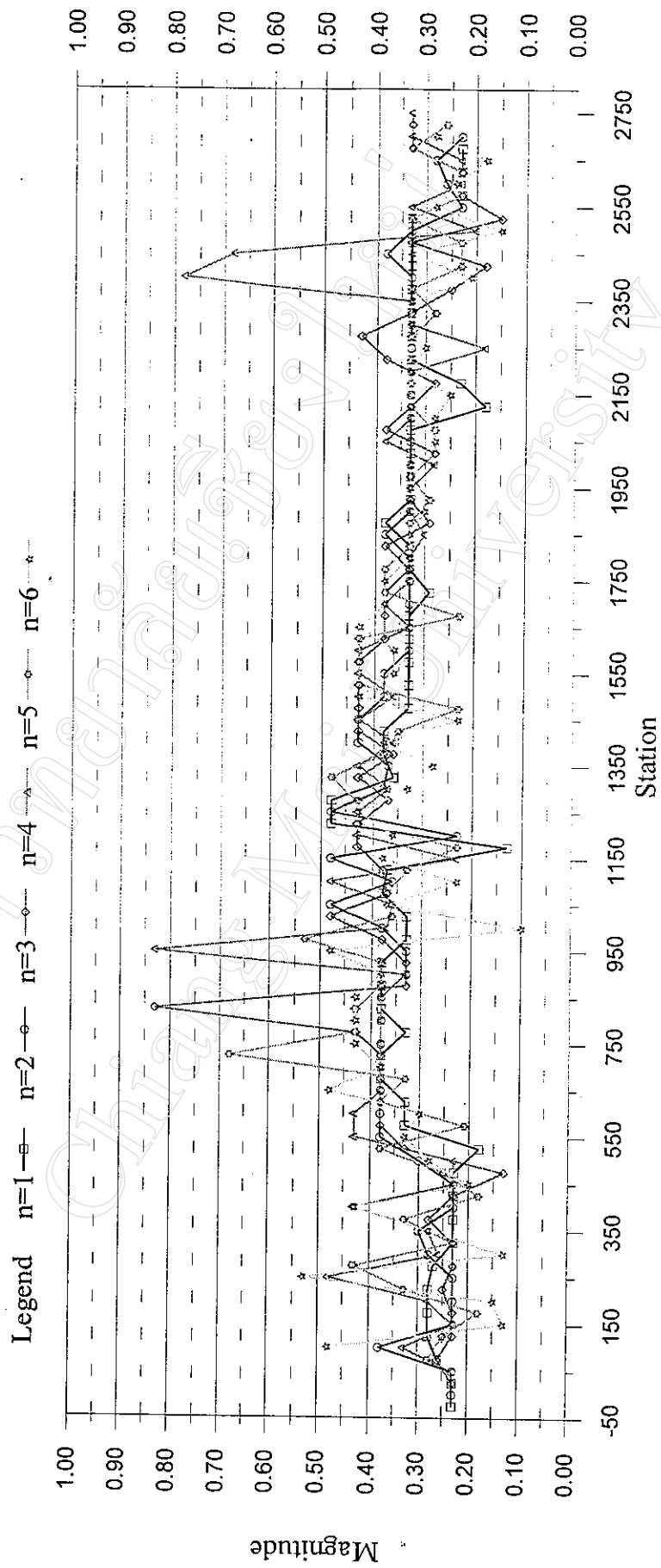


Figure 4.12 Stacked profile plot of frequency dependent of Mae Chong sulphide deposit.  
Pole-dipole array of 10 meter dipole separation.

electromagnetic coupling, not means the anomalous zone. Figure 4.4(e) shows pseudosection plot of the frequency dependent, high value distributes over station 500 to station 2500 represents by yellow to pink color and then the background value represents by blue color.

Profile plot of time constant is shown in Figure 4.13. For  $n=1$  to  $n=6$ , there are distinctive two values of time constant, it is used to separate anomalous zone from non-anomalous zone. Time constant is of 20 seconds for anomalous value and about 5 seconds for background value which is clearly shown in stacked profile of Figure 4.14. At some points there are anomalously high and low peaks that is classified as overshooting anomalous value. Figure 4.4(f) shows pseudosection plot of time constant parameter, high time constant value covers over station 500 to station 2500 represented by red color and background value represented by blue color. There is a very good relationship between time constant and frequency dependent parameters, high time constant with high frequency dependent and low time constant with low frequency dependent.

#### **4.5 Results of Khao Khi Nok graphite deposit**

Induced polarization survey of this area was acquired with the dipole-dipole array configuration of 10 meter dipole separation. Transmitting time of the transmitter TSQ-3 is 2 seconds. Traverse line is laid out in NW-SE direction. Survey station is allocated from station 150 to station 1000, with the total length of 850 meters.

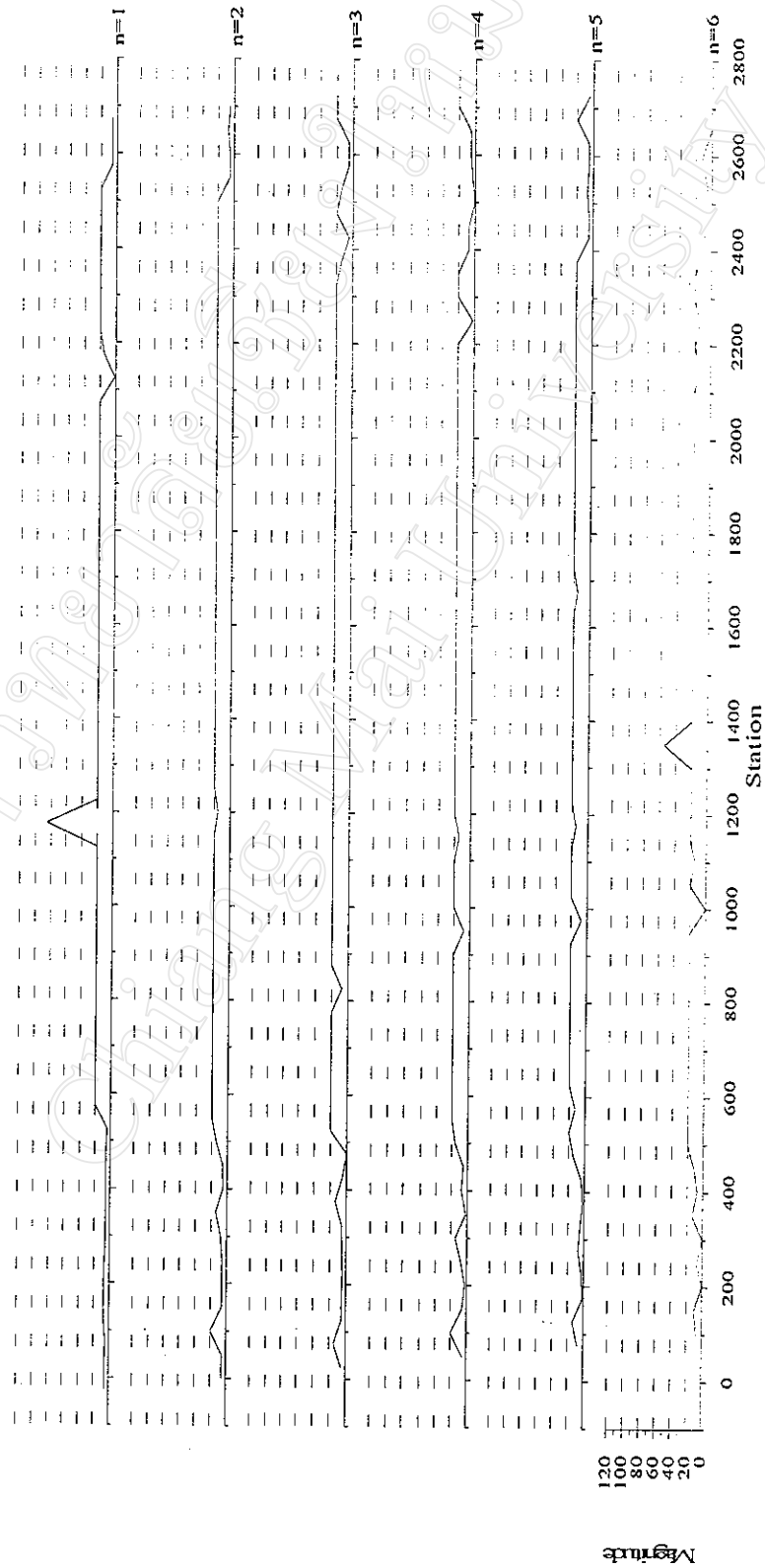


Figure 4.13 Profile plot of time constant of Mae Chong sulphide deposit.  
Pole-dipole array of 10 meter dipole separation.

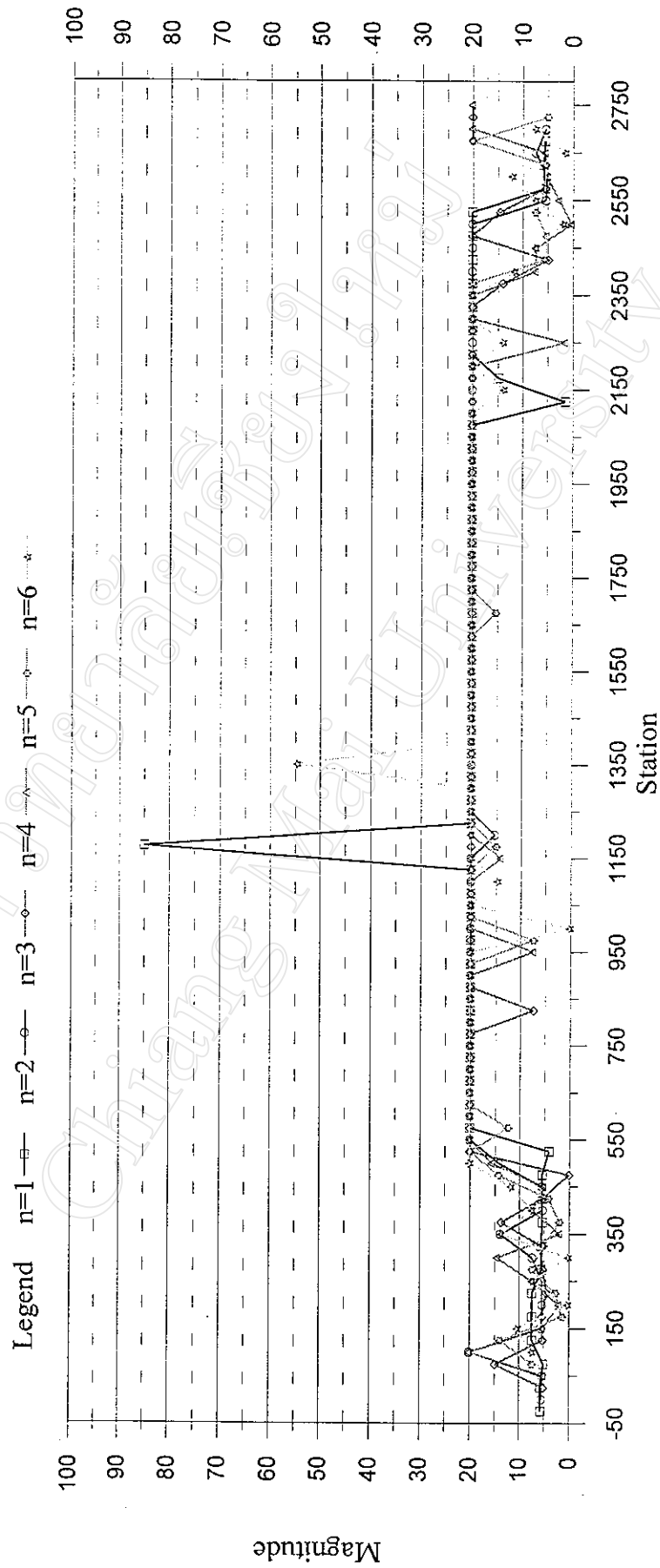


Figure 4.14 Stacked profile plot of time constant of Mae Chong sulphide deposit.  
Pole-dipole array of 10 meter dipole separation.

#### 4.5.1 Conventional parameters

Apparent resistivity profiles are plotted in Figure 4.15, the anomalous zone is defined by its lower magnitude than the vicinity, that zone locate about station 250 of 10 ohm-meter resistivity and about station 450 with very low resistivity, not exceed 5 ohm-meter. Background level of this area is quite flat and is located from station 600 to station 1000, its value is about 100 ohm-meter. It clearly shows the anomalous zone in the stacked profile plot in Figure 4.16. It should be noted that the stacked profile of the anomalous zone has not the same value of the apparent resistivity that mean it has variation in grain size or there is some other mixture of a conductive mineral present. Whereas, the non-anomalous zone has change in its resistivity with depth which implies that it is the resistivity of the layered earth. Pseudosection plot of the apparent resistivity is shown in Figure 4.17(a), the anomalous zone is represented by blue color is distinctly shown at left side of the section whereas the non-anomalous zone is represented by red to pink color located from center to right side of the survey line.

Apparent chargeability profiles are plotted in Figure 4.18. From the figure, the apparent chargeability has magnitude of 5 millivolts per volt about station 220 from the pseudodepth of  $n=1$  to  $n=4$ . From station 400 to station 500, the apparent chargeability is very high and there is an abruptly change in magnitude at station 460, from the pseudodepth of  $n=5$  to  $n=6$ . From stacked profile plot in Figure 4.19, the anomalous zone can be identified about station 250 and station 450. Highest magnitude is located at station 450 at pseudodepth  $n=4$ . Background

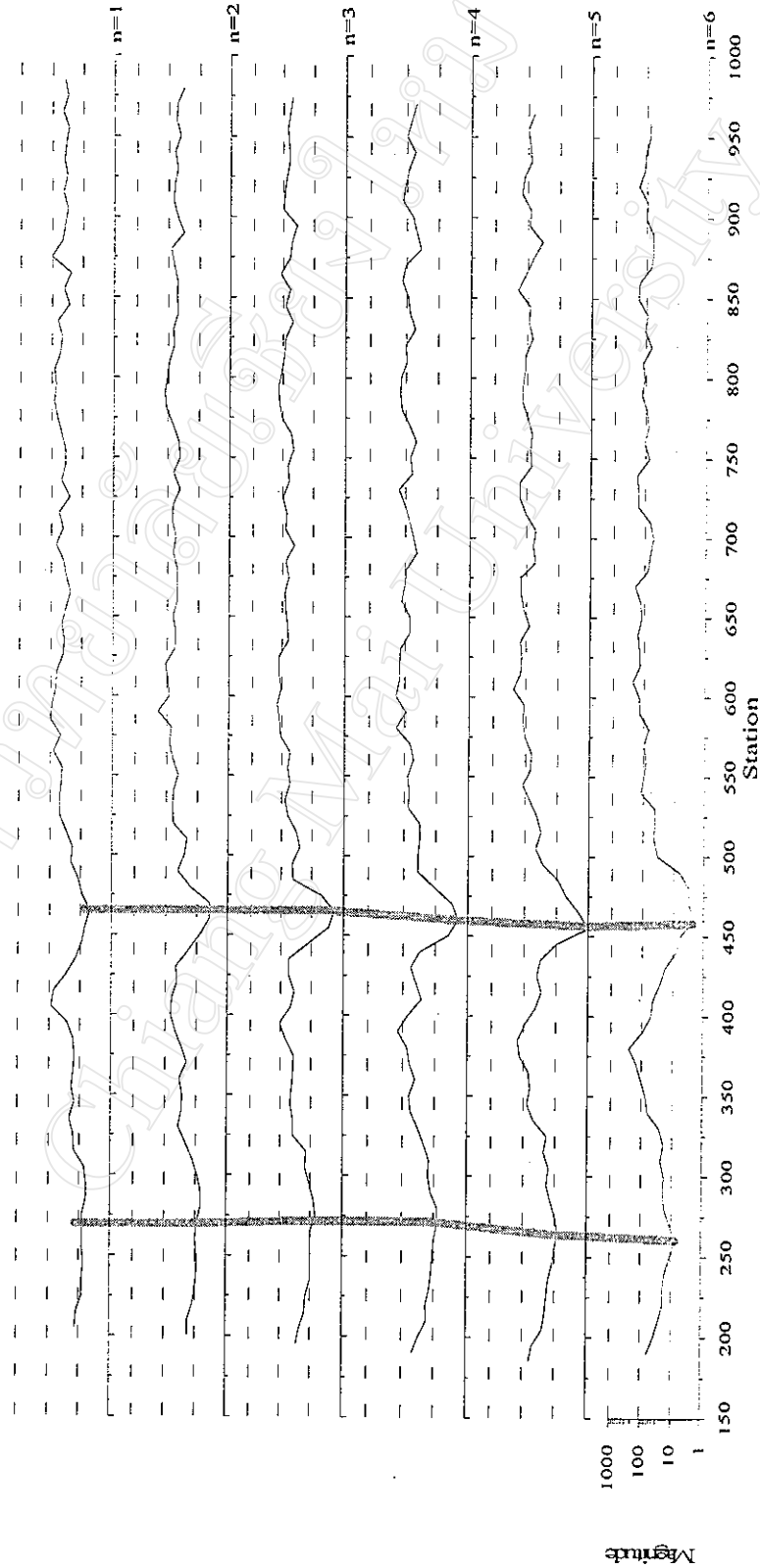


Figure 4.15 Profile plot of apparent resistivity of Khao Khi Nok graphite deposit.

Dipole-dipole array of 10 meter dipole separation. Solid lines are the trend of low apparent resistivity.

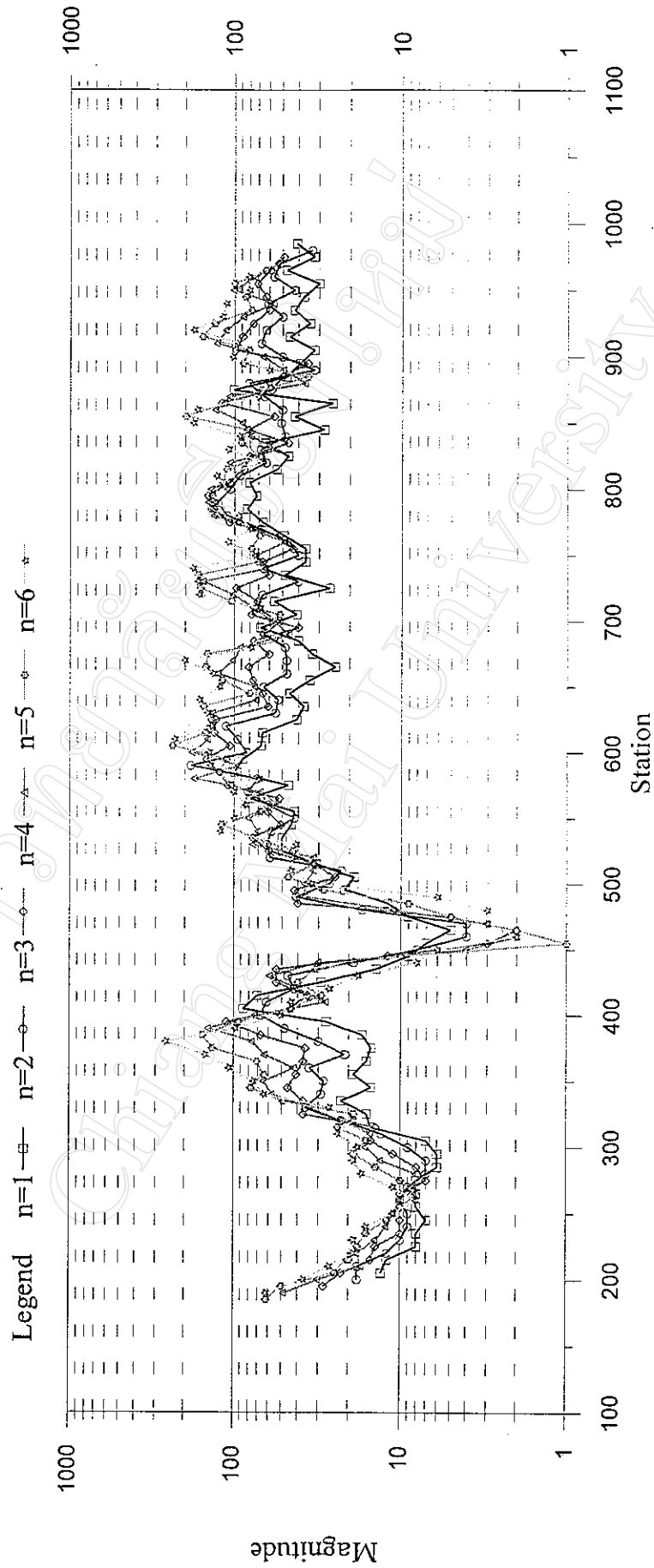
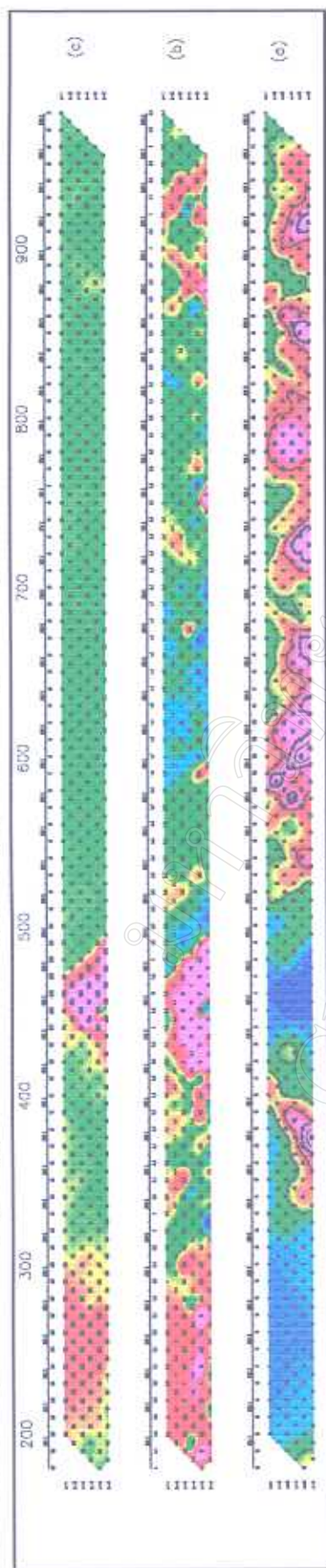


Figure 4.16 Stacked profile plot of apparent resistivity of Khao Khi Nok graphite deposit.  
DiDipole-dipole array of 10 meter dipole separation.

Conventional parameters; (a) apparent resistivity, (b) apparent chargeability, (c) metal factor



Complex resistivity parameters; (d) chargeability, (e) frequency dependent, (f) time constant

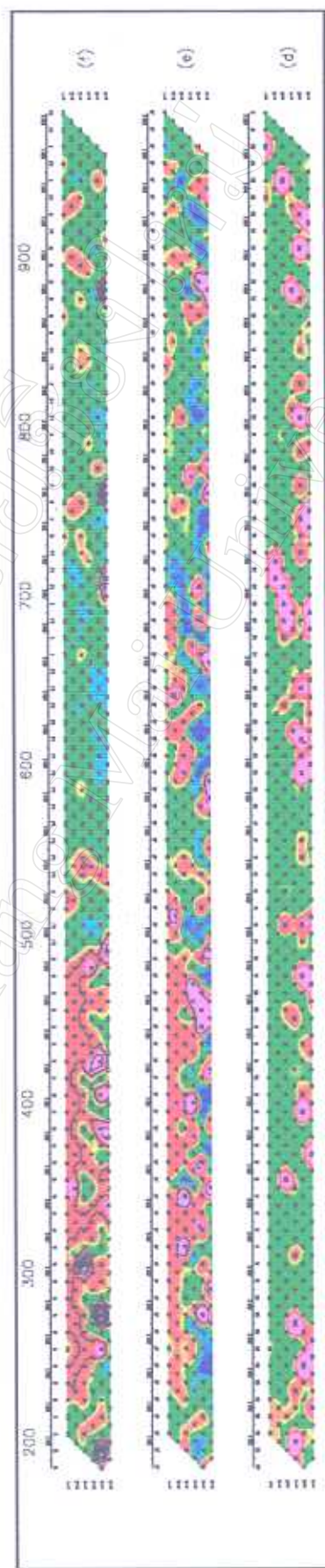


Figure 4.17 Conventional and complex resistivity pseudosections plot of Khao Khi Nok graphite deposit.

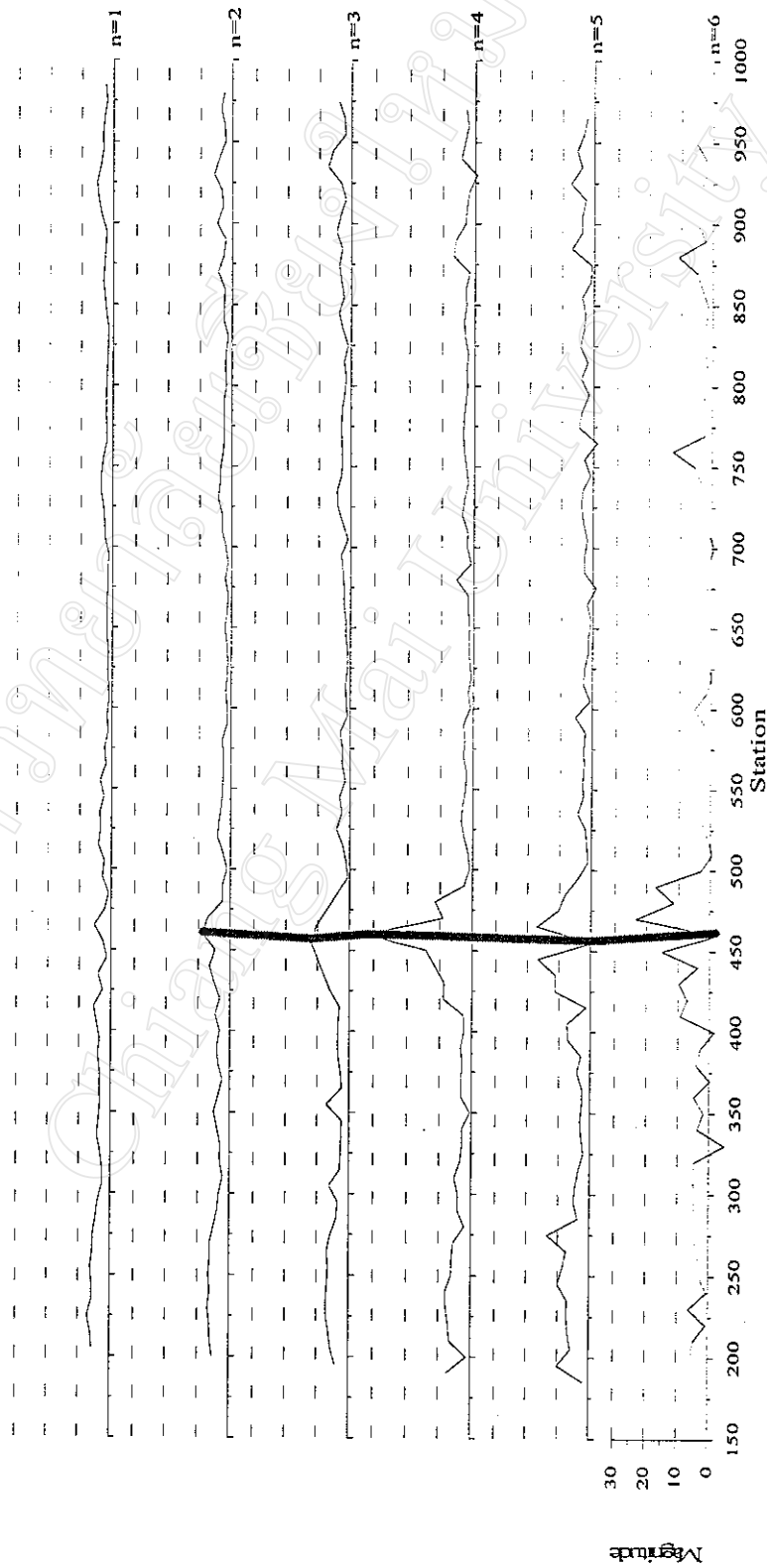


Figure 4.18 Profile plot of apparent chargeability of Khao Khi Nok graphite deposit.

Dipole-dipole array of 10 meter dipole separation. Solid line is the trend of high apparent chargeability.

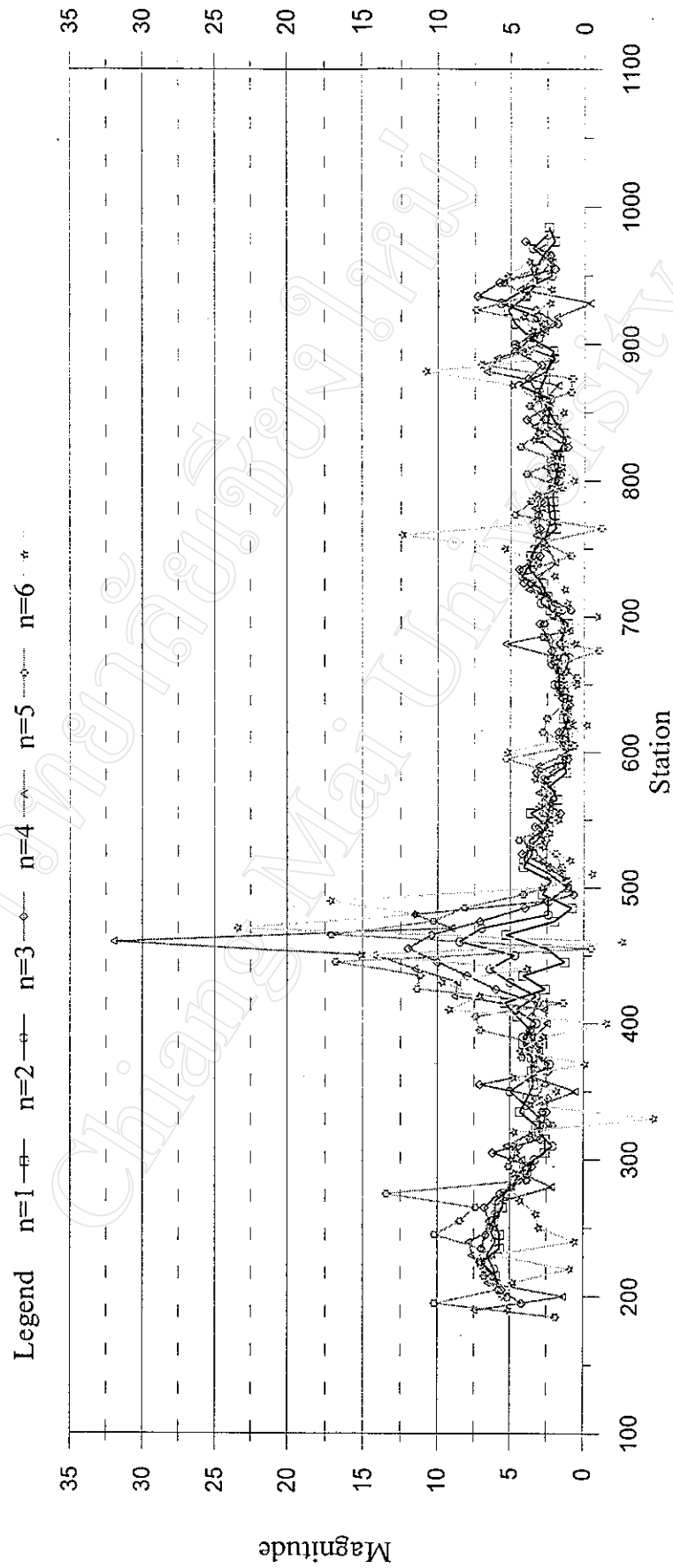


Figure 4.19 Stacked profile plot of apparent chargeability of Khao Khi Nok graphite deposit.  
Dipole-dipole array of 10 meter dipole separation.

value is clearly observed and quite smooth with value about 2.5 millivolts per volt. Then, pseudosection is plotted in Figure 4.17(b) which shows these two anomalous zone.

Metal factor profiles are shown in Figure 4.20, there is a strong correlation of the metal factor with the apparent resistivity and the apparent chargeability, it has high magnitude at the pseudodepth of  $n=3$  to  $n=6$  which highest at pseudodepth  $n=4$ . Figure 4.21 shows stacked profile of the metal factor which has high magnitude about station 250 and very high about station 450. But in Figure 4.17(c), the anomaly can be located at the left portion of the survey line, about station 440.

#### 4.5.2 Complex resistivity parameters

Chargeability profiles are shown in Figure 4.22, it shows a strongly influence of this parameter with depth, from  $n=3$  to  $n=6$ . For  $n=1$  and  $n=2$ , the chargeability is quite flat. Stacked profile is shown in Figure 4.23, a background value is about 50. It cannot locate an anomalous zone from this parameter because of non-uniformity of shape of the profiles. Pseudosection plot in Figure 4.17(d) shows an ambiguous zone which is located close to station 250.

Frequency dependent profiles are plotted in Figure 4.24. For  $n=1$  and  $n=2$ , the shallower, it has uniform value of about 0.2, but from  $n=3$  to  $n=6$  there is strong variation. It appears that there is an electromagnetic coupling indicated by high value of frequency dependent parameter. Figure 4.25 shows clearly stacked profile of strong noise interference which increases frequency dependent value up to 0.9, this means that there is a strong variation in grain size with depth.

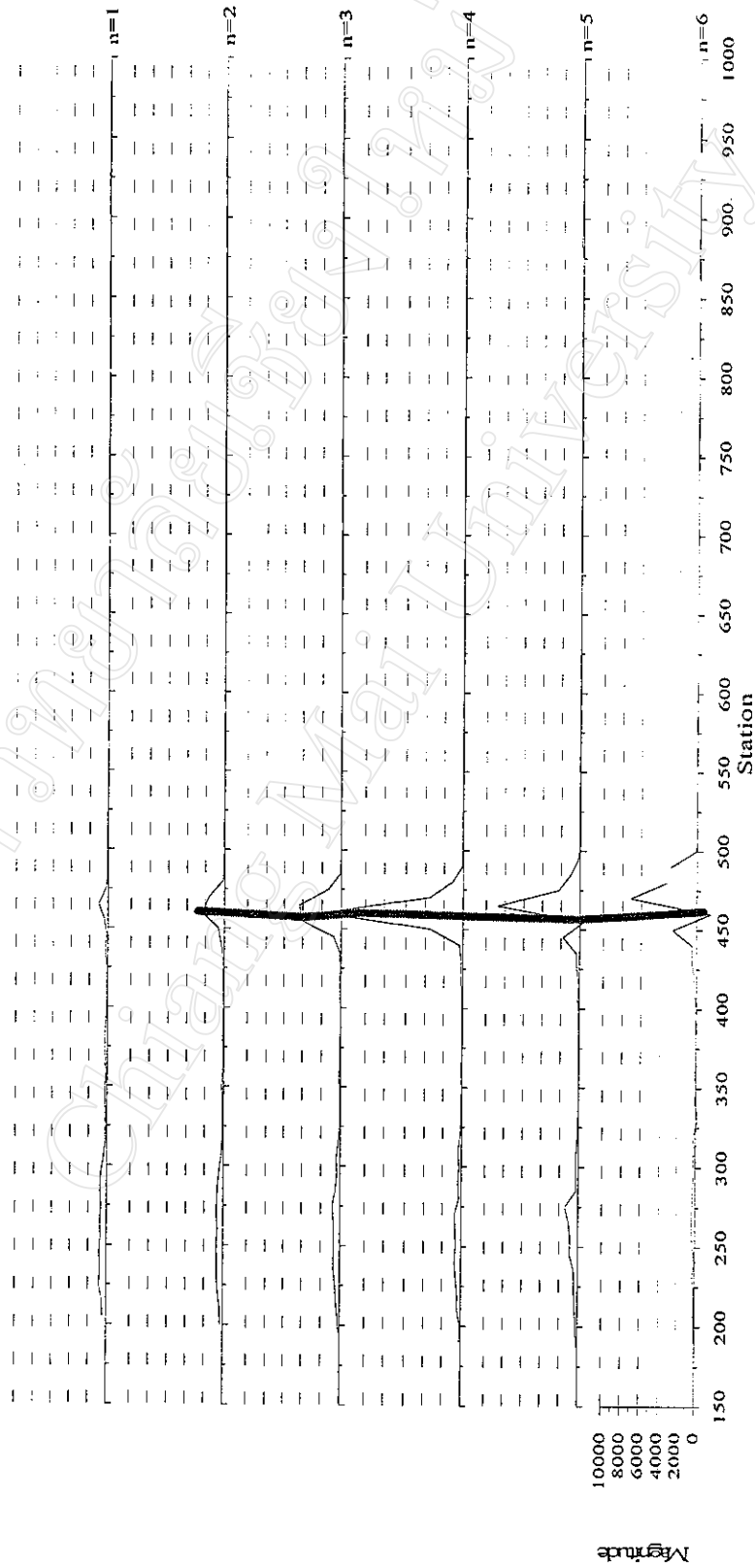


Figure 4.20 Profile plot of metal factor of Khao Khi Nok graphite deposit.  
Dipole-dipole array of 10 meter dipole separation. Solid line is the trend of high metal factor.

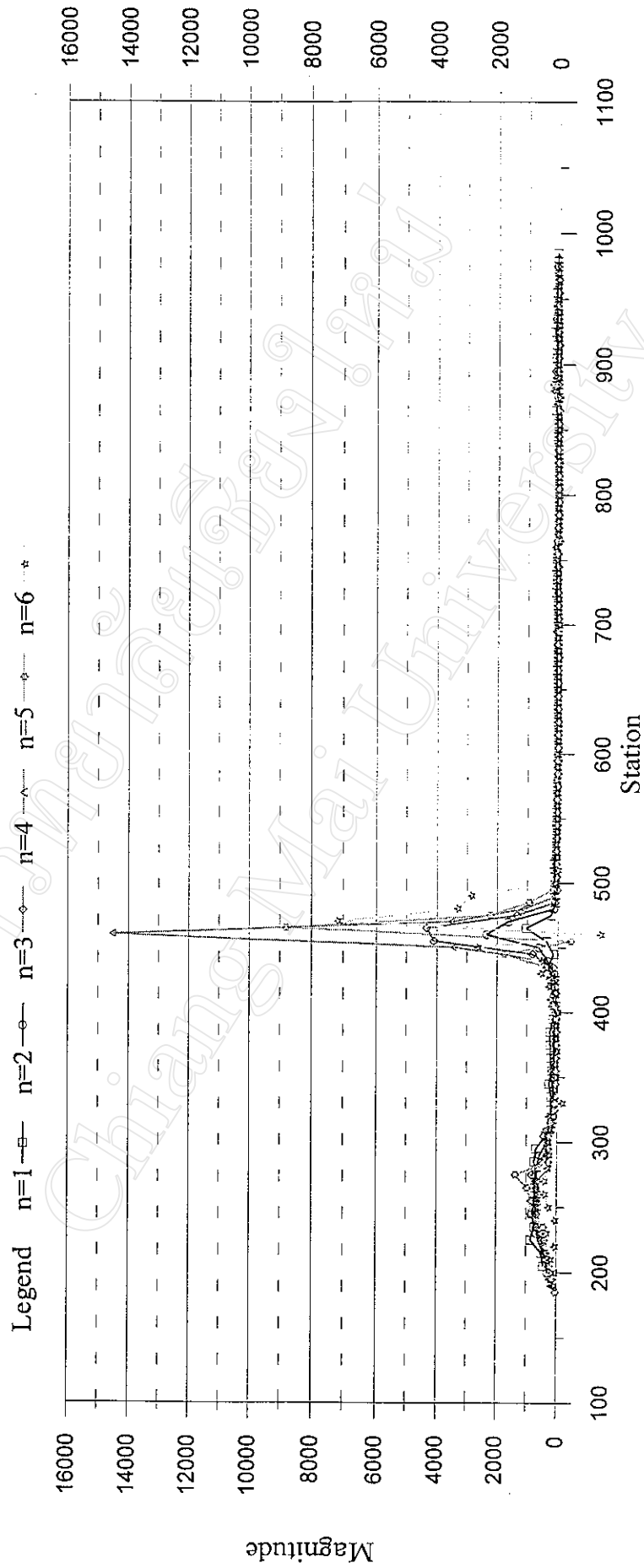


Figure 4.21 Stacked profile plot of metal factor of Khao Khi Nok graphite deposit.  
Dipole-dipole array of 10 meter dipole separation.

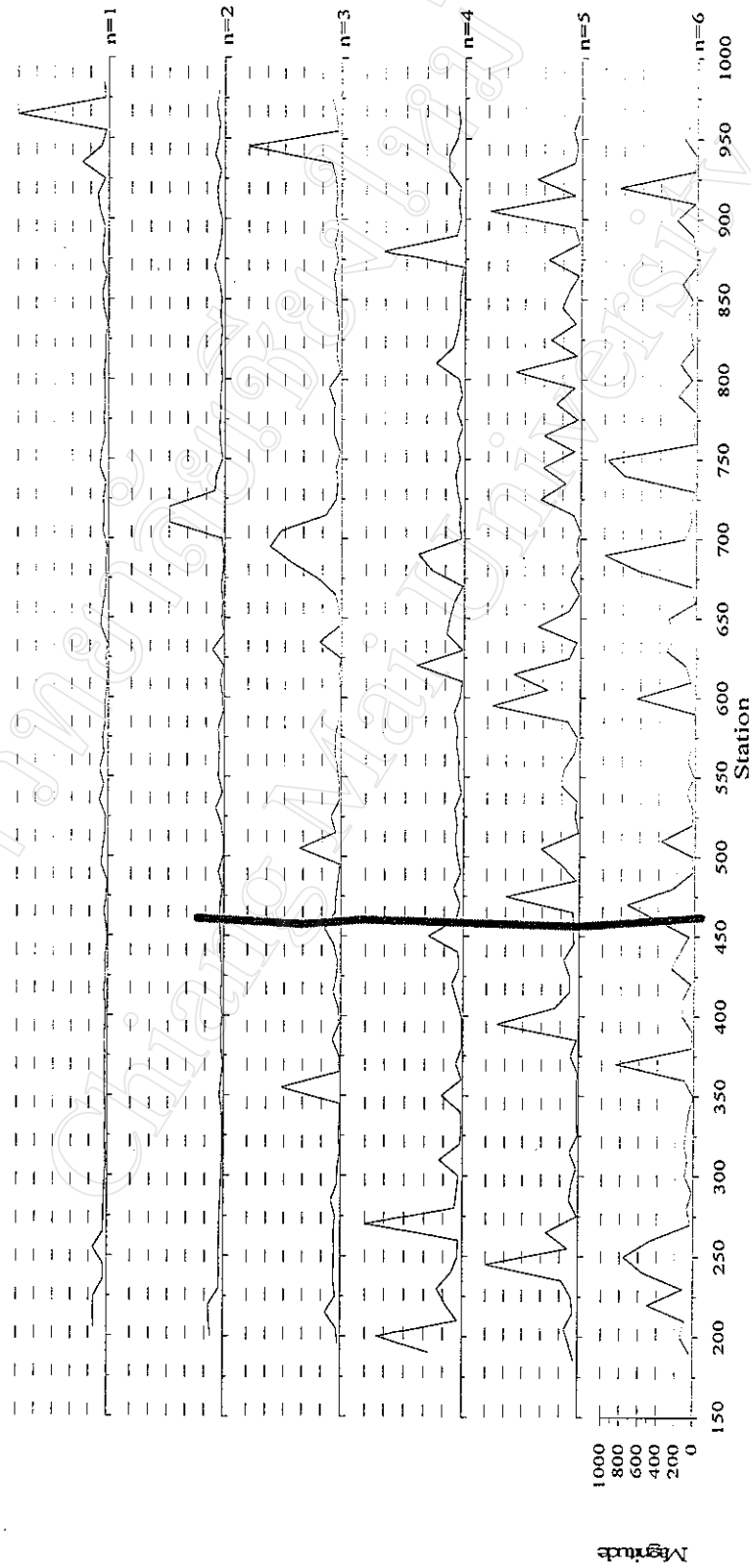


Figure 4.22 Profile plot of chargeability of Khao Khi Nok graphite deposit. Dipole-dipole array of 10 meter dipole separation. Solid line is the trend which correlated with high metal factor.

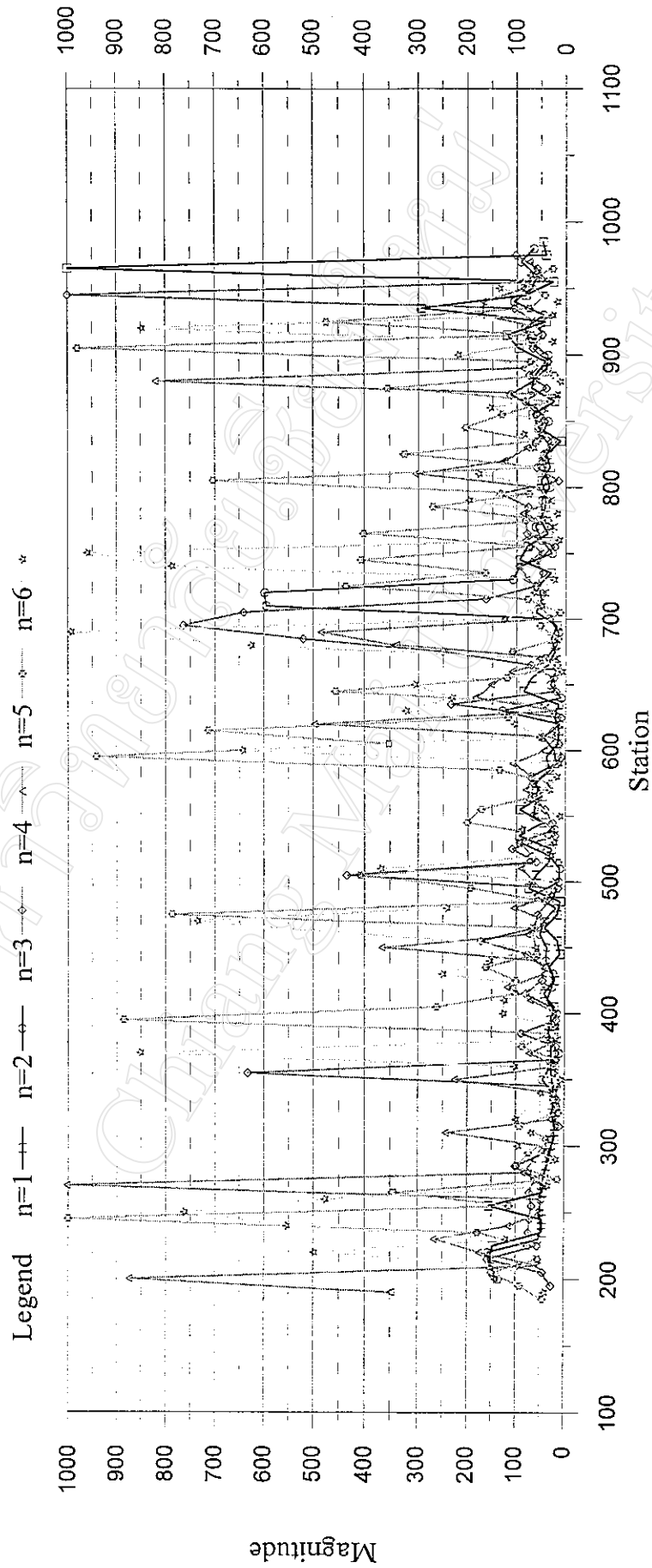


Figure 4.23 Stacked profile plot of chargeability of Khao Khi Nok graphite deposit.  
Dipole-dipole array of 10 meter dipole separation.

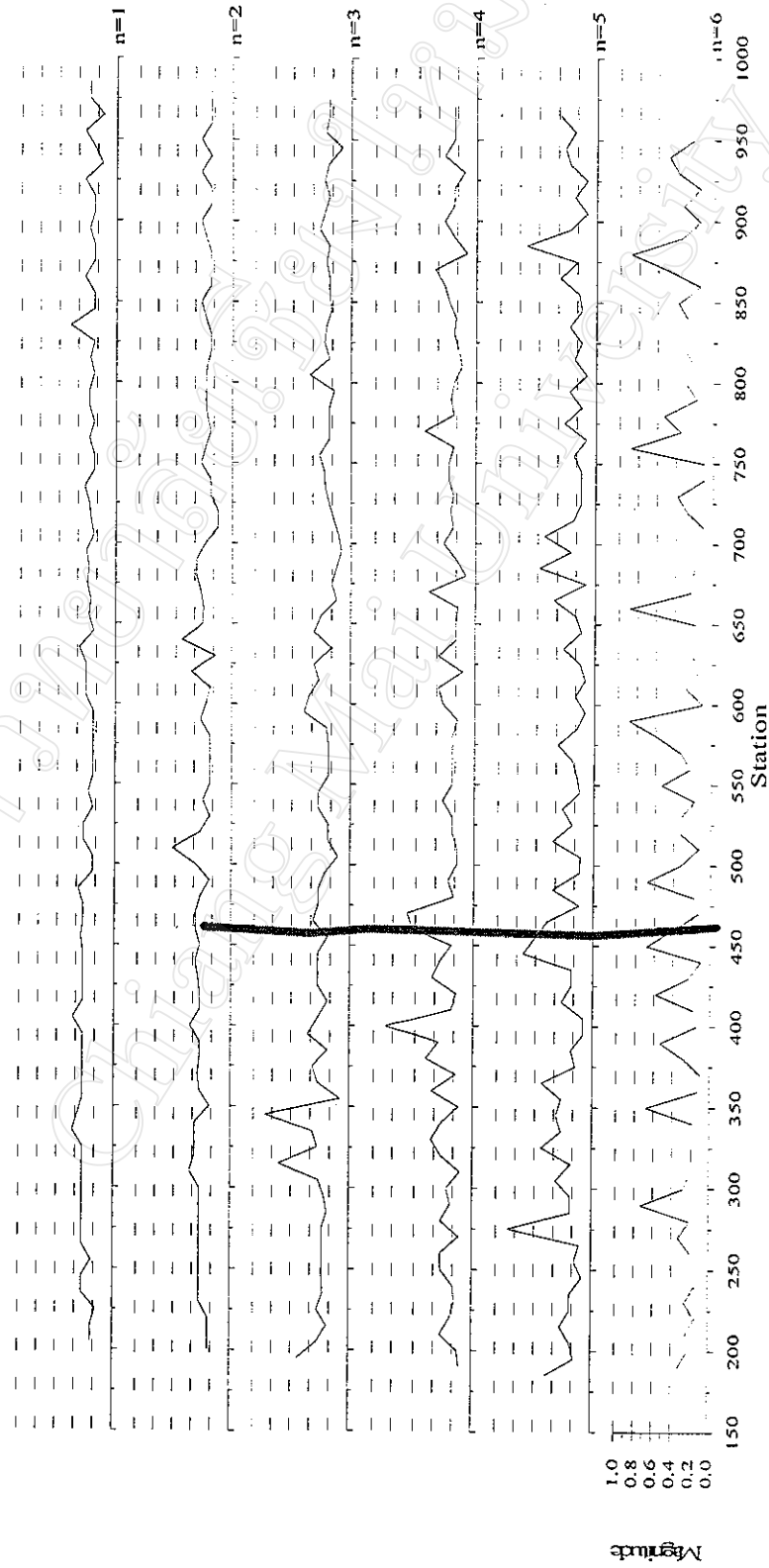


Figure 4.24 Profile plot of frequency dependent of Khao Khi Nok graphite deposit. Dipole-dipole array of 10 meter dipole separation. Solid line is the trend which correlated with high metal factor.

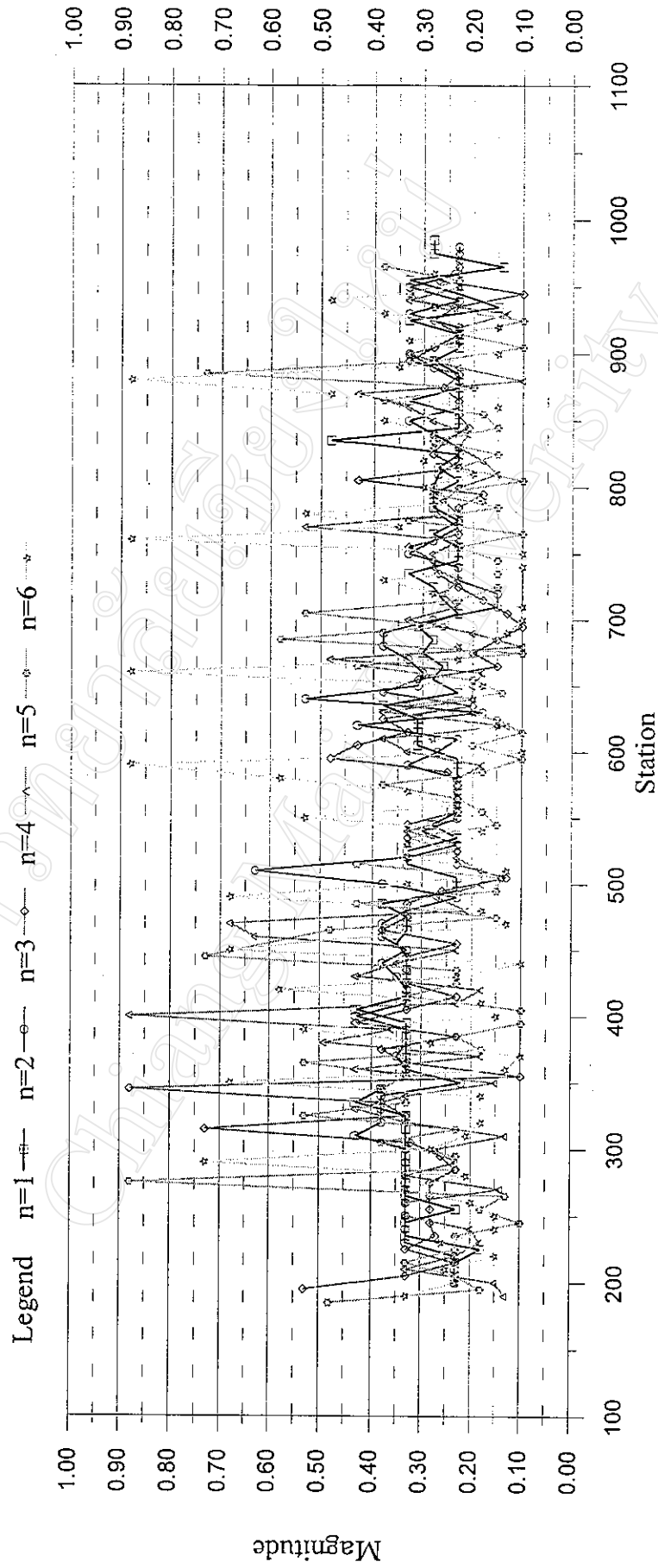


Figure 4.25 Stacked profile plot of frequency dependent of Khao Khi Nok graphite deposit.  
Dipole-dipole array of 10 meter dipole separation.

Pseudosection plot in Figure 4.17(e) shows an anomalous zone from station 250 to station 450.

Time constant profiles are plotted in Figure 4.26. For  $n=1$  to  $n=2$ , it has high time constant value cover both anomalous zones, from station 230 to station 480. There is some value of the time constant which is more steeply higher than the vicinity. This value is not defined as an anomaly because the magnitude is not continuously change. From a stacked profile plot in Figure 4.27, the time constant in the anomalous zone is about 20 milliseconds and a background value is lower than 10 milliseconds. Pseudosection plot of the time constant is shown in Figure 4.17(f), there is very good relationship of high frequency dependent and high value of time constant.

## **4.6 Results of Pong Nok Gaew clay deposit**

Induced polarization data is selected from dipole-dipole array configuration of 10 meter dipole separation. Transmitting time of a transmitter is of 2 seconds. A traverse line is allocated in E-W direction from station 0 to station 800, with total length of 800 meters.

### **4.6.1 Conventional parameters**

Apparent resistivity profiles are shown in Figure 4.28, for  $n=1$  it clearly shows an anomalous zone at the center of a survey line, closed to station 400, with very low apparent resistivity value of about 1 ohm-meter. For  $n=2$  to  $n=4$ , the anomalous zone gave very low apparent resistivity value and increases up at  $n=5$  and  $n=6$ . At the left portion of the anomalous zone, a background value increases with depth that is indicated the apparent resistivity of a non-anomalous zone. Stacked

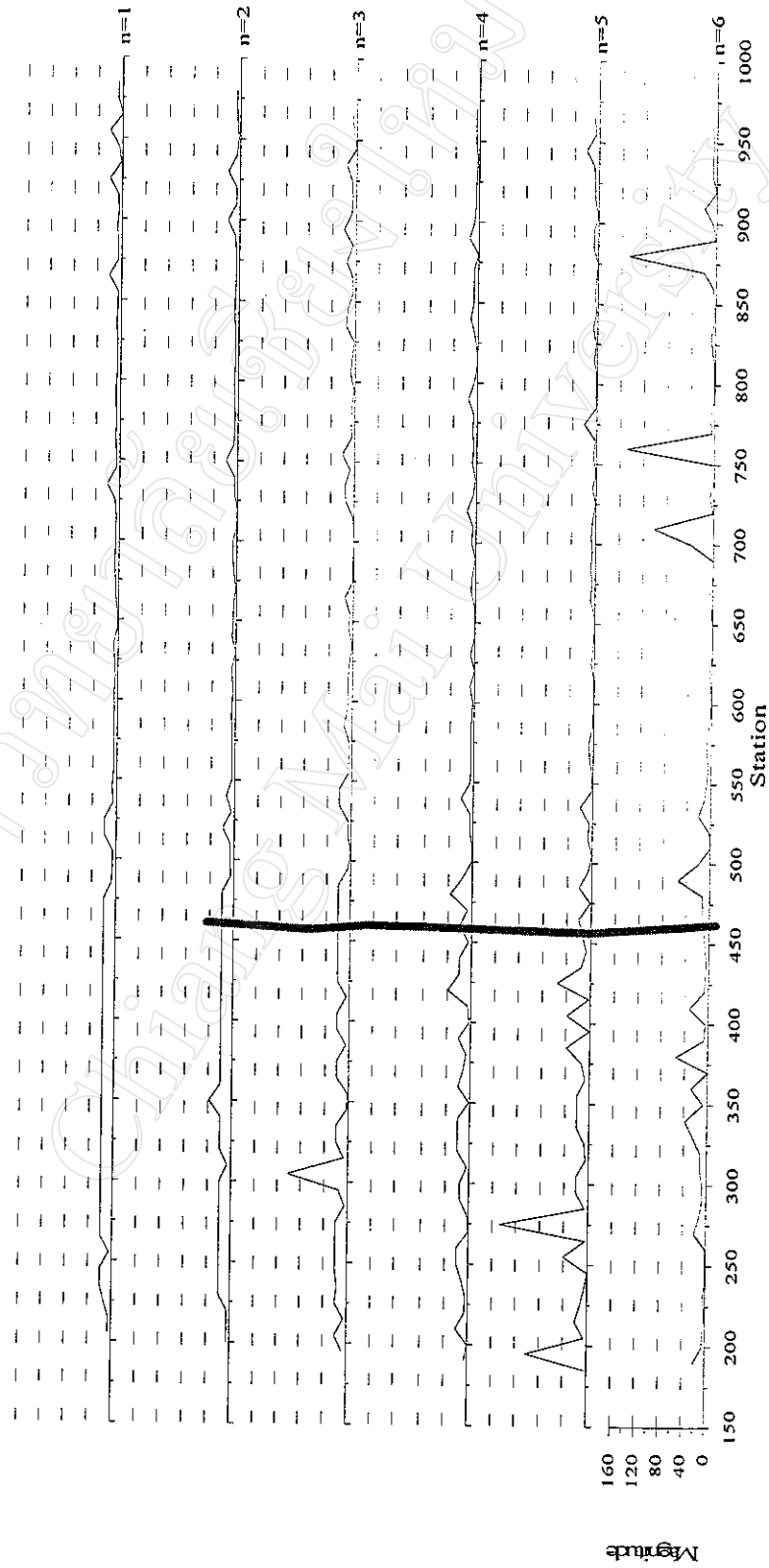


Figure 5.26 Profile plot of time constant of Khao Khi Nok graphite deposit. Dipole-dipole array of 10 meter dipole separation. Solid line is the trend which correlated with high metal factor.

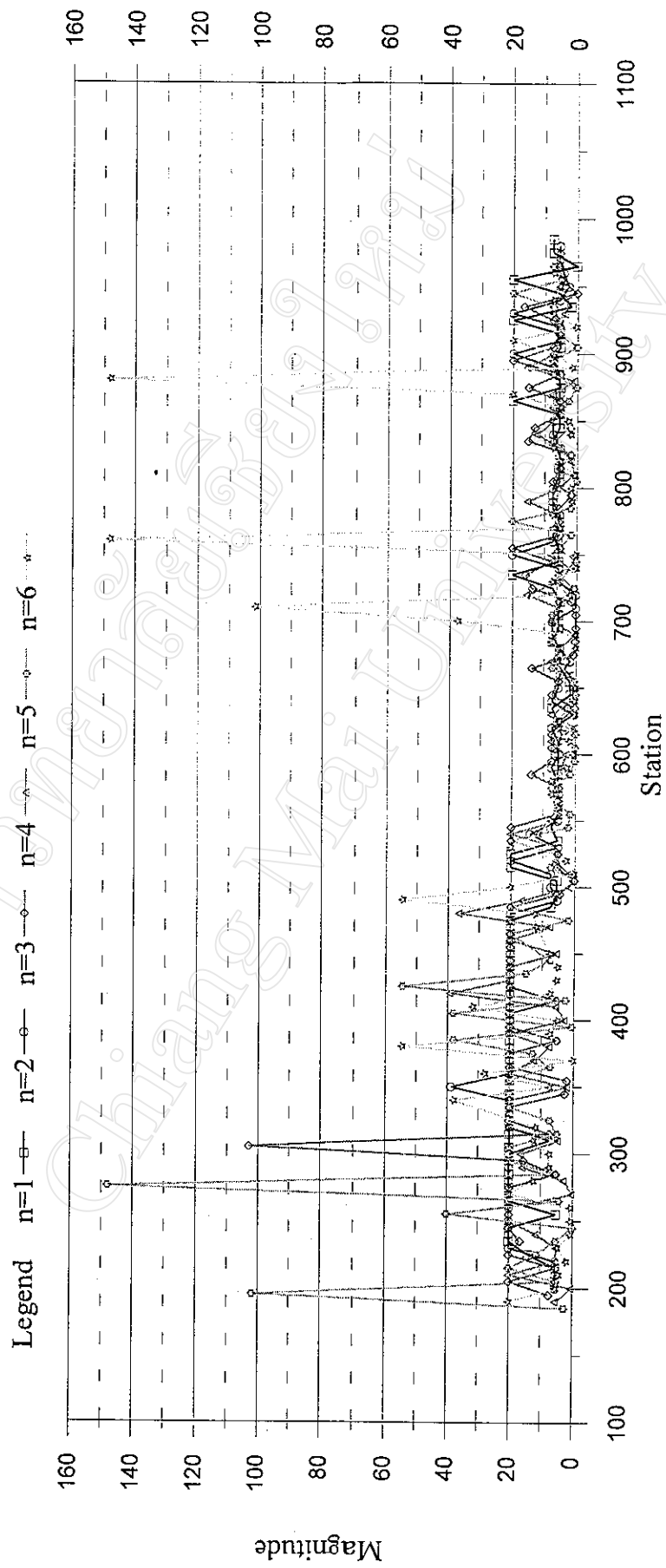


Figure 5.27 Stacked profile plot of time constant of Khao Khi Nok graphite deposit.  
Dipole-dipole array of 10 meter dipole separation.

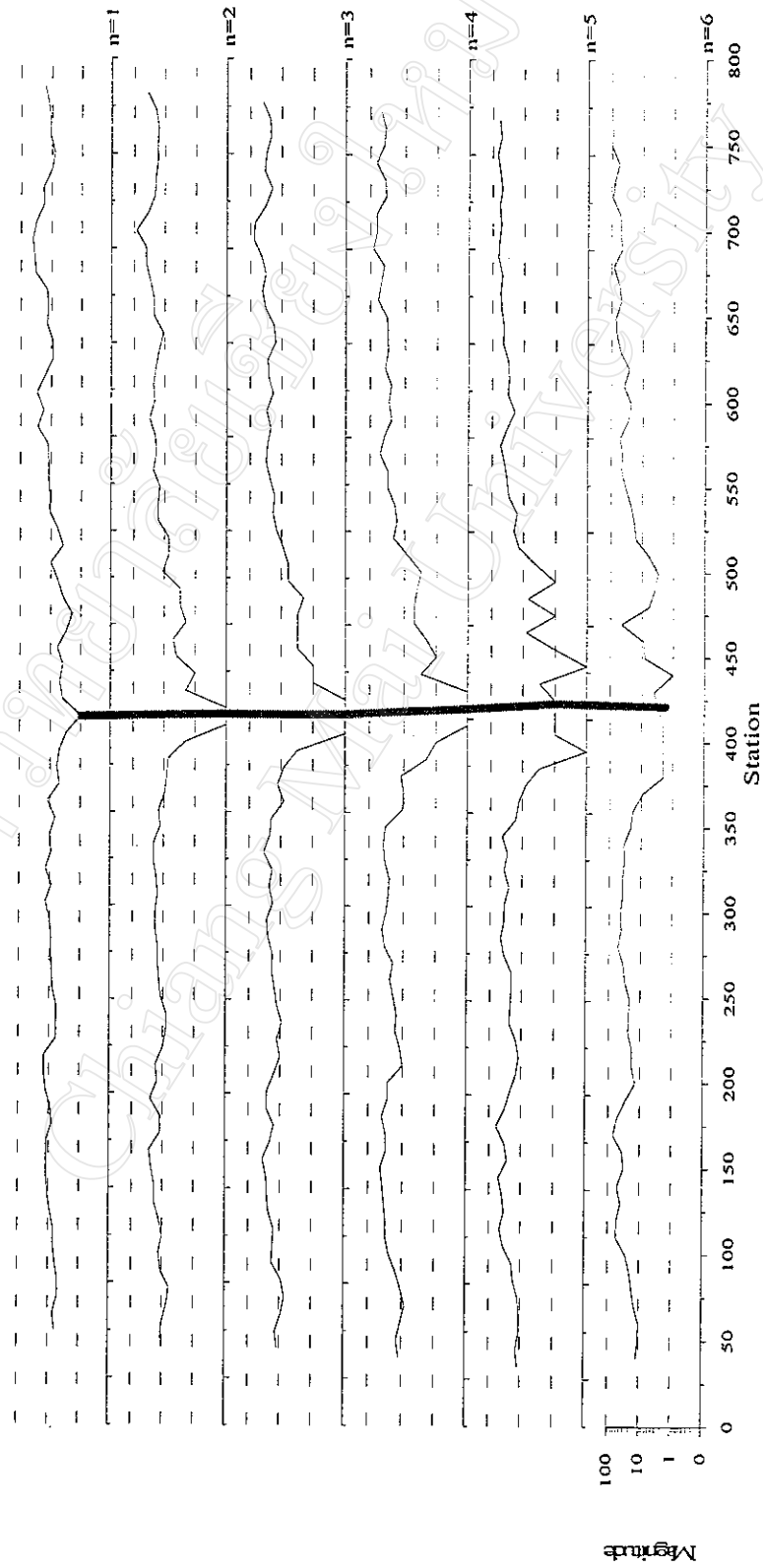


Figure 4.28 Profile plot of apparent resistivity of Pong Nok Gaew clays deposit.

Dipole-dipole array of 10 meter dipole separation. Solid line is the trend of low apparent resistivity.

profile plot in Figure 4.29 shows the anomalous zone at station 420, resistivity value is decreased with depth that means conductive body located at great depth. At station 60, 210, and 600, apparent resistivity value seem not change considerably, that like the other low resistivity zones. Background value is about 100 ohm-meter at depth  $n=1$  and increases up to almost 1000 ohm-meter at depth  $n=6$ . In pseudosection plot in Figure 4.30(a) there is a strong low resistivity zone located at the center of the survey line represents by blue color.

Apparent chargeability profiles are shown in Figure 4.31, an anomalous zone is allocated in three zones. Thick solid lines are drawn to track these anomalous zones. At station 60 and station 230, apparent chargeability value is reached 40 millivolts per volt. While station 430 has very high apparent chargeability, reaching 160 millivolts per volt. Stacked profile plot in Figure 4.32 shows the whole three anomalous zones which has the apparent chargeability value increases with the depth that means a source of the polarization effect is come from the great depth. Figure 4.30(b) shows a pseudosection of the apparent chargeability which is very high magnitude at the center of the survey line that correlates well with the apparent resistivity value.

Metal factor profiles are plotted in Figure 4.33, it can be seen that at station 420 metal factor value increases with depth and reaches the maximum at the depth of  $n=4$ . This can identify that an anomalous body located below station 450 with shallow depth. In Figure 4.34 stacked profile shows quite good location of the anomalous zone. Pseudosection of this parameter shows in Figure 4.30(c) indicates the anomalous zone

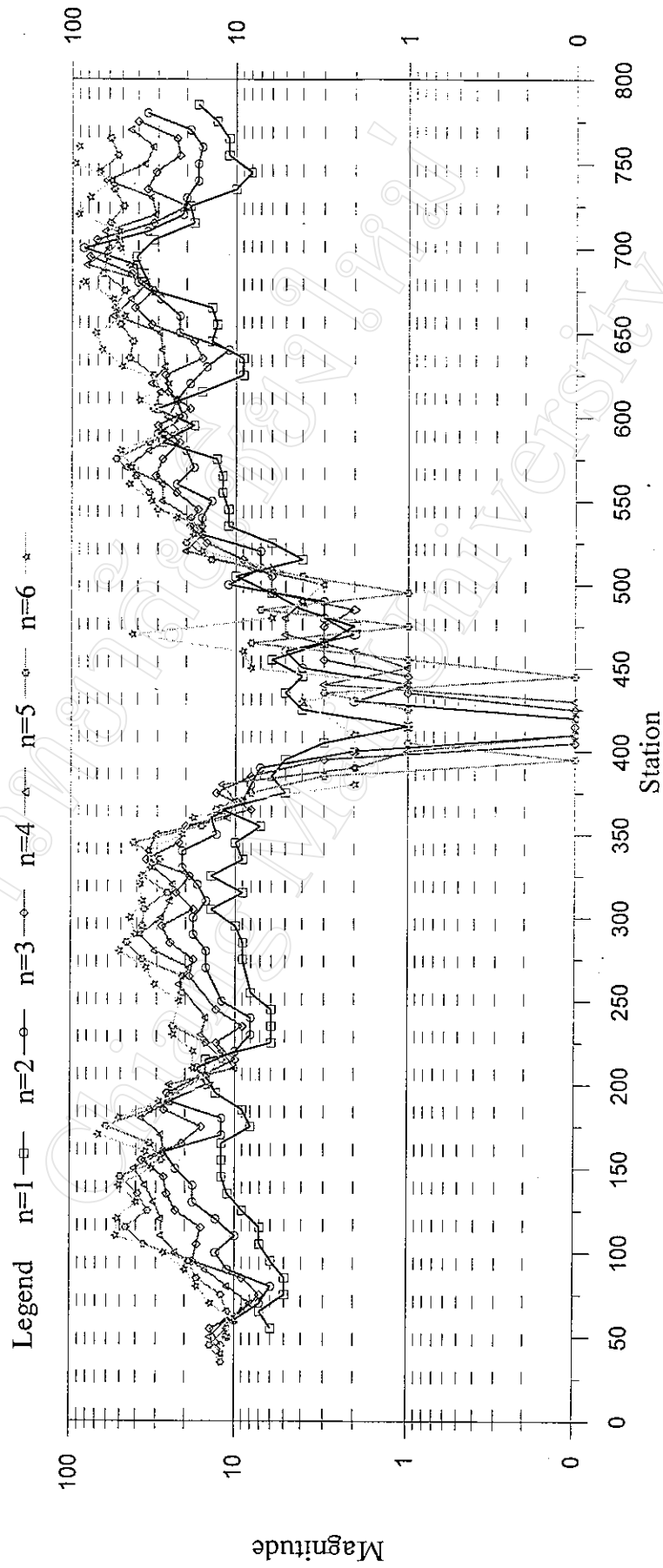
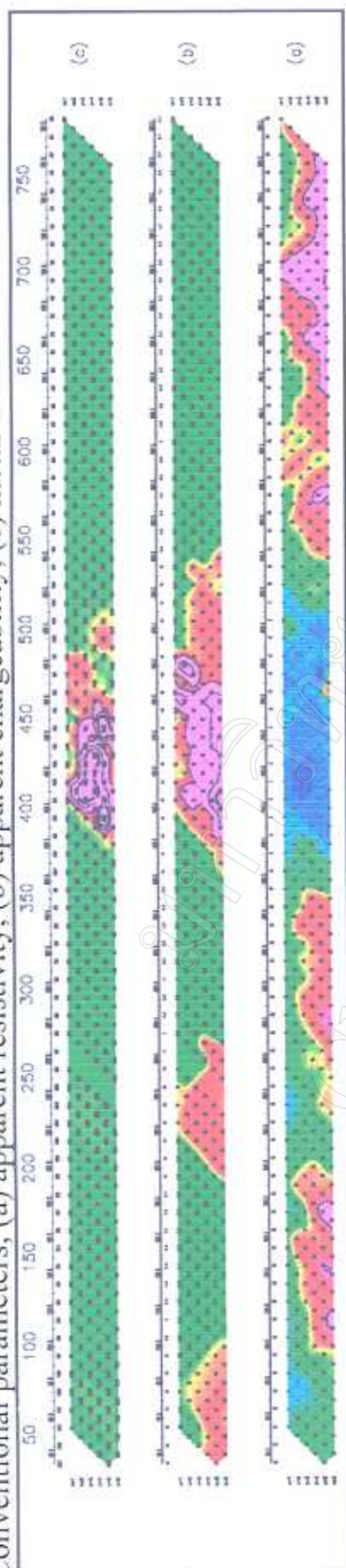


Figure 5.29 Stacked profile plot of apparent resistivity of Pong Nok Gaew clays deposit.  
Dipole-dipole array of 10 meter dipole separation.

Conventional parameters; (a) apparent resistivity, (b) apparent chargeability, (c) metal factor



Complex resistivity parameters; (d) chargeability, (e) frequency dependent, (f) time constant

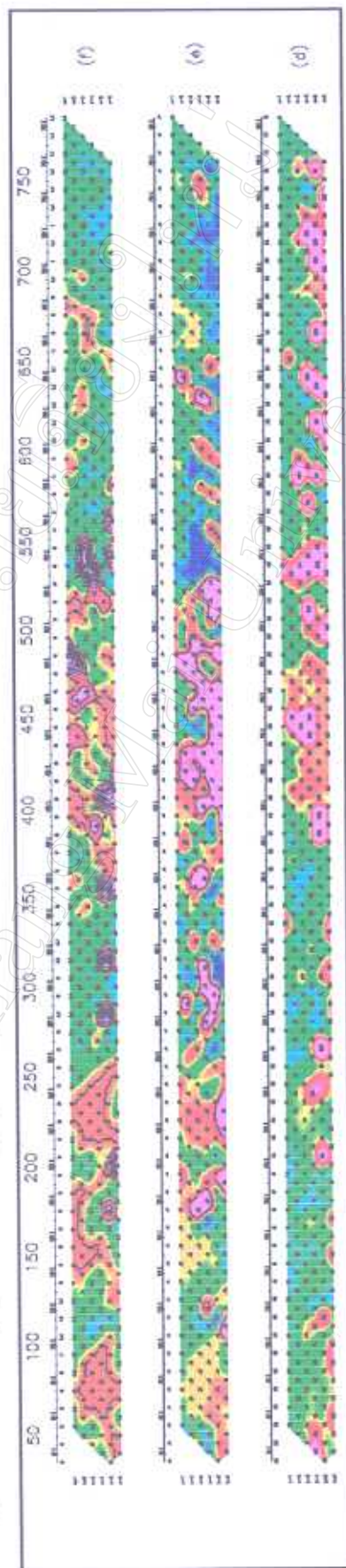


Figure 4.30 Conventional and complex resistivity pseudosections plot of Pong Nok Gaew clay deposit.

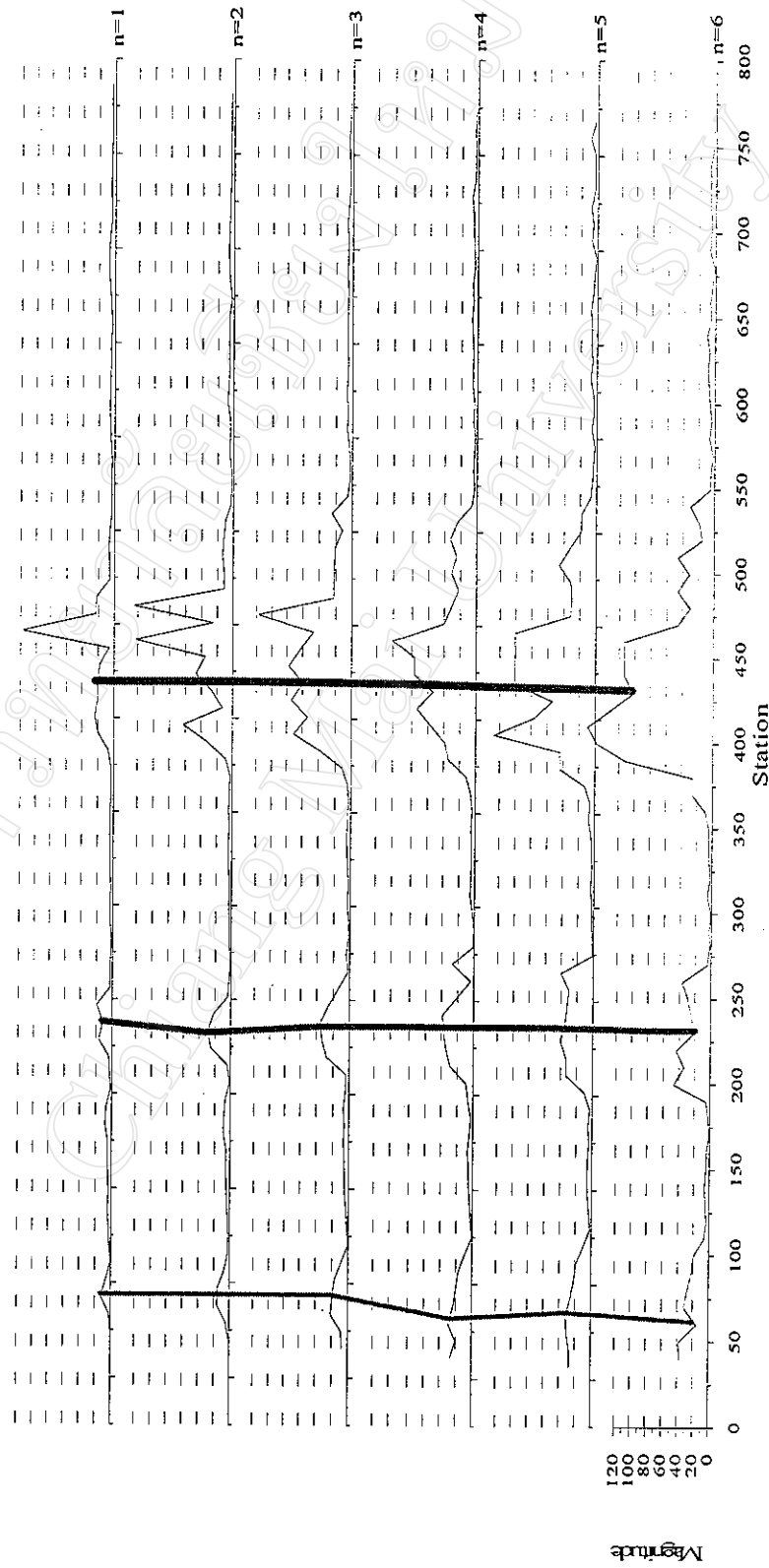


Figure 5.31. Profile plot of apparent chargeability of Pong Nok Gaew clays deposit.

Dipole-dipole array of 10 meter dipole separation. Solid lines are the trend of high apparent chargeability.

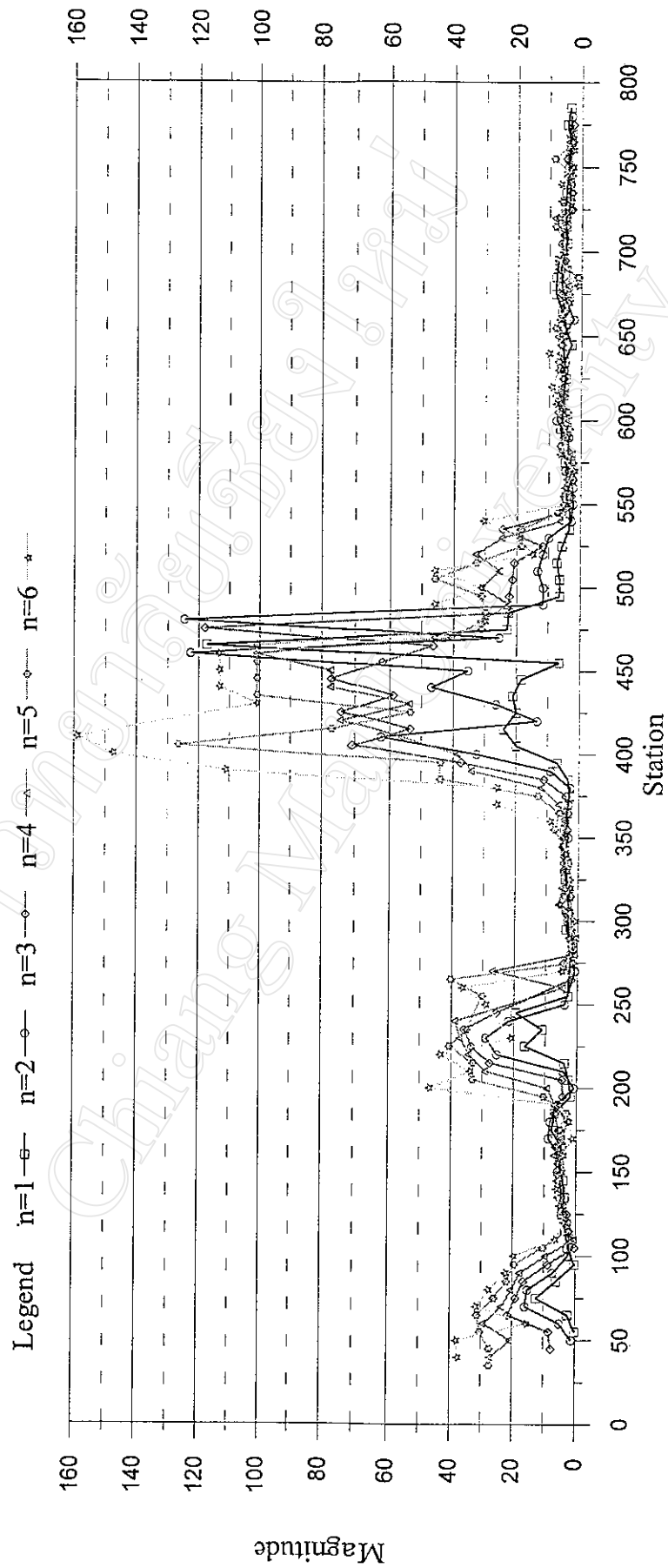


Figure 5.32. Stacked profile plot of apparent chargeability of Pong Nok Gaew clays deposit.  
Dipole-dipole array of 10 meter dipole separation.

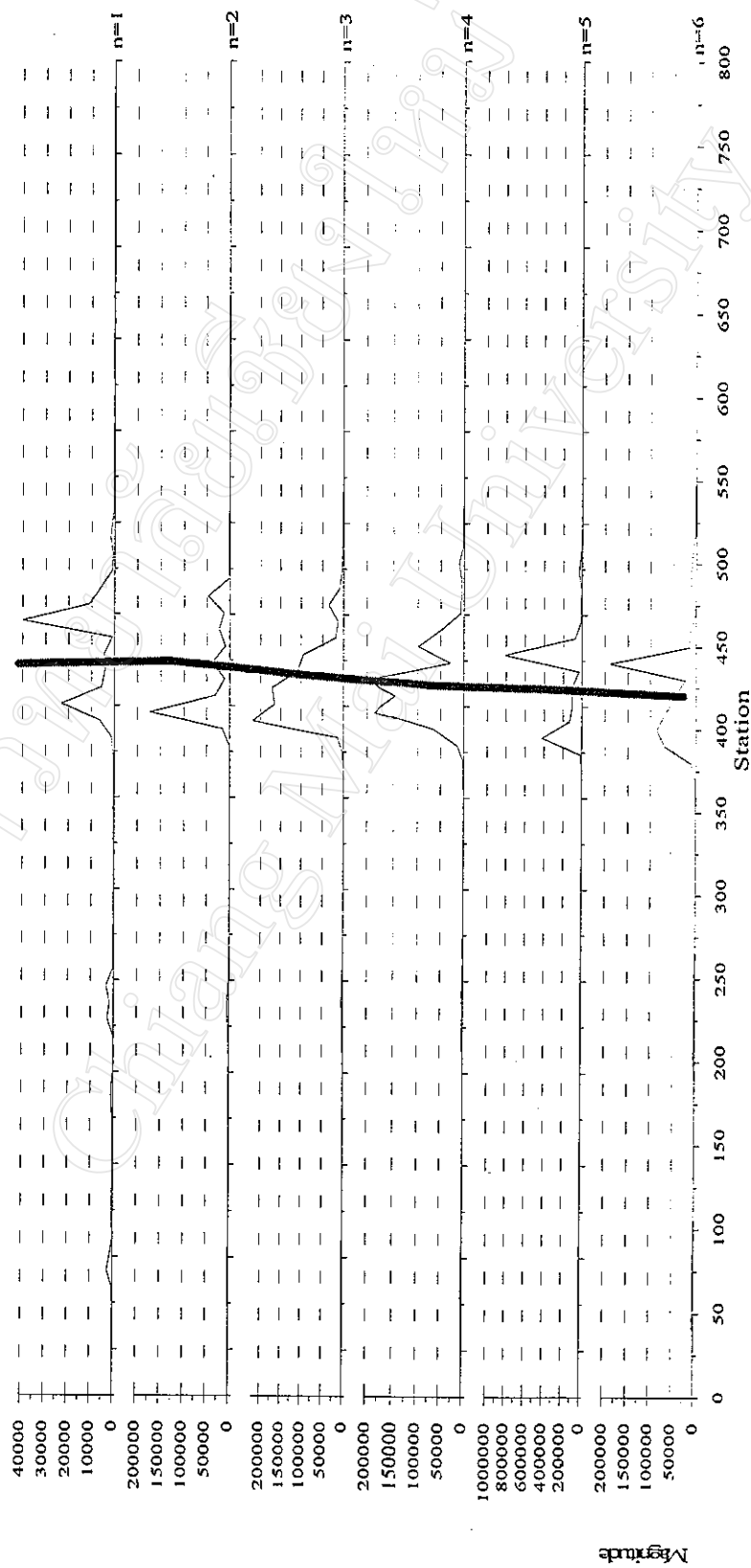


Figure 5.33 Profile plot of metal factor of Pong Nok Gaew clays deposit.

Dipole-dipole array of 10 meter dipole separation. Solid line is the trend of high metal factor.

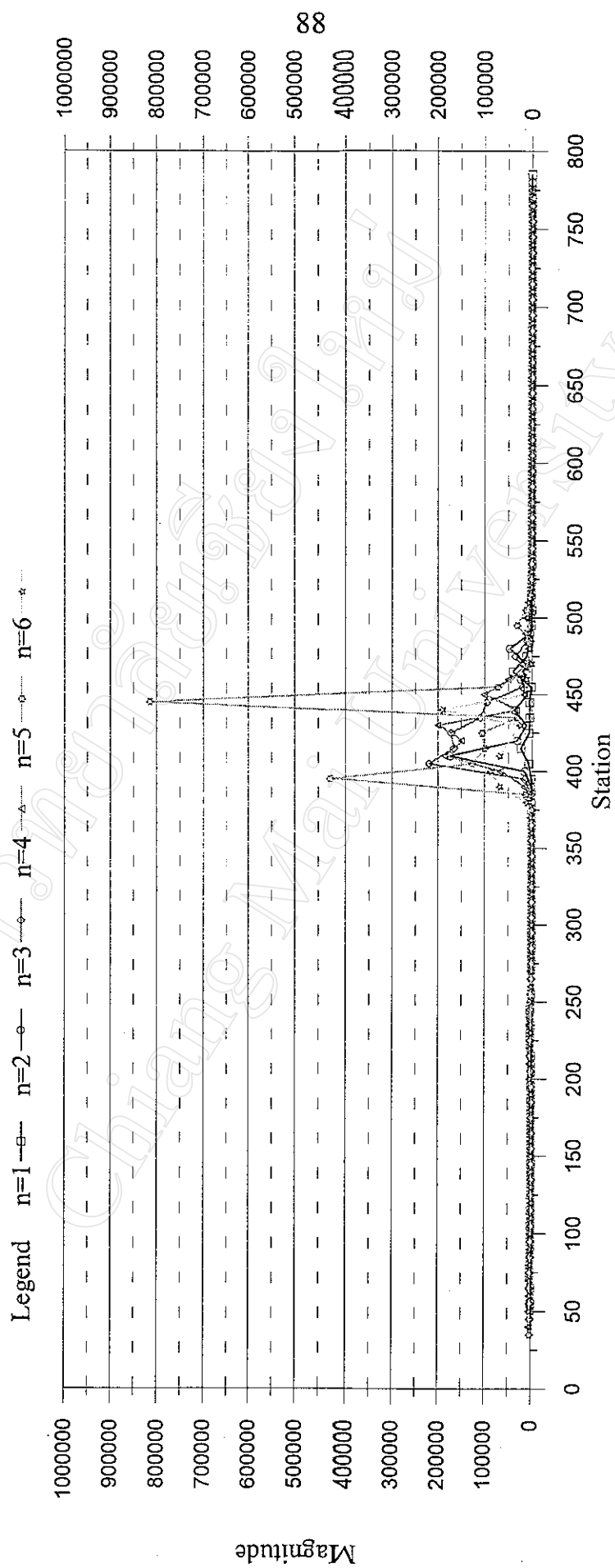


Figure 5.34 Stacked profile plot of metal factor of Pong Nok Gaew clays deposit.  
Dipole-dipole array of 10 meter dipole separation.

that correlates well with both the apparent resistivity and the apparent chargeability values.

#### 4.6.2 Complex resistivity parameters

Chargeability profiles are plotted in Figure 4.35 and its stacked profile is plotted in Figure 4.36. For  $n=1$ , this parameter shows more smoother profiles than the other pseudodepth. Pseudosection is plotted in Figure 4.30(d), it shows high value in three distinctive zone about station 360 to station 600.

Frequency dependent profiles are plotted in Figure 4.37 and its stacked profile is plotted in Figure 4.38. It has uniform value in background zone below station 250 with 0.4 in magnitude. In an anomalous zone, from station 300 to station 450, the value is between 0.2 to 0.5, with an average value 0.34. In the right portion this parameter has strong variation that cannot identify the anomalous zone. Pseudosection is plotted in Figure 4.30(e) that shows high value in left portion.

Time constant profiles are plotted in Figure 4.39, it shows that a background value is very low, not exceed 10 milliseconds. At an anomalous zone, the time constant is very high but it is not continuous in the vicinity. Generally, the time constant value of 20 milliseconds is distributed over this survey line. By this reason, it is very difficult to use this parameter to locate the anomalous zone. From pseudo-depth of  $n=5$  and  $n=6$ , there are many strong influences that manifest itself discontinuously. Stacked profile of time constant is shown in Figure 4.40, it can be seen that a background value is lower than 10

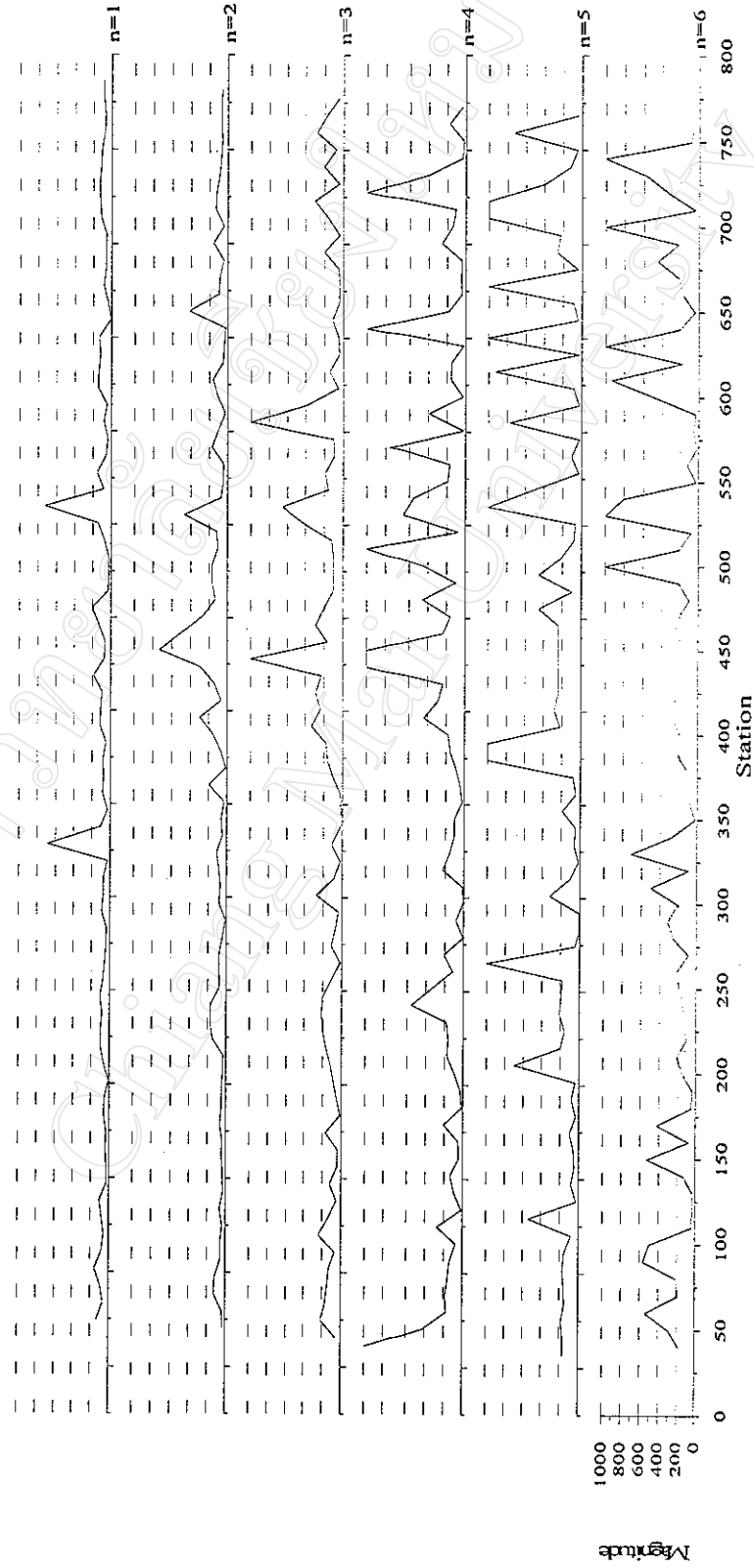


Figure 5.35 Profile plot of chargeability of Pong Nok Gaew clays deposit.  
Dipole-dipole array of 10 meter dipole separation.

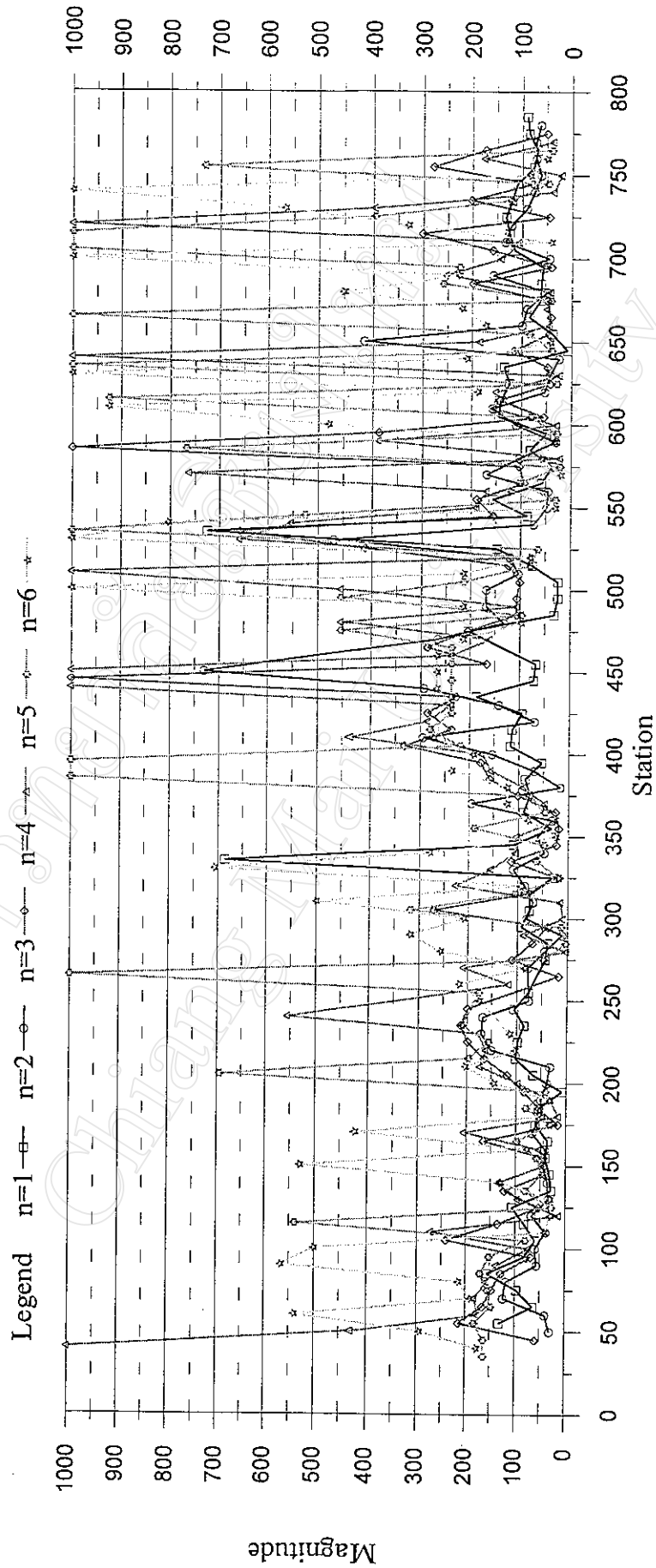


Figure 5.36 Stacked profile plot of chargeability of Pong Nok Gaew clays deposit.  
Dipole-dipole array of 10 meter dipole separation.

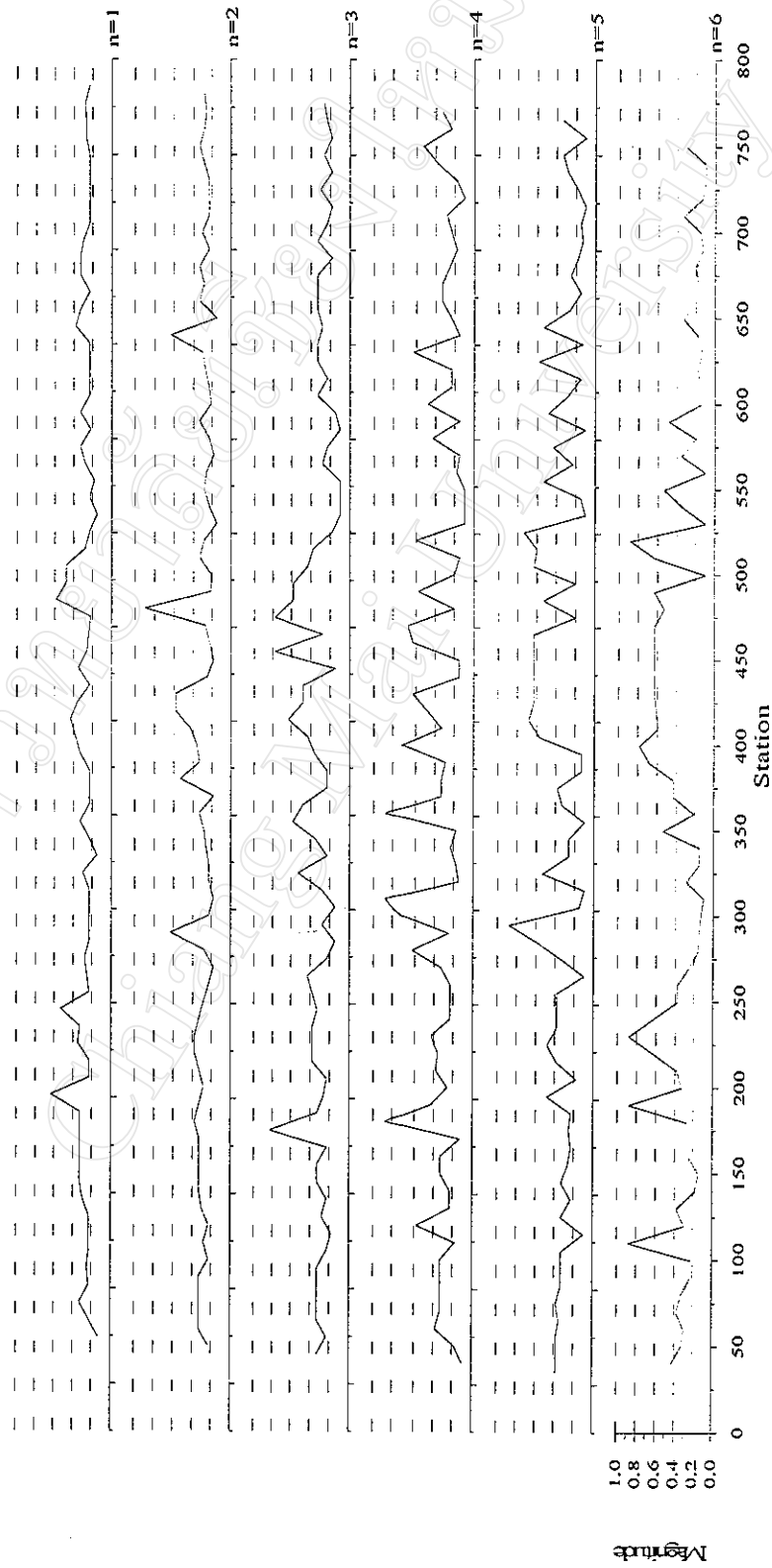


Figure 5.37 Profile plot of frequency dependent of Pong Nok Gaew clays deposit.  
Dipole-dipole array of 10 meter dipole separation.

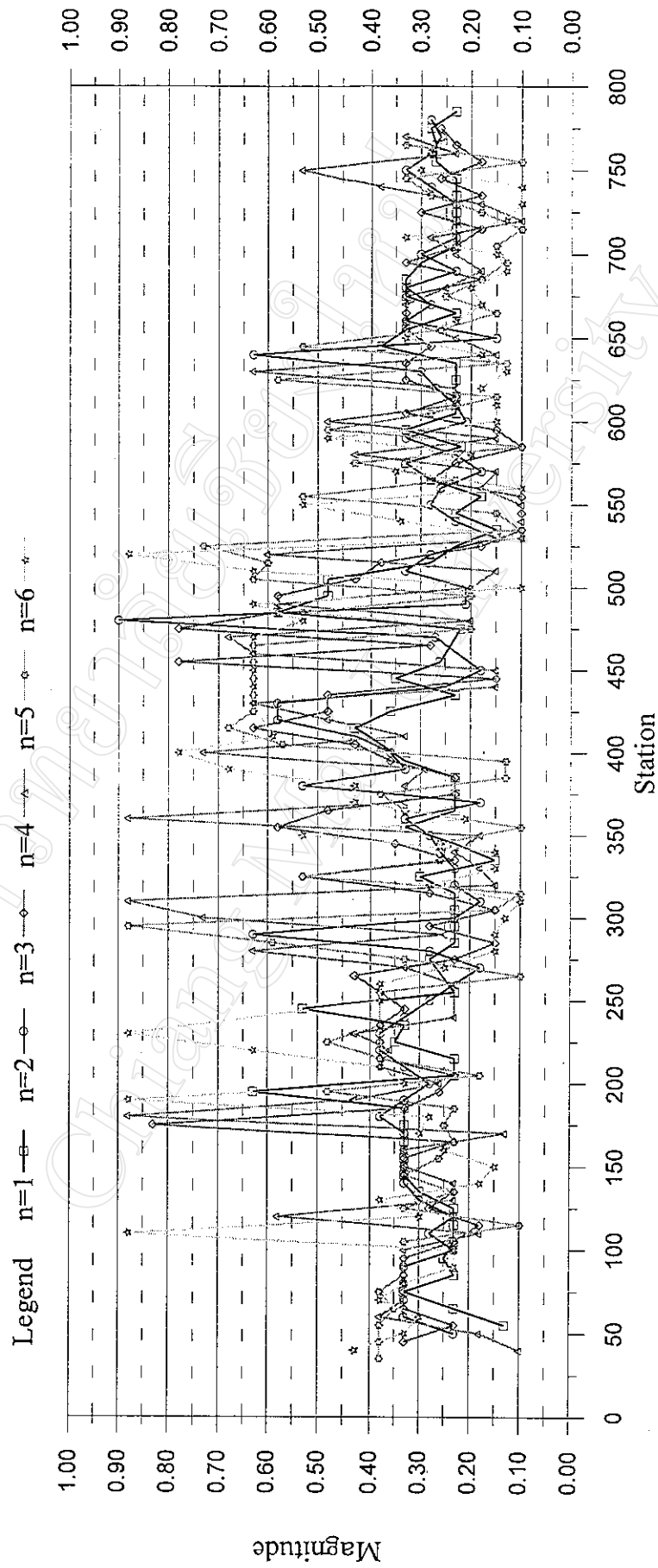


Figure 5.38 Stacked profile plot of frequency dependent of Pong Nok Gaew clays deposit.  
Dipole-dipole array of 10 meter dipole separation.

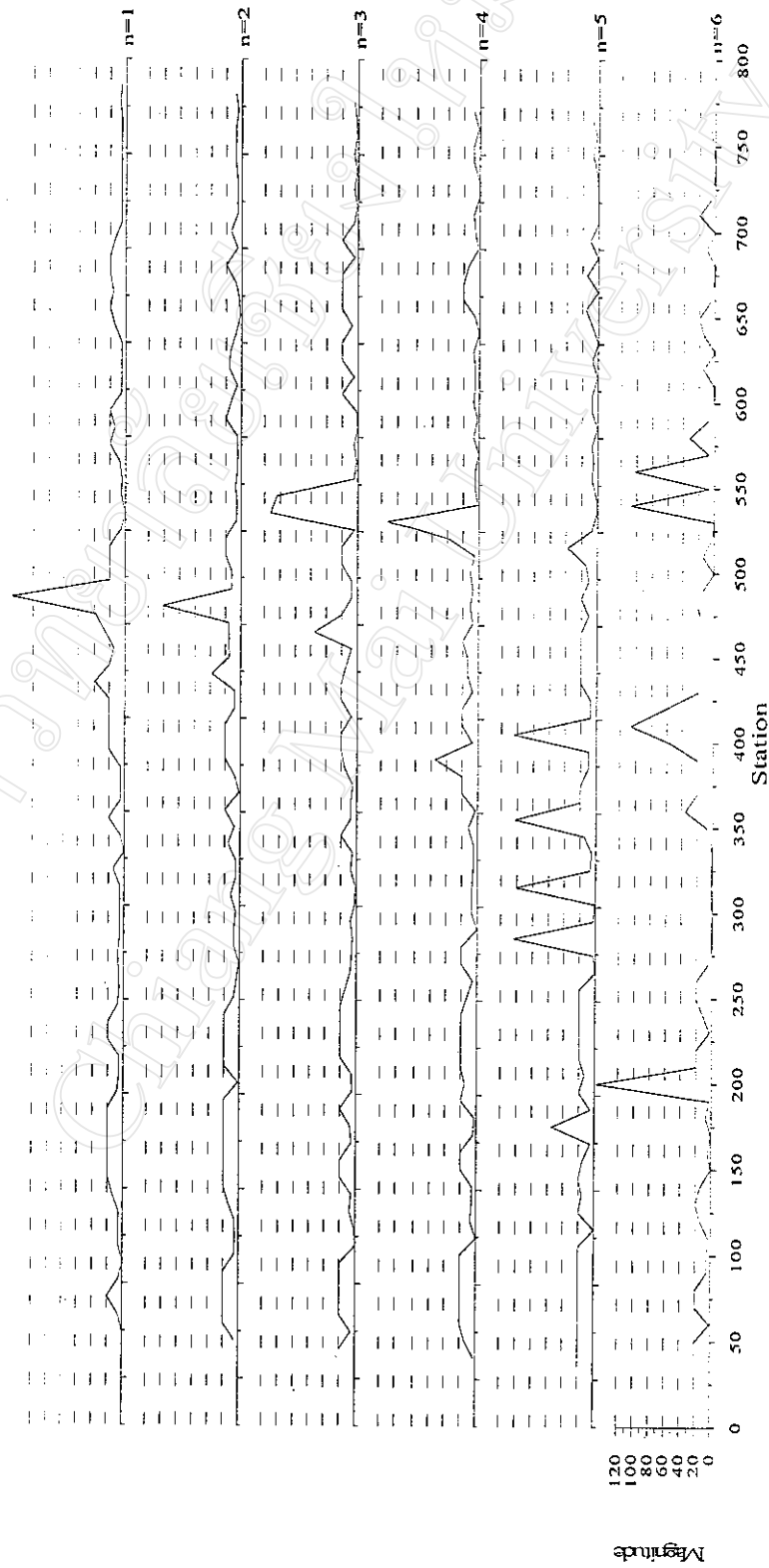


Figure 5.39 Profile plot of time constant of Pong Nok Gaew clays deposit.  
Dipole-dipole array of 10 meter dipole separation.

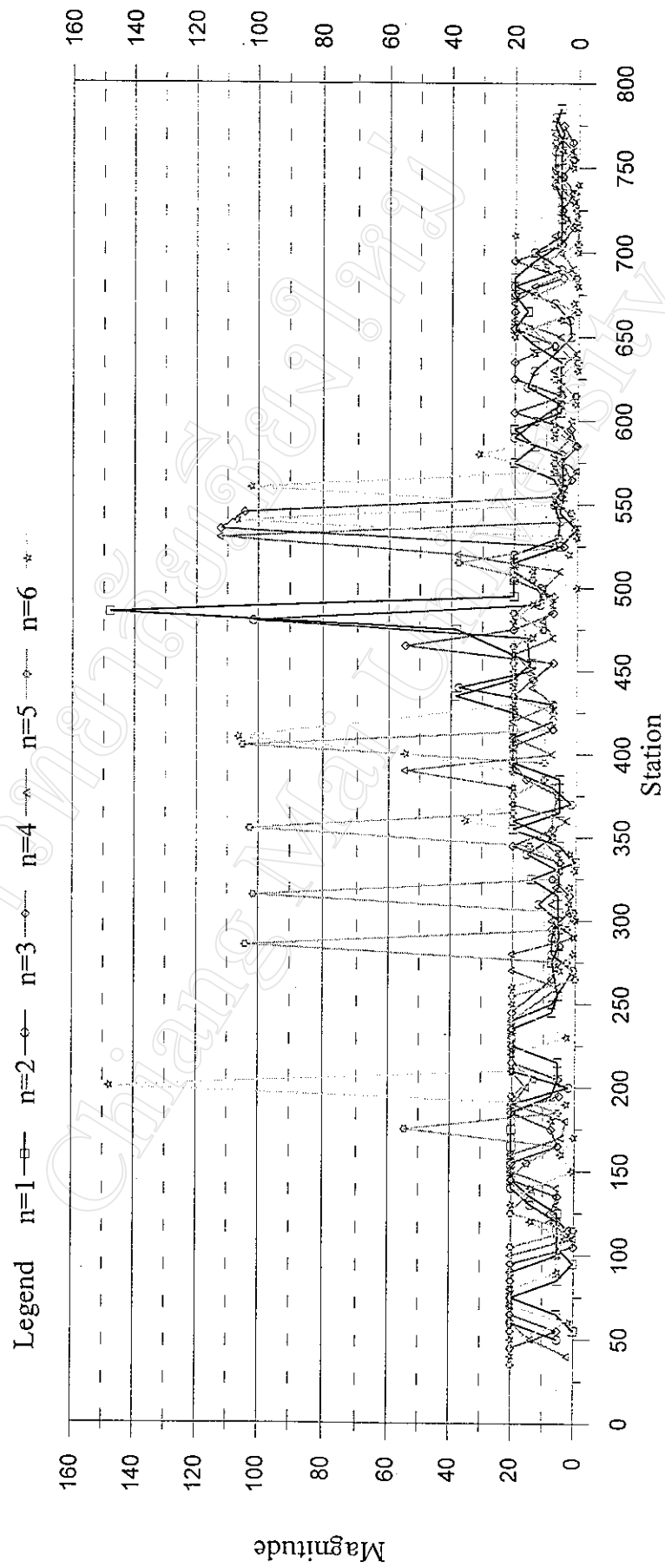


Figure 5.40 Stacked profile plot of time constant of Pong Nok Gaew clays deposit.  
Dipole-dipole array of 10 meter dipole separation.

milliseconds and the anomalous zone has high time constant over 20 milliseconds. Figure 4.30(f) shows a pseudosection plot of the time constant that is not meaningful in case of locating the anomalous zone.

Table 4.3, 4.4, and 4.5 show summarization of those three areas.

## **4.7 Decay curve characteristics**

This section present how the induced polarization response of the ground behave under impressed external force. Decay characteristic of each mineralization shown in anomalous and non-anomalous decay curves. Furthermore, an effect of survey parameter will be presented due to comparison of responding result in spite of further analysis.

### **4.7.1 Anomalous and non-anomalous decay curves**

Decay curves of each mineral deposit are plotted to obtain shape and magnitude of them. Decay curves of anomalous and non-anomalous zone are selected from point which completely decay shape, noise free data. Decay curves are plotted first separate each mineral to individually observe and plotted together to separate each mineral.

#### ***4.7.1.1 Mae Chong sulphide deposit***

Non-anomalous decay curves are shown in Figure 4.41 (lower). Non-anomalous zone is selected from area of high apparent resistivity (refer to resistivity stacked profile) and low apparent chargeability (refer to chargeability stacked profile). Decay curves of this zone have low magnitude at the early time and have nearly the same magnitude at the later time. The analysis intends at the early time rather than late time.

Table 4.3 Summary of sulphide mineralization.

Parameter	Background	Anomaly
Apparent resistivity	over 100 (highest 180)	below 100 (lowest 2)
Apparent chargeability	about 5	over 5 (highest 107)
Metal factor	low (about 0)	high (max. 62,000)
Frequency dependent	0.23	0.33
Time constant	5	20

Table 4.4 Summary of graphite mineralization.

Parameter	Background	Anomaly
Apparent resistivity	over 30 (highest 250)	below 10 (lowest 1)
Apparent chargeability	below 5	over 5 (highest 32)
Metal factor	low (about 0)	high (max. 15,000)
Frequency dependent	0.23	0.33
Time constant	5	20

Table 4.5 Summary of clay mineralization.

Parameter	Background	Anomaly
Apparent resistivity	over 10 (highest 100)	below 10 (lowest ~0)
Apparent chargeability	5	over 10 (highest 160)
Metal factor	low	high
Frequency dependent	0.23	(0.33) and 0.63
Time constant	below 5	(20) over up to 150

Note: value in parenthesis is found but not located as anomalous zone

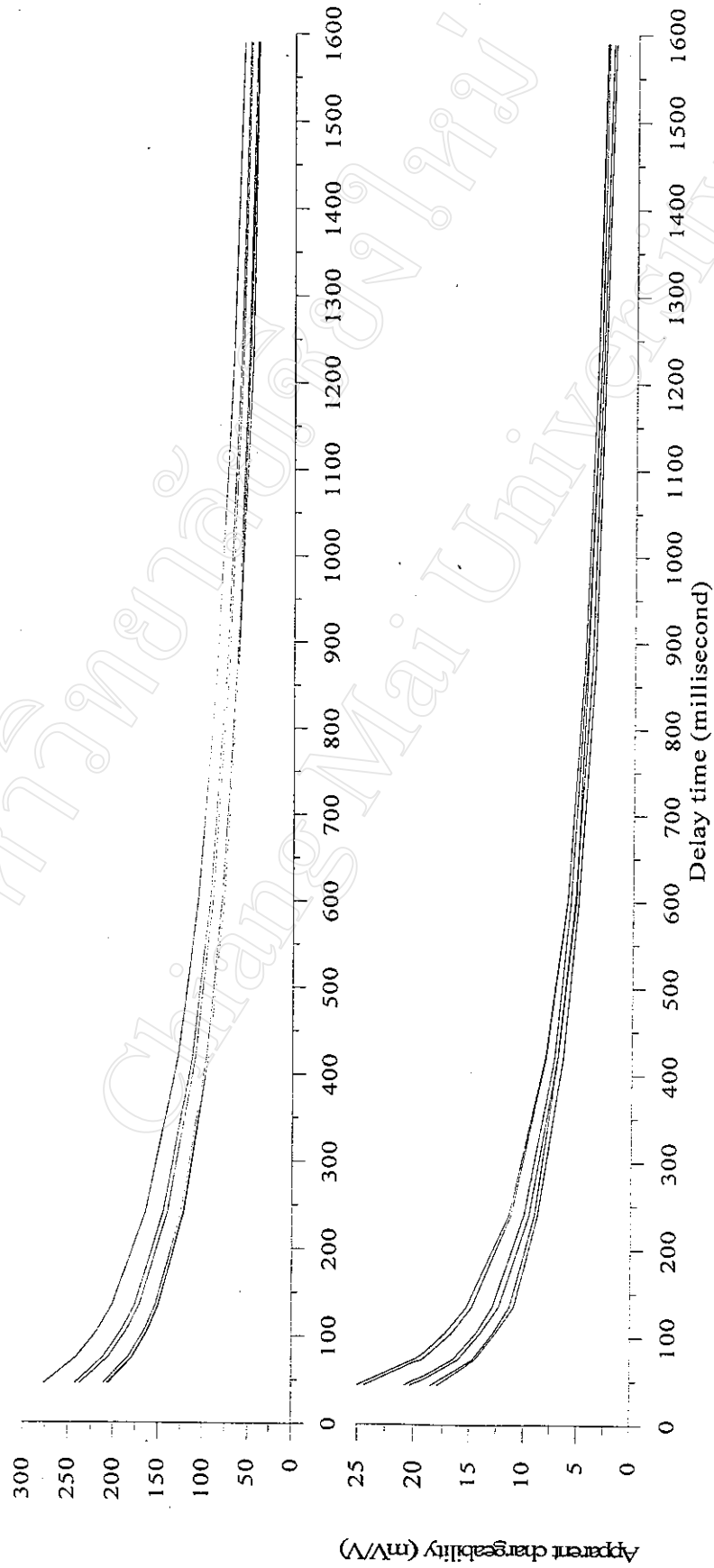


Figure 4.41 Top is decay curves of an anomalous zone and bottom is decay curves of non-anomalous zone of Mae Chong sulphide deposit. Array configuration is pole-dipole of 50 meter dipole separation.

The magnitude for non-anomalous decay curve is from about 10 millivolts per volt up to, not exceed, 35 millivolts per volt.

Anomalous zone is selected from area of low apparent resistivity and high apparent chargeability. Decay curves of this anomalous zone is shown in Figure 4.41 (upper), the magnitude of decay curve in early portion is very high compare to non-anomalous zone even in late portion. It can be easily separated out an anomalous zone from a non-anomalous zone by shape of the decay curve.

Figure 4.42 shows a combined decay curve plot of an anomalous, non-anomalous, and overshoot anomalous zones. It can be easily observed from the figure that the non-anomalous zone have very low amplitude, called a background value that is not exceed 50 milliseconds and have similar in shape. Anomalous decay curves have strongly high amplitude and change in the early time of their decay curve with the magnitude from 100 up to 300 milliseconds.

#### ***4.7.1.2 Khao Khi Nok graphite deposit***

Decay curves of non-anomalous zone are shown in Figure 4.43 (lower), shape of the decay curve is quite uniform and has nearly the same magnitude. Magnitude of the non-anomalous decay curve is very low, not exceed 20 millivolts per volt.

In an anomalous zone, the decay curves are shown in Figure 4.43 (upper). It can be clearly observed that, in the early portion, there is very strong negative electromagnetic coupling. Refer to the apparent chargeability plotting, topic 4.4.3, it is only negative induced polarization effect.

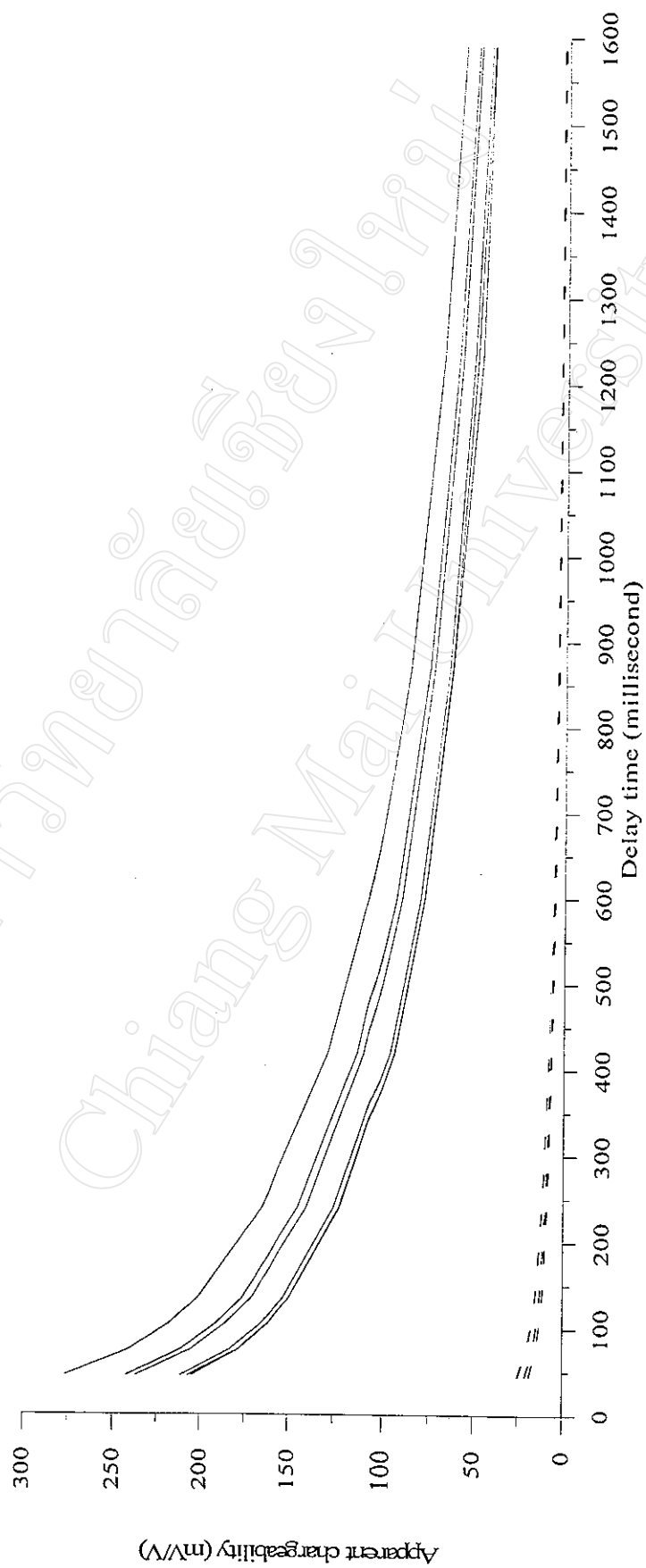


Figure 4.42 Combined plot of anomalous and non-anomalous zones of Mae Chong area.

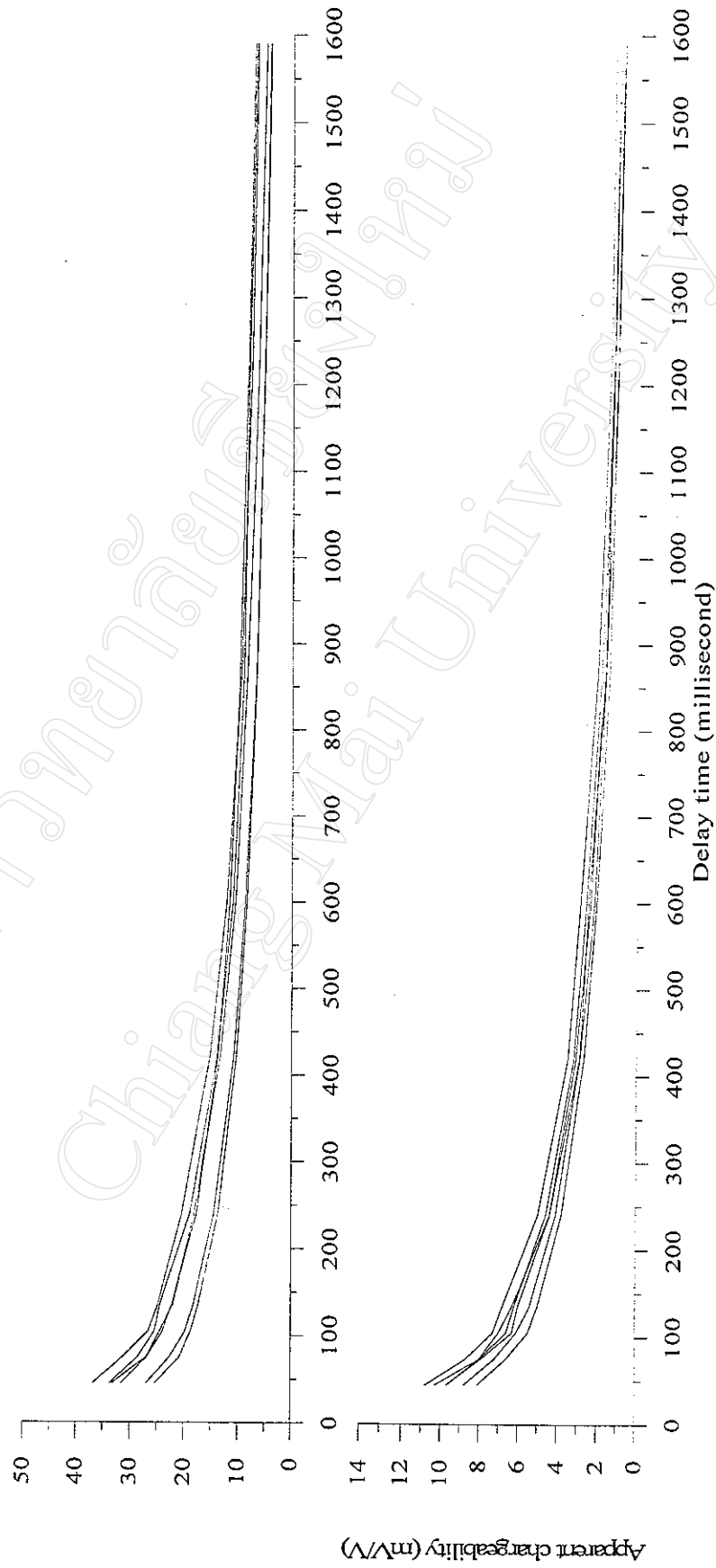


Figure 4.43 Top is decay curves of an anomalous zone and bottom is decay curves of non-anomalous zone of Khao Khi Nok graphite deposit. Array configuration is dipole-dipole of 10 meter dipole separation.

Figure 4.44 shows a combine plot of the non-anomalous and the anomalous decay curves that can be separated each other by this plot.

#### ***4.7.1.3 Pong Nok Gaew clay deposit***

Decay curves of a non-anomalous zone are shown in Figure 4.45 (lower). Shape of the decay curve is highly uniform with the change in magnitude not exceeds 40 millivolts per volt.

Decay curve of the anomalous zone are plotted in Figure 4.45 (upper). The magnitude of this zone is very high compare with the non-anomalous zone and there is some curve interferes by noise at the early time. Anomalous decay curve has the magnitude three time higher than the background decay curve in the early time.

Figure 4.46 shows a combine plot of these three kinds of decay curve. From the combined plot, the anomalous decay curves can be distinguished from the background decay curves.

#### ***4.7.1.4 Summary***

Figure 4.47 shows combined plot of the non-anomalous zone and the anomalous zone of sulphide, graphite, and clay in the study areas.

It shows that graphite has lowest background value than clay and sulphide is the highest background value. Background value of these minerals are not exceed 50 millivolts per volt.

In an anomaly portion, the upper part, sulphide still has the highest magnitude more than the other two. Decay curve of sulphide nearly uniform compare which of clay. Moreover, graphite decay curve has the lowest magnitude and rather uniform in shape and magnitude than clay.

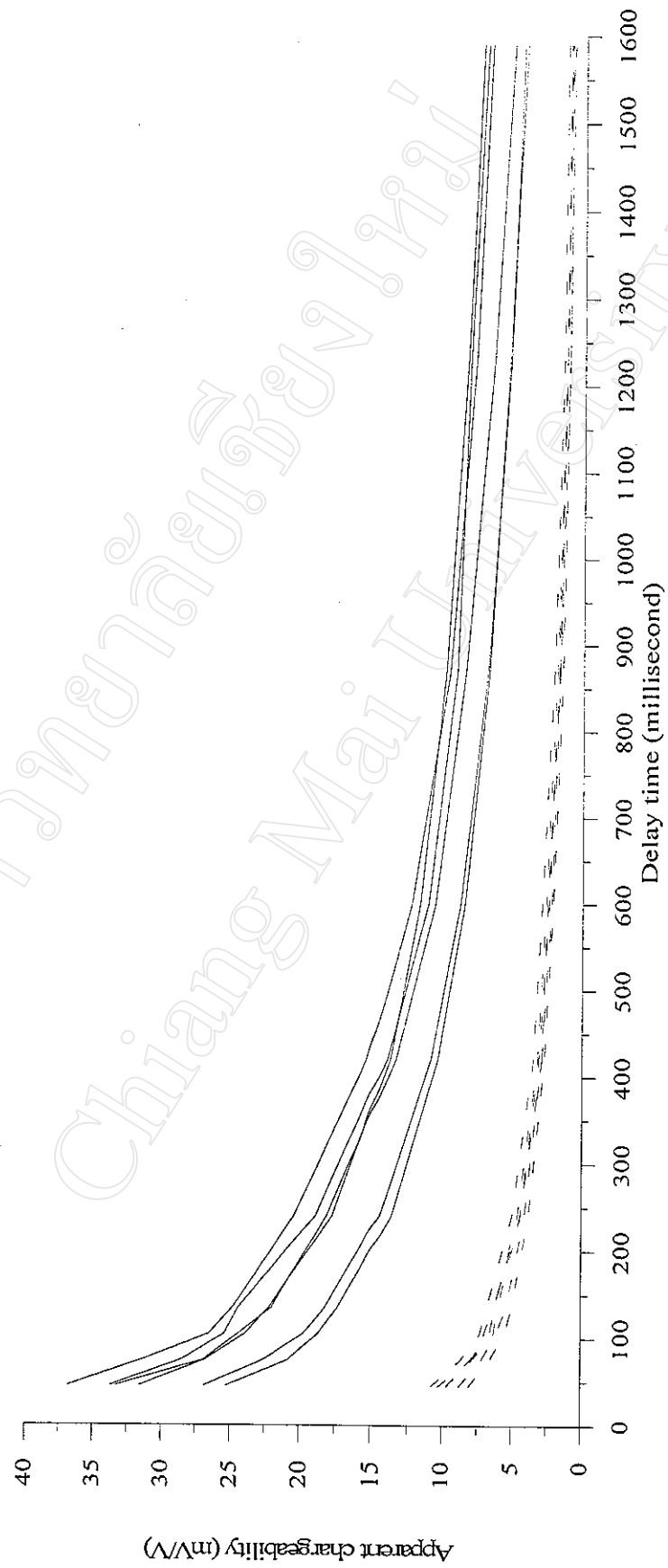


Figure 4.44 Combined plot of anomalous and non-anomalous zones of Khao Khi Nok area.

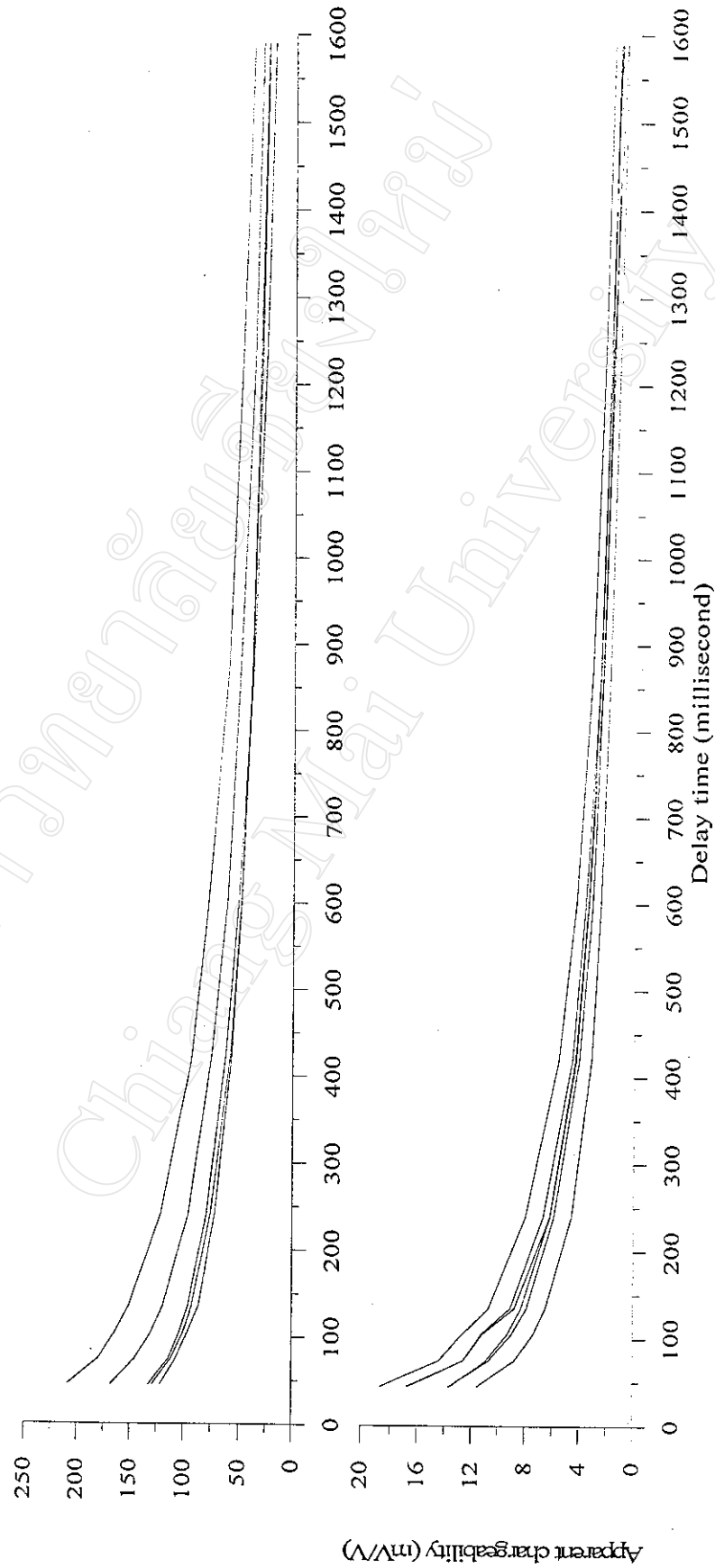


Figure 4.45 Top is decay curves of an anomalous zone and bottom is decay curves of non-anomalous zone of Pong Nok Gaew clays deposit. Array configuration is dipole-dipole of 10 meter dipole separation.

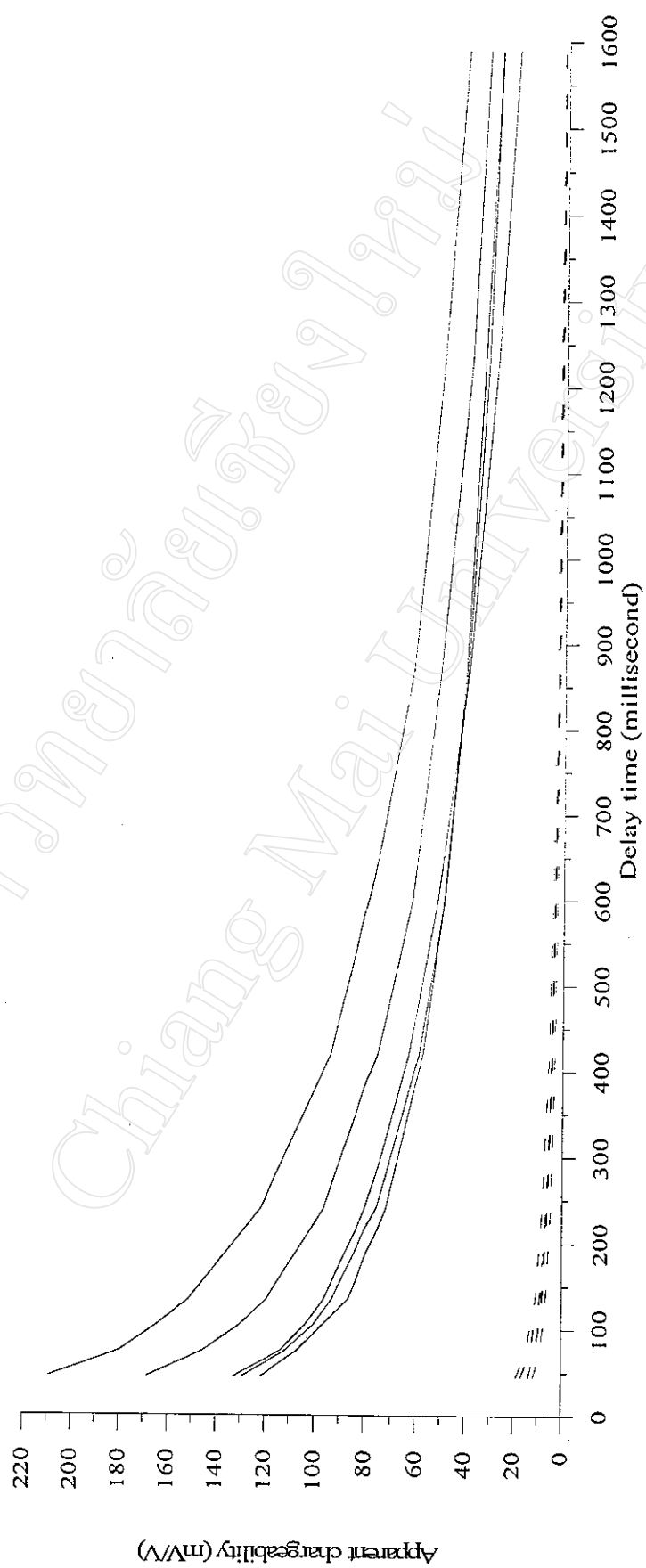


Figure 4.46 Combined plot of anomalous and non-anomalous zones of Pong Nok Gaew area.

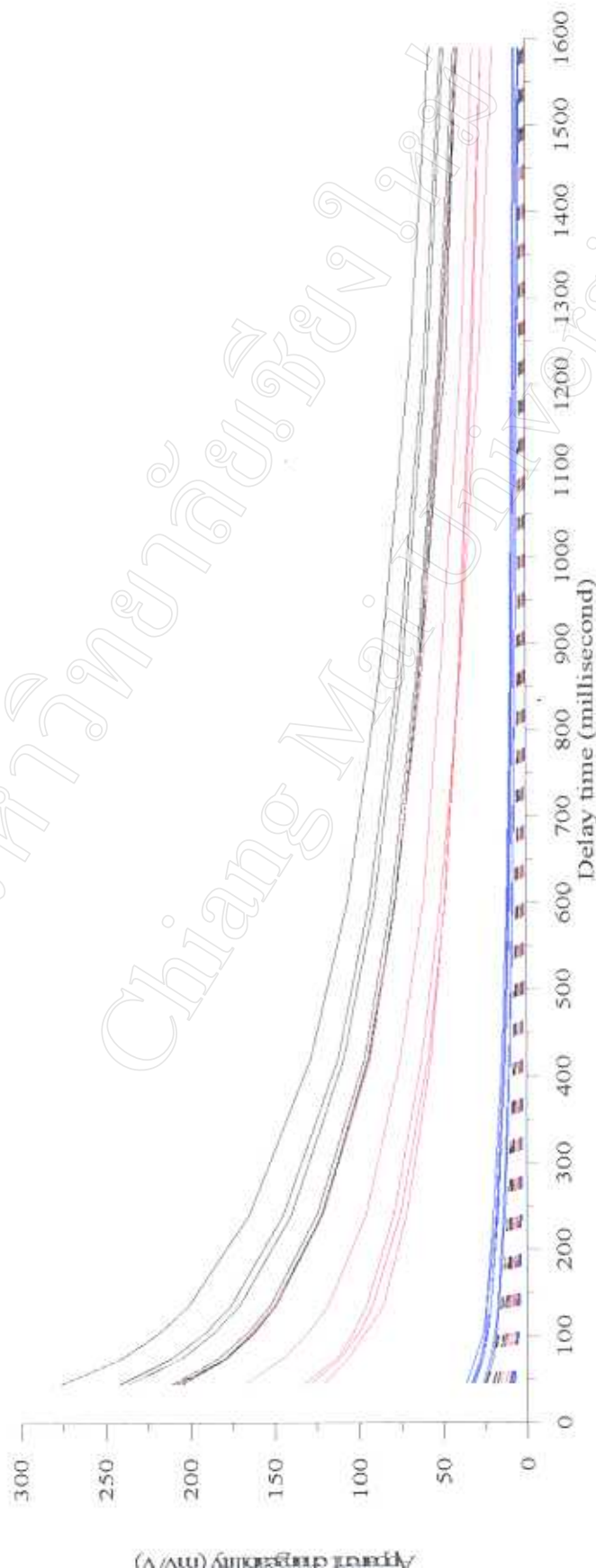


Figure 4.47 Combined plot of sulphide, graphite, and clays deposits of Mae Chong, Khao Khi Nok, and Pong Nok Gaew areas. Solid line represent anomalous decay curves; black of sulphide, blue of graphite, and red of clays. Dash line represent non-anomalous decay curves; black of sulphide, blue of graphite, and red of clays (Note: plot in linear-linear scale)

So that it can be concluded that sulphide and graphite has the uniform shape of decay curve and has distinctive magnitude that separate them out. While clay has strong variation in its shape of decay curve and also has strong variation in its magnitude. Decay curve of clay overlays between the decay curve of sulphide and graphite.

#### **4.7.2 Effect of survey parameter on decay curve**

Induced polarization data of Khao Khi Nok and Pong Nok Gaew were acquired with various parameters, except for Mae Chong where has only a single set of data. By this benefit, we can classified them into three groups of survey parameter as: (1) array configuration, (2) dipole separation, and (3) transmitting time duration of transmitter.

In this study, two kinds of array configuration are chosen because of their wide-spread used in the mineral exploration, there are pole-dipole and dipole-dipole arrays. Dipole separation of 10, 20, and 40 meters are selected because it can operate easily during the surveys operation. Last, transmitting time of the transmitter is chosen with 2 seconds and 4 seconds, generally use 2 seconds rather than 4 seconds because of the benefit of shorter time operation in each survey line. So that it can derives an effect of those parameter as the following section.

##### ***4.7.2.1 Effect of array configuration***

This section attempts to find out an effect of array configuration with shape of a decay curve. Theoretically, the pole-dipole and the dipole-dipole arrays are different in the measurement of an electric field over the ground. By this reason, it seems that the decay curve should be different in magnitude rather than its shape.

Figure 4.48 shows the relationship of the pole-dipole and the dipole-dipole arrays of dipole separation 40 meters at Khao Khi Nok graphite deposit. Both array configurations are surveyed with 2 seconds transmitting time. Black solid lines represent decay curve of the pole-dipole array and blue solid lines represent the dipole-dipole array. The decay curves of both arrays are quite similar in their shape. This figure points out that the change in array configuration is less effective on shape of the decay curve.

It can be summarized that the array configuration of the pole-dipole and the dipole-dipole arrays gave similar shape of the responded decay curve.

#### ***4.7.2.2 Effect of dipole separation***

In fact, the change in dipole separation means that the depth of investigation is changed, so that this effect should not be involved with the decay curve characteristics. However, this section attempts to observe the change in decay shape of a different array size by neglecting its skin depth.

Figure 4.49 shows the comparison of different dipole separation, the dipole separation are of 10 meter (black color) and 20 meter (blue color). The decay curves are selected from Khao Khi Nok graphite deposit. The array configuration is the pole-dipole array configuration. The figure shows that decay shape of both 10 meters and 20 meters dipole separation is quite similar.

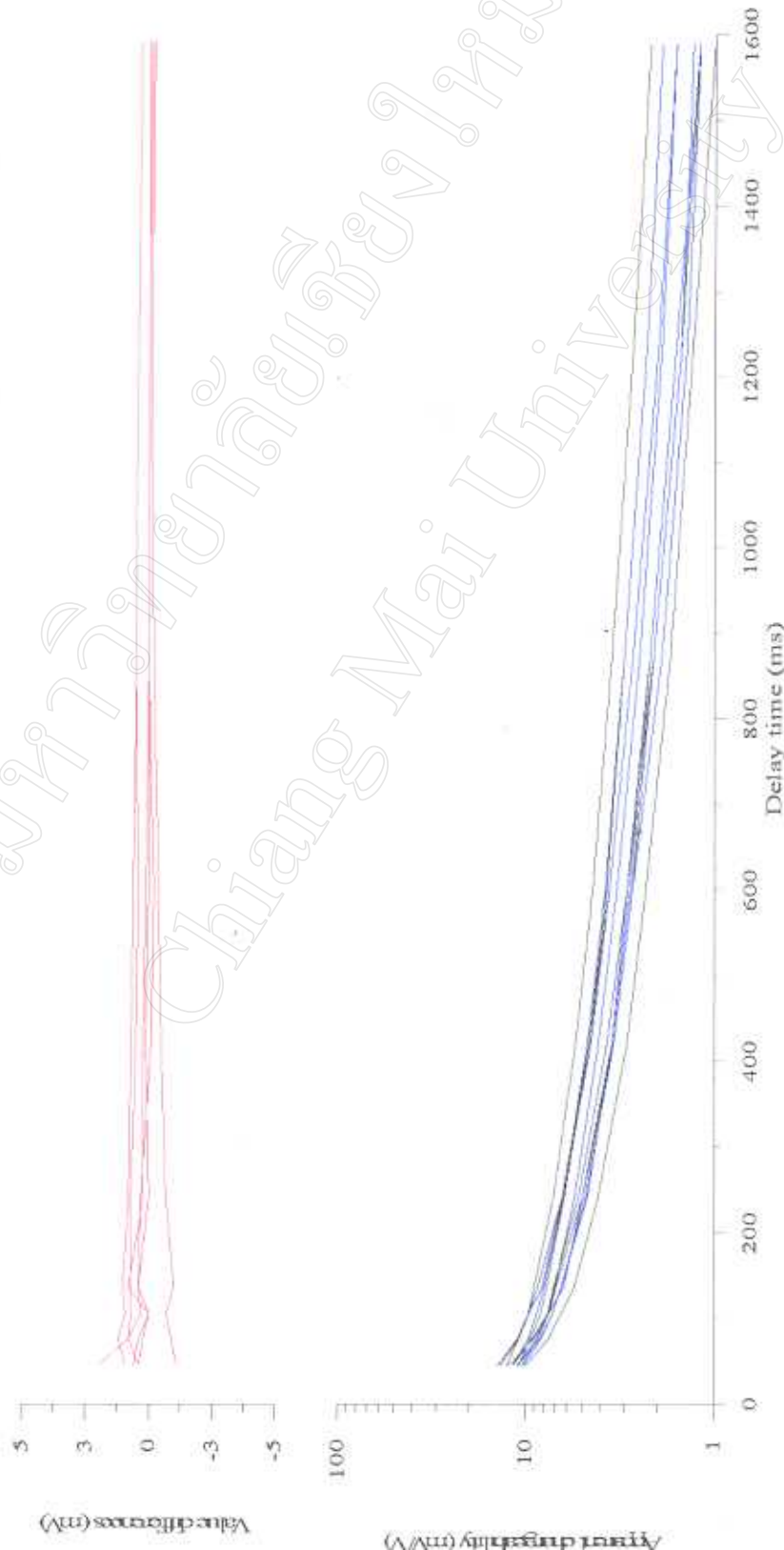


Figure 4.48 Comparison of array configuration of Khao Khi Nok graphite deposit. Array are pole-dipole and dipole-dipole of 40 meter dipole separation.

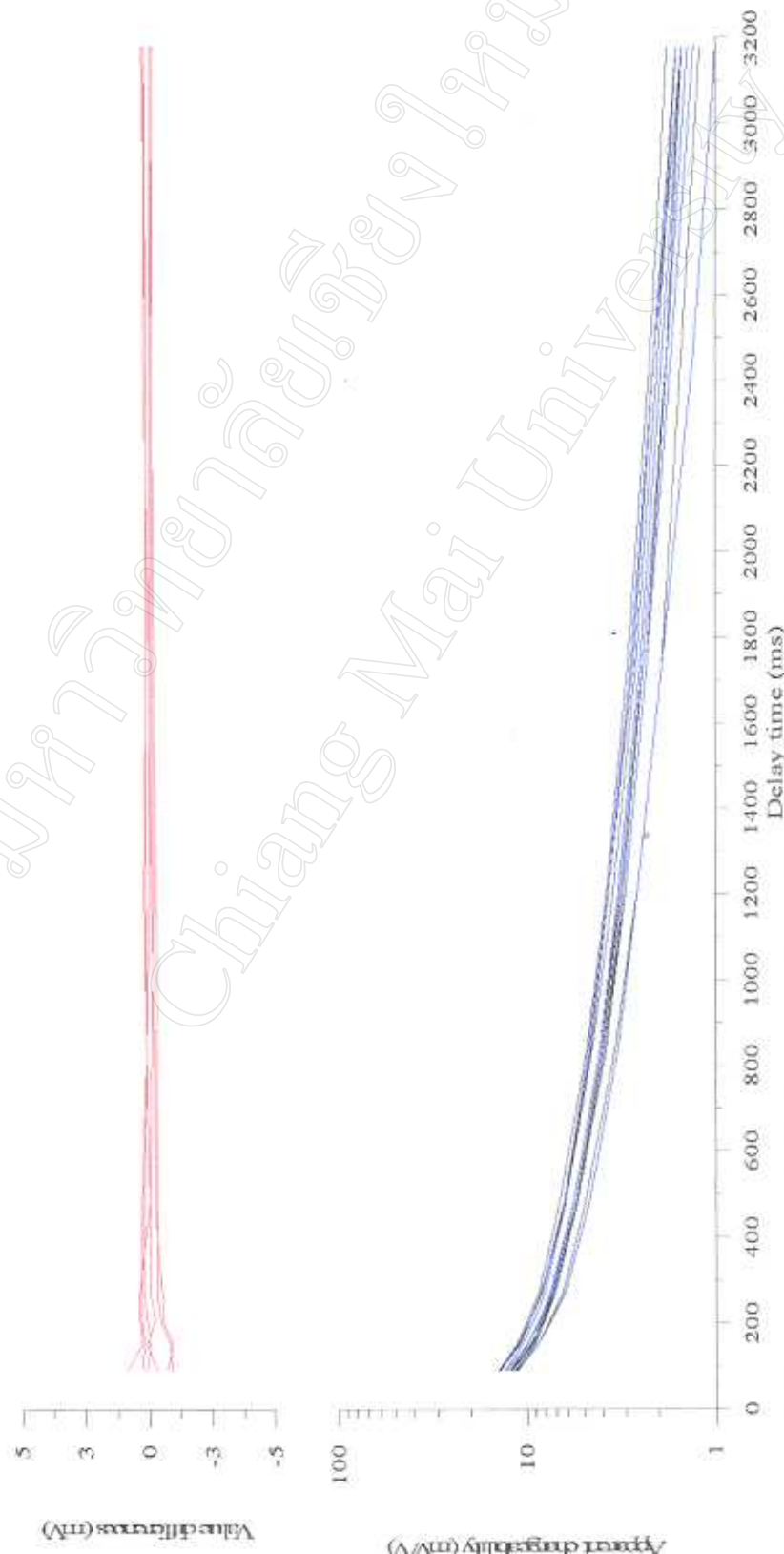


Figure 4.49 Comparison of dipole separation of Pong Nok Gaew clays deposit. Dipole separation are 10 and 20 meter of pole-dipole array.

It can be summarized that the change in dipole separation is not affect too much on decay shape but it seems that the magnitude of the decay curve changed only at the early time interval.

#### ***4.7.2.3 Effect of transmitting time duration***

From the theory of induced polarization effect, time duration of emitted current seem to be a major source of measured potential. While short transmitting time is applied, a polarization effect cannot be completely established since the measured potential should be lower than an applying of long transmitting time duration.

Figure 4.50 shows the relationship of decay shape and transmitting time duration. Black solid lines represent the dipole-dipole array of 10 meters dipole separation and blue solid lines represent the dipole-dipole array with 20 meters dipole separation. Both set of decay curves are of 2 seconds transmitting time duration. Red solid lines represent the pole-dipole array of 10 meters dipole separation and pink solid lines represent the pole-dipole array of 20 meters dipole separation. Both sets are of 4 seconds transmitting time duration. From the figure, it can be observed the differences in decay shape while the transmitting time duration is changed.

It can be summarized that length of transmitting time give different shape of decay curve. The magnitude of the decay curve slowly decreases whereas the transmitting time is longer.

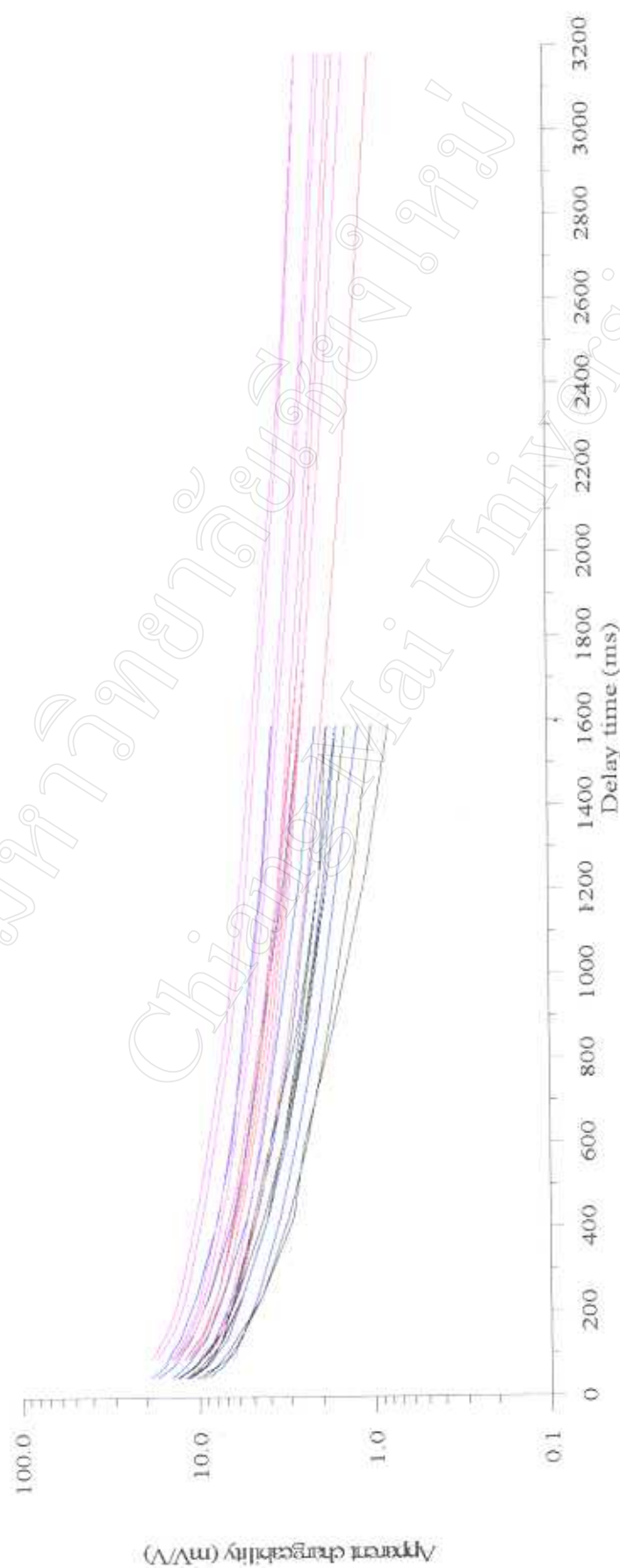


Figure 4.50 Comparison of transmitting time duration of Khao Khi Nok graphite deposit. Transmitting time are 2 second, shorter, and 4 second, longer.

#### 4.7.2.4 Summary

It can be concluded that the decay curve of each minerals differ with slightly variation. It may be occurs from the variation in grain size of mineral and percent of mineral accumulation. The effect of different array used in the prospecting and the effect of changing dipole separation are not influence on shape of decay curve. In case of transmitting time duration, this parameter has strongly effect on shape of the decay curve, while increases transmitting time duration the decay curve slowly decrease in the later. Thus it should be noted that if time constant of decay curve is used in order for the purpose of mineral discrimination, i.e. *Pelton et. al.* (1978), the data must be acquired by the same survey parameter.

### 4.8 Relationship of resistivity and chargeability parameters

This section attempts to generalize the relationship between apparent resistivity and apparent chargeability parameters of those three mineralizations. In spite of the relationship of decay characteristic that varies considerably in apparent chargeability more than that of apparent resistivity. Thus, their relationship should be differentiate in term of the apparent chargeability rather than the apparent resistivity. Subsequently, this relationship might be one of localize characteristic of each mineralization, individually.

By plotting apparent resistivity,  $\rho$ , in x-axis and apparent chargeability,  $M$ , in y-axis, the relationship of these parameters can be obtained by drawing a trend line overlays a plot. By observing the characteristic of the apparent chargeability and the apparent resistivity,

in both anomalous zone and non-anomalous zone, their relationship can be represented by the negative linear relationship. So that the trend line is generated by  $M = ap + b$ , the linear relationship formula. The examples of the plot are shown in Figure 4.51, 4.52, and 4.53 for the pseudodepth of  $n=1$  of Mae Chong, Khao Khi Nok, and Pong Nok Gaew areas, respectively.

The linear trend line parameters,  $a$  and  $b$ , are calculated separately with each  $n$ -pseudodepth and, moreover, separated in each time slice of the decay curve. Consequently, those parameters can be summarized in Table 4.6 for Mae Chong area, in Table 4.7 for Khao Khi Nok area, and in Table 4.8 for Pong Nok Gaew area.

Thereafter, both  $a$  and  $b$  parameters of every  $n$ -pseudodepth are separately plotted for three mineralizations. These parameters are plotted in Figure 4.54 for Mae Chong, in Figure 4.55 for Khao Khi Nok, and in Figure 4.56 for Pong Nok Gaew.

### **Summary**

For Mae Chong area, it can be observed that, for slice 1 to 10, there is a good relationship of the apparent resistivity and the apparent chargeability. At low apparent resistivity zone, the apparent chargeability is strongly high, meanwhile, beside that zone this parameter are uniformly low. The anomalous zone can be identified by the apparent resistivity value lower than about 100 ohm-meter that there is more higher apparent chargeability value. While the non-anomalous zone is identified by the apparent resistivity higher than 100 ohm-meter, the apparent chargeability is not changed significantly.

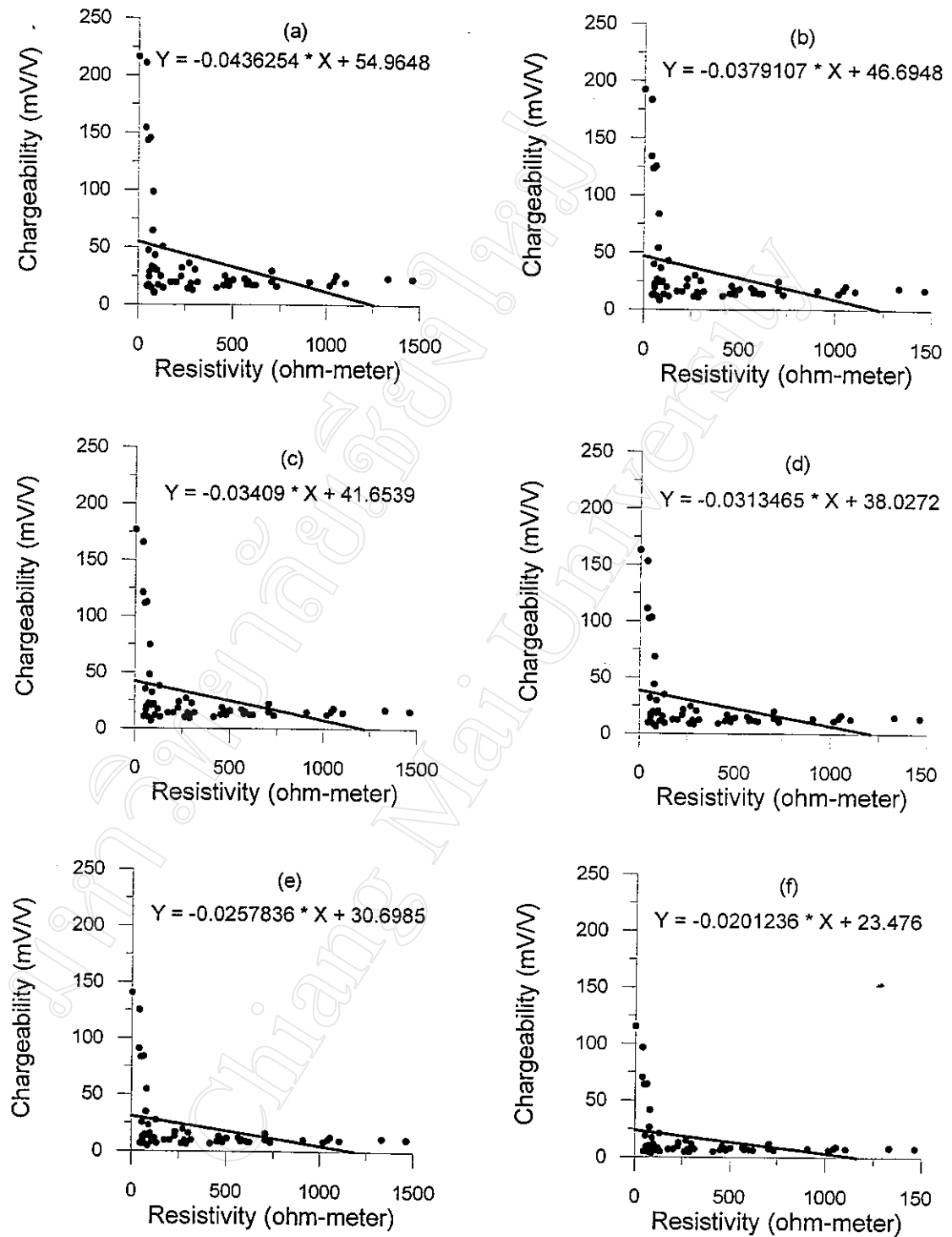
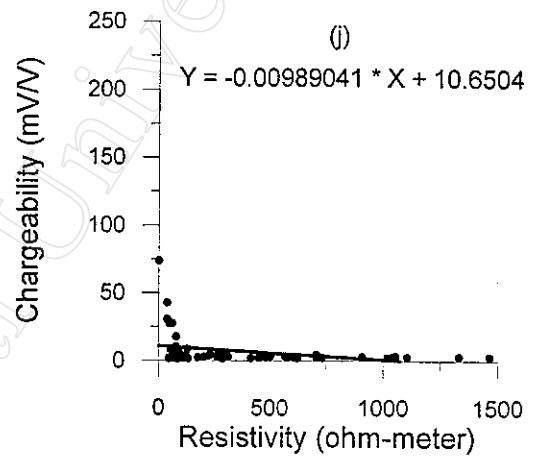
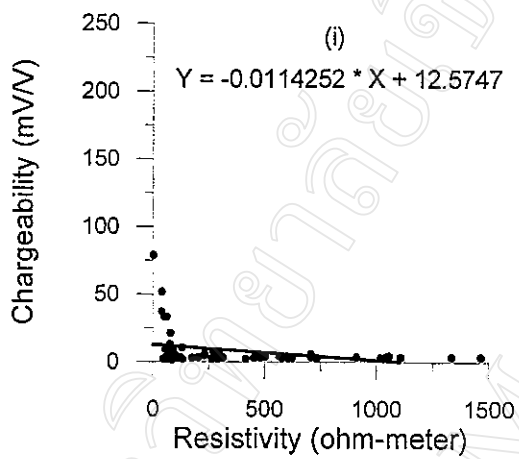
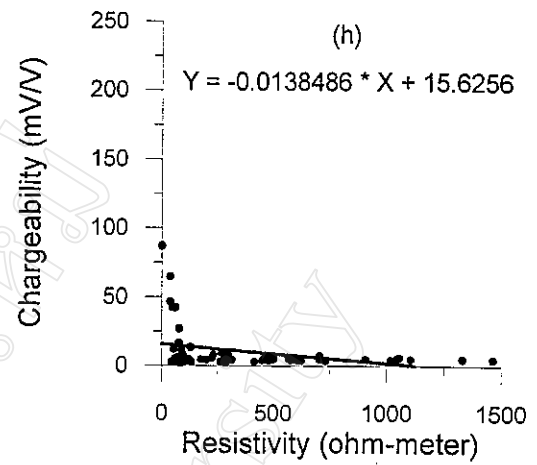
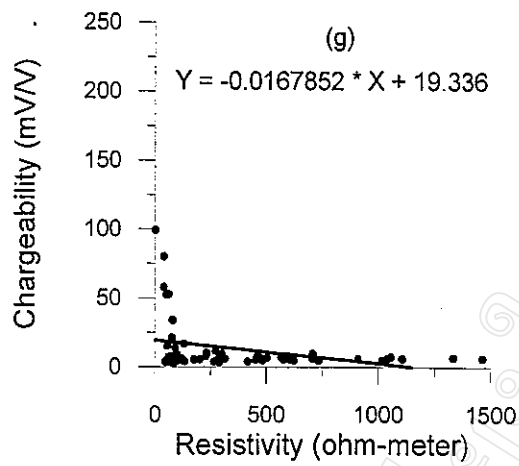


Figure 4.51 Graphs of apparent resistivity and apparent chargeability for  $n=1$  of Mae Chong sulphide deposit.

Plots are of slice (a) 1st, (b) 2nd, (c) 3rd, (d) 4th, (e) 5th, (f) 6th, (g) 7th, (h) 8th, (i) 9th, and (j) 10th.



(continued)

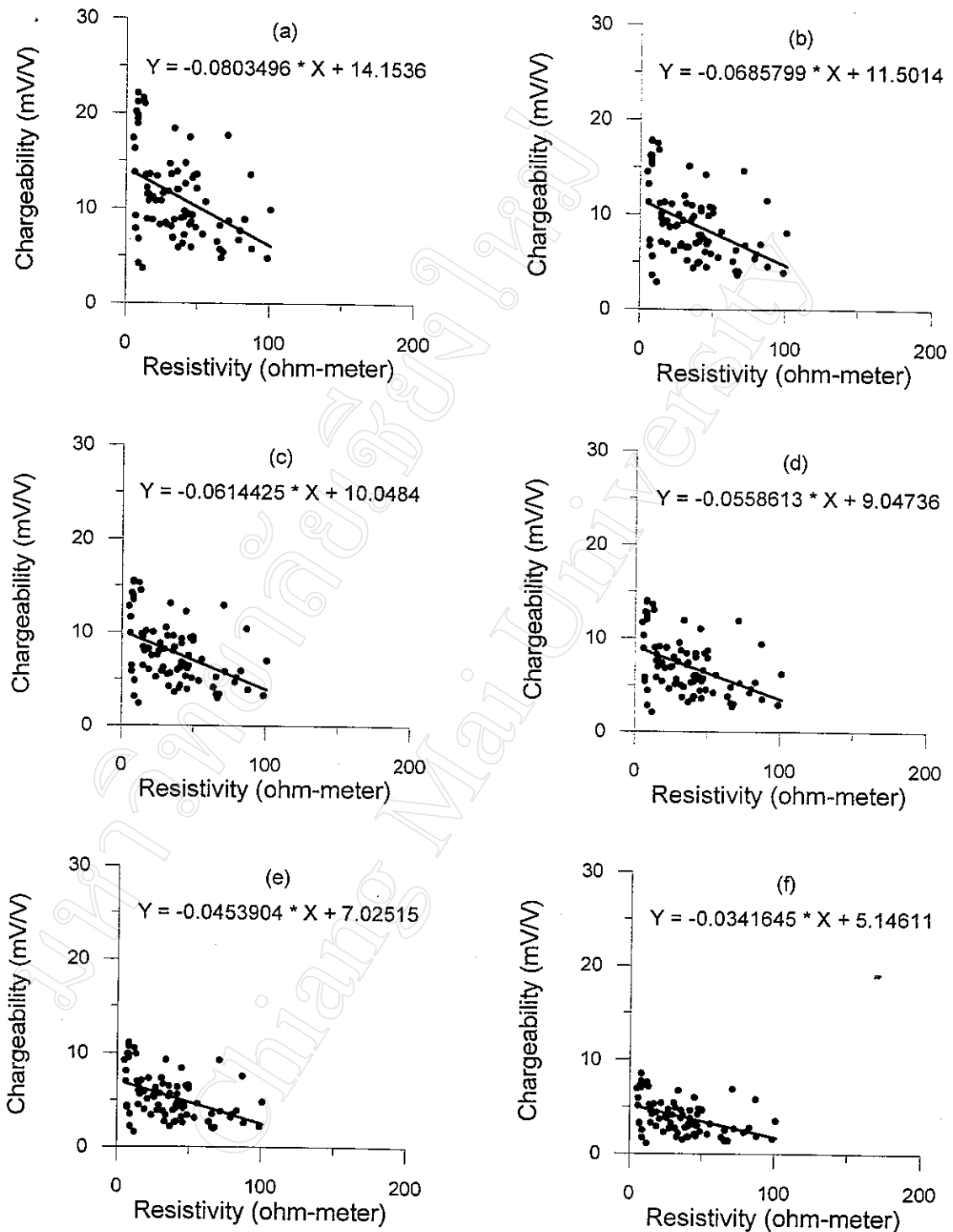
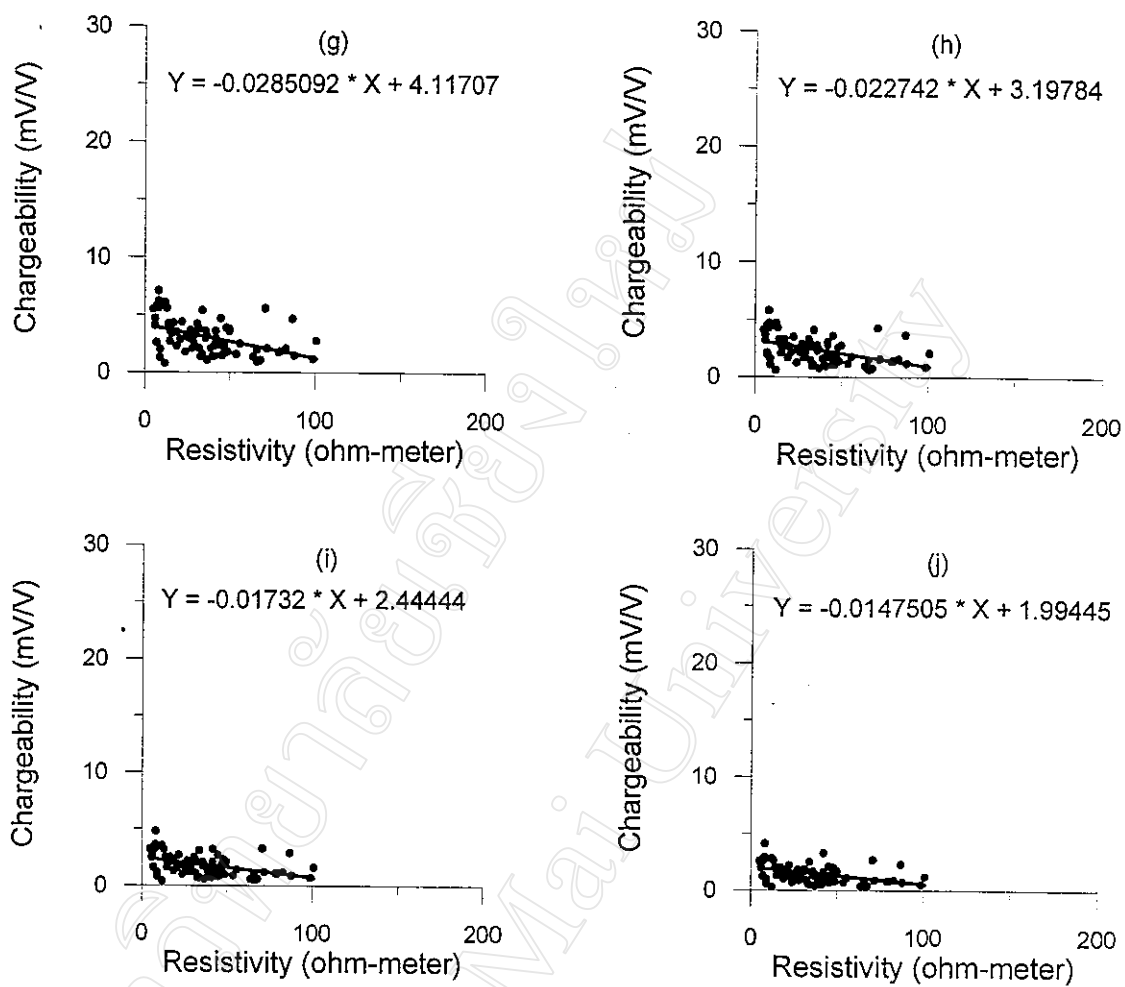


Figure 4.52 Graphs of apparent resistivity and apparent chargeability for  $n=1$  of Khao Khi Nok graphite deposit.

Plots are of slice (a) 1st, (b) 2nd, (c) 3rd, (d) 4th, (e) 5th, (f) 6th, (g) 7th, (h) 8th, (i) 9th, and (j) 10th.



(continued)

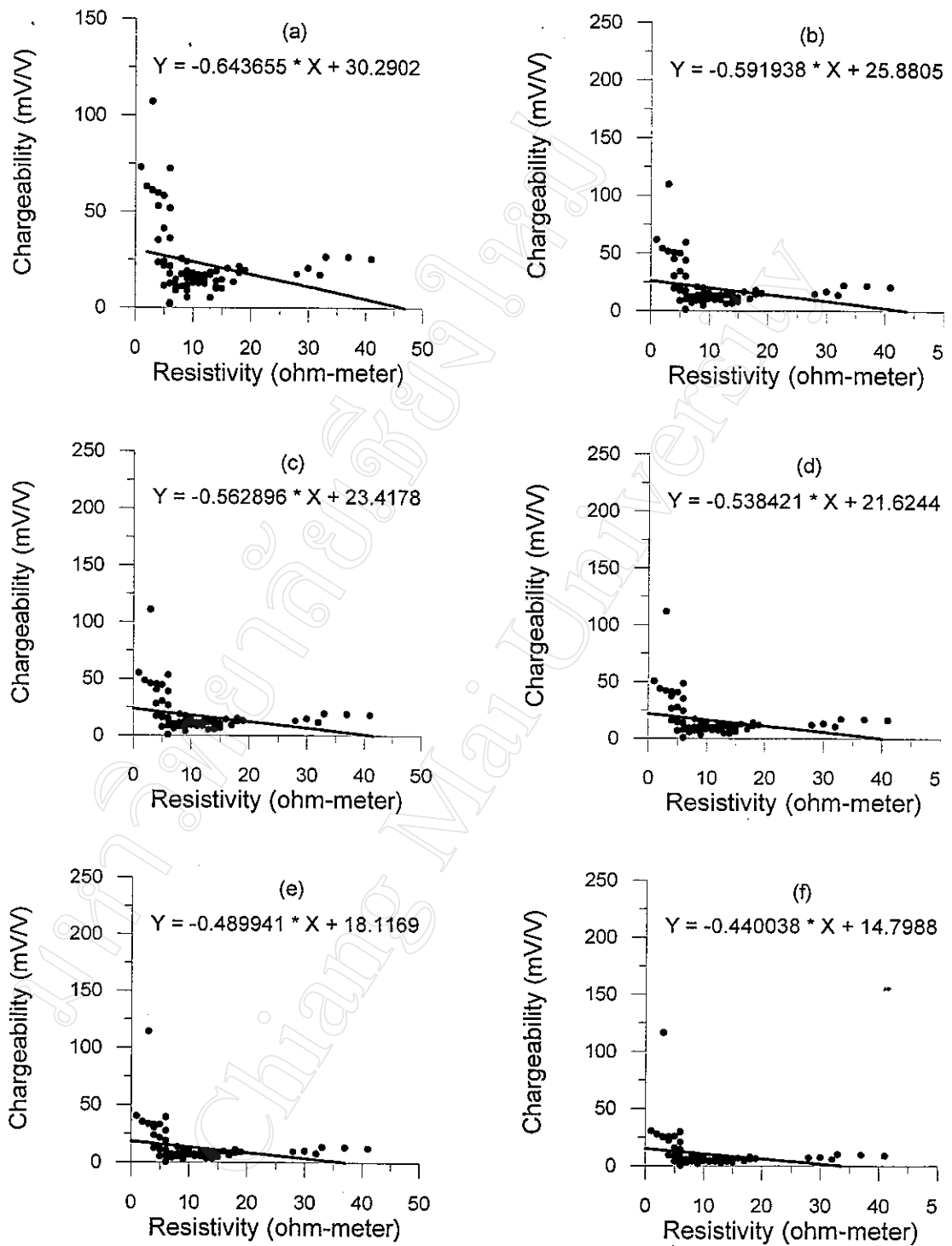
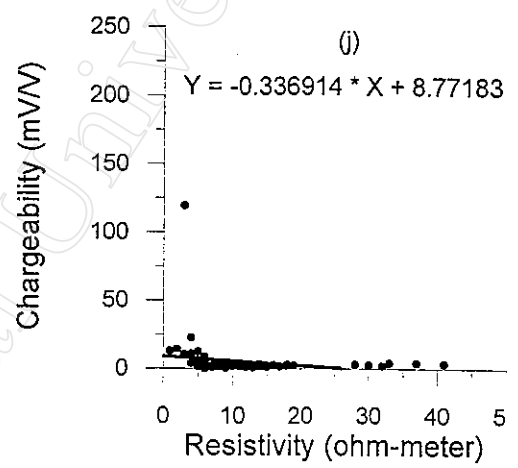
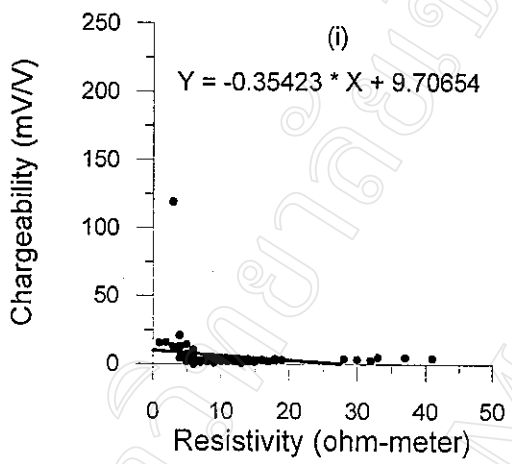
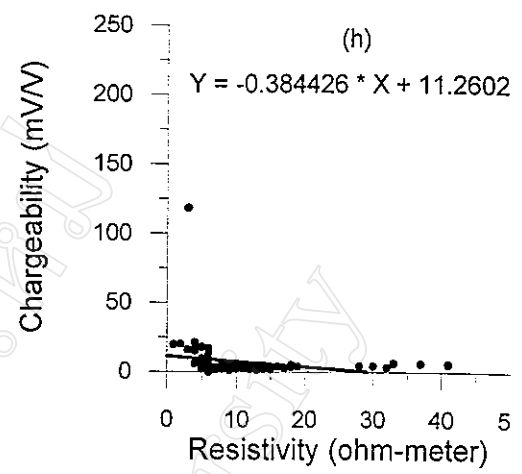
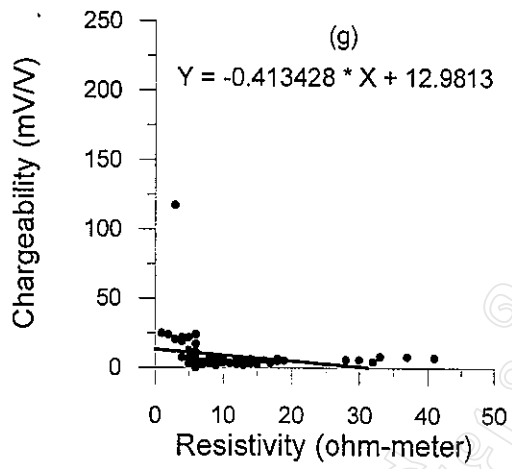


Figure 4.53 Graphs of apparent resistivity and apparent chargeability for  $n=1$  of Mae Chong sulphide deposit.

Plots are of slice (a) 1st, (b) 2nd, (c) 3rd, (d) 4th, (e) 5th, (f) 6th, (g) 7th, (h) 8th, (i) 9th, and (j) 10th.



(continued)



Figure 4.54 Plots of fitted parameters of Mae Chong sulphide deposit. Parameters plotted are (a) a and (b) b parameters.

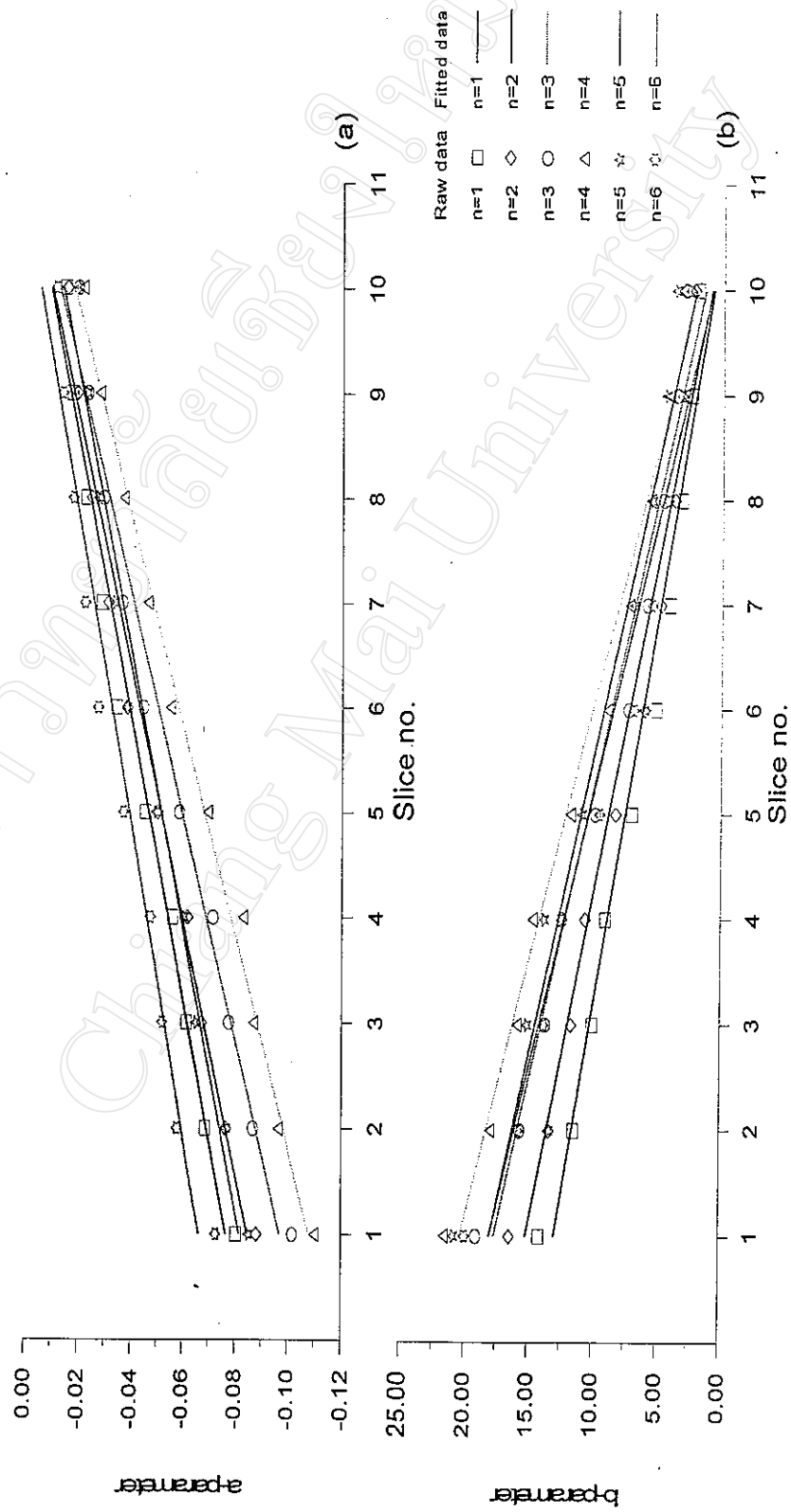


Figure 4.55 Plots of fitted parameters of Khao Khi Nok graphite deposit. Parameters plot are (a) a and (b) b parameters

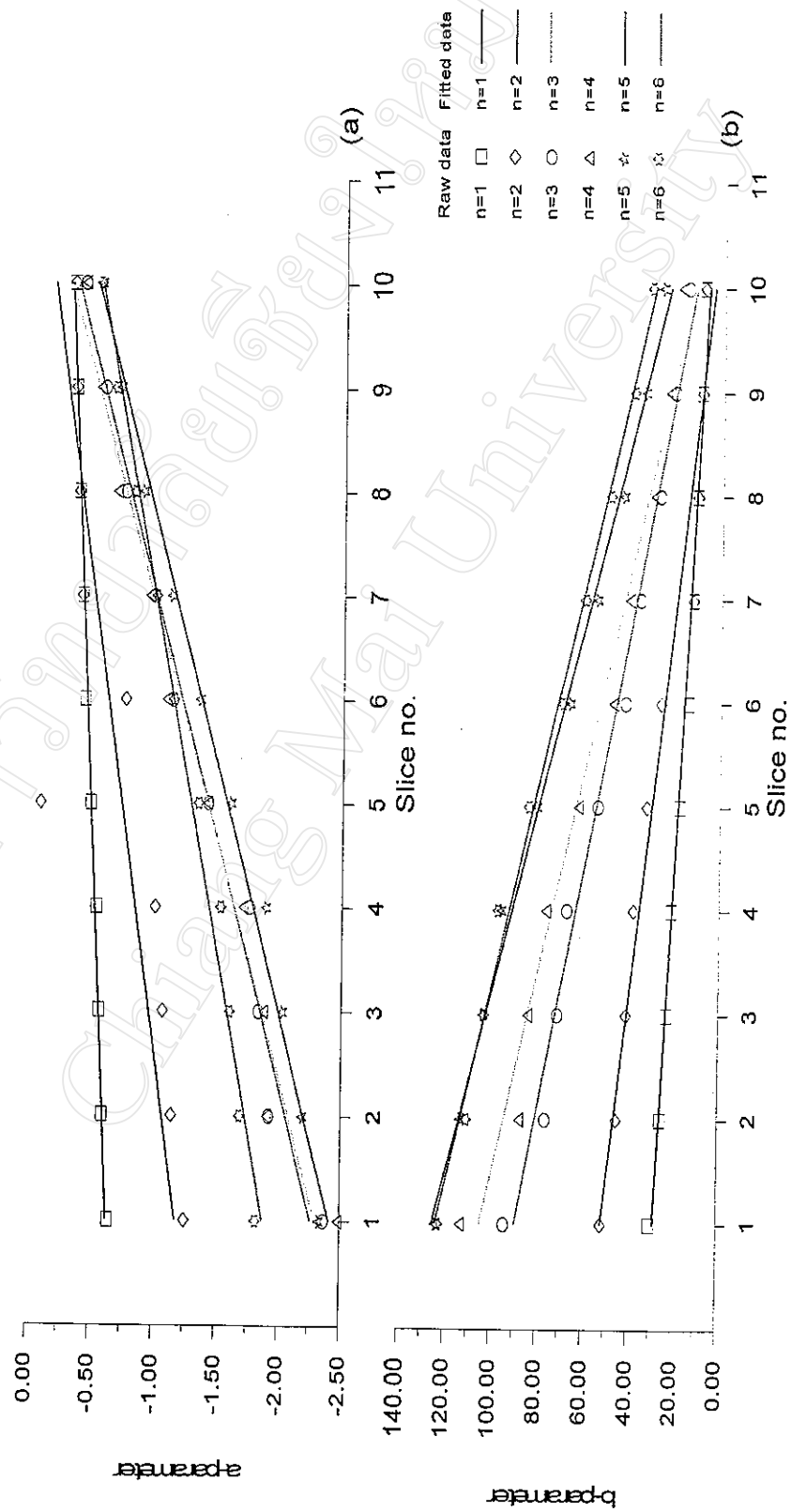


Figure 4.56 Plots of fitted parameters of Pong Nok Gaew clays deposit. Parameters plot are (a) a and (b) b parameters.

Table 4.6 Calculated parameters, a and b, of Mae Chong area.

slice	a(n=1)	a(n=2)	a(n=3)	a(n=4)	a(n=5)	a(n=6)	b(n=1)	b(n=2)	b(n=3)	b(n=4)	b(n=5)	b(n=6)
1	-0.043625	-0.035200	-0.046342	-0.063005	-0.054881	-0.046439	54.9648	53.8347	60.9863	71.0094	71.052	71.0095
2	-0.037910	-0.030596	-0.039865	-0.054073	-0.048427	-0.039837	46.6948	45.8072	51.9246	60.2883	59.7023	59.9169
3	-0.03409	-0.027581	-0.035811	-0.057230	-0.041932	-0.03495	41.6539	40.8264	46.3598	59.7738	53.4444	52.9045
4	-0.031346	-0.024447	-0.033147	-0.044846	-0.038752	-0.031978	38.0272	37.1275	42.5672	49.3341	48.9428	48.3201
5	-0.025783	-0.020493	-0.016936	-0.029335	-0.031841	-0.026031	30.6985	29.8268	33.3706	40.5494	39.4553	38.6404
6	-0.020123	-0.015877	-0.020824	-0.027622	-0.024437	-0.019879	23.476	22.7417	25.9919	30.3866	29.9746	29.3513
7	-0.016785	-0.013035	-0.017285	-0.023173	-0.020451	-0.018437	19.336	18.5201	21.4041	24.7453	24.6813	25.1094
8	-0.013848	-0.010415	-0.013836	-0.01856	-0.016040	-0.014927	15.6256	14.6962	17.002	19.6509	19.3388	20.0108
9	-0.011425	-8.07E-02	-0.010862	-0.014681	-0.012221	-0.012132	12.5747	11.3811	13.3022	15.3655	14.8474	15.8797
10	-9.89E-02	-6.74E-02	-8.84E-02	-0.012018	-9.84E-02	-0.010373	10.6504	9.38791	10.8646	12.5413	12.0715	13.2711

Table 4.7 Calculated parameters, a and b, of Khao Khi Nok area.

slice	a(n=1)	a(n=2)	a(n=3)	a(n=4)	a(n=5)	a(n=6)	b(n=1)	b(n=2)	b(n=3)	b(n=4)	b(n=5)	b(n=6)
1	-0.080346	-0.088099	-0.101898	-0.11007	-0.084946	-0.072655	14.1536	16.4294	19.0897	21.562	20.8306	19.9723
2	-0.068579	-0.076384	-0.086628	-0.096271	-0.076384	-0.057705	11.5014	13.4236	15.6445	17.9856	13.4236	15.7729
3	-0.061442	-0.067219	-0.077453	-0.086748	-0.065027	-0.051880	10.0484	11.715	13.7282	15.8716	15.1112	13.8546
4	-0.055861	-0.061857	-0.071376	-0.082622	-0.060515	-0.047252	9.04736	10.628	12.4736	14.7015	13.8093	12.4427
5	-0.045390	-0.049985	-0.058497	-0.069348	-0.049350	-0.036849	7.02515	8.27526	9.85549	11.8008	10.9111	9.53188
6	-0.034164	-0.038279	-0.044472	-0.054811	-0.038279	-0.027203	5.14611	6.09137	7.31019	8.92172	6.09137	6.91234
7	-0.028509	-0.030994	-0.036258	-0.046095	-0.033428	-0.022223	4.11707	4.85135	5.88251	7.26686	6.88482	5.51788
8	-0.022742	-0.02466	-0.029115	-0.036767	-0.027146	-0.017783	3.19784	3.76892	4.6422	5.65079	5.52771	4.29574
9	-0.01732	-0.019147	-0.023124	-0.027634	-0.0222908	-0.013714	2.44444	2.85049	3.60908	4.21732	4.4631	3.27563
10	-0.014750	-0.015454	-0.019536	-0.021275	-0.019835	-0.011317	1.99445	2.27362	2.98354	3.26217	3.7448	2.63536

Table 4.8 Calculated parameters, a and b, of Pong Nok Gaew area.

slice	a(n=1)	a(n=2)	a(n=3)	a(n=4)	a(n=5)	a(n=6)	b(n=1)	b(n=2)	b(n=3)	b(n=4)	b(n=5)	b(n=6)
1	-0.643655	-1.25347	-2.36998	-2.48327	-2.33498	-1.81693	30.2902	51.7015	94.0601	112.971	123.566	122.581
2	-0.591938	-1.14174	-1.92058	-1.9044	-2.19678	-1.68446	25.8805	45.2725	76.3493	87.7017	113.221	110.796
3	-0.562896	-1.06836	-1.83125	-1.87352	-2.03038	-1.60195	23.4178	41.3823	71.3507	84.1898	103.624	103.445
4	-0.538421	-1.00484	-1.75888	-1.70448	-1.89041	-1.52654	21.6244	38.4364	67.6186	76.4941	95.9973	97.5435
5	-0.489941	-0.089283	-1.42432	-1.41733	-1.60596	-1.34436	18.1169	32.8989	54.4799	63.0119	80.8043	84.337
6	-0.440038	-0.760612	-1.13602	-1.08626	-1.35337	-1.13846	14.7988	26.9967	42.8266	48.0745	66.8085	70.0274
7	-0.413428	-0.413428	-0.980762	-0.947422	-1.12228	-0.999551	12.9813	12.9813	36.5349	41.3845	55.3639	60.8962
8	-0.384426	-0.384426	-0.752466	-0.683658	-0.894643	-0.826638	11.2602	11.2602	28.1895	30.3886	44.2894	50.0312
9	-0.35423	-0.35423	-0.583777	-0.548916	-0.70837	-0.667501	9.70654	9.70654	21.836	24.2479	34.8498	40.0929
10	-0.336914	-0.336914	-0.420128	-0.426428	-0.553059	-0.543224	8.77183	8.77183	16.0527	18.9707	27.3106	32.5115

For Khao Khi Nok area, both parameters,  $a$  and  $b$ , are uniformly distribute throughout this study area. It is distinctly differ from Mae Chong and Pong Nok Gaew areas in case of the distribution of those parameter. The anomalous zone cannot identify from non-anomalous zone by this relationship because there is not a contact point, the magnitude is abruptly changed, that separate such two zones apart.

For Pong Nok Gaew area, this area has nearly the same relationship with Mae Chong area. The lower apparent resistivity of about 5 ohm-meter is steeply changed with the high apparent chargeability. In contrary, the more higher apparent resistivity than 5 ohm-meter is not considerably changed with the low apparent chargeability. However, in the later slice, this relationship can be observed separately. The anomalous zone is the zone of low apparent resistivity, lower than 5 ohm-meter, that comprises with the increased apparent chargeability. In the other hand, the non-anomalous zone is the high apparent resistivity zone that has not changed significantly in the apparent chargeability and the apparent resistivity.

In case of parameter  $a$ , the slope of Mae Chong sulphide deposit is about 0.003 to 0.006 millisiemens with an average value of 0.004 millisiemens . While the slope of Khao Khi Nok graphite deposit is about 0.007 to 0.010 millisiemens with average value of 0.008 millisiemens . Whereas the slope of Pong Nok Gaew clay deposit is about 0.340 to 0.229 millisiemens with average value of 0.205 millisiemens .

For parameter  $b$ , the slope of Mae Chong sulphide deposit is about -4.924 to -6.553 millivolts per volt with an average value of -5.816 millivolts per volt. While the slope of Khao Khi Nok graphite deposit is about -1.351 to -2.033 millivolts per volt with average value of -1.762 millivolts per volt. Whereas the slope of Pong Nok Gaew clay deposit is about -2.391 to -10.695 millivolts per volt with an average value of -7.831 millivolts per volt.

#### **4.9 Conclusion of results**

This part summarizes the result of analyzing technique and its efficiency when applied to the other areas that might be related in the geological conditions. It can be concluded herein as:

(1) Sulphide mineralization gave high responses in magnitude of an apparent chargeability, more than 5 up to 107 millivolts per volt, with low apparent resistivity, below 100 down to 2 ohm-meter. Metal factor in an anomalous zone is highest at 62,000. In case of Cole-Cole parameter, a chargeability ( $M$ ) is not meaningful throughout this study area. While frequency dependent is about 0.23 for background and about 0.33 for anomalous zone. Time constant is about 5 milliseconds for a background value and about 20 milliseconds for an anomalous zone.

(2) Graphite mineralization gave low responses in a magnitude of an apparent chargeability due to its low apparent resistivity. Electrical charges which accumulate at each end of mineral grain while current on-time will be discharged when electric current corrupted, graphite has very low resistivity so that the electrical charges can migrate rapidly

through its grain. An apparent chargeability of graphite is more than 5 millivolts per volt and reach the maximum at 32 millivolts per volt comprises with its low apparent resistivity that lower than 5 ohm-meter. Meanwhile in the non-mineralized zone, the apparent chargeability is lower than 10 millivolts per volt down to 1 millivolts per volt, whereas the apparent resistivity is more higher than 30 ohm-meter up to 250 ohm-meter. The metal factor in the mineralized zone is risen up to 15,000. The frequency dependent is 0.23 for the non-mineralized zone and 0.33 for the anomalous body. Then, the time constant is 5 milliseconds for the background and increases up to 20 milliseconds in the mineralized zone.

(3) Clay mineralization gave high responses in the magnitude of the apparent chargeability, nearly the same as of sulphide response. Apparent chargeability in the anomalous zone is higher than 10 millivolts per volt up to 160 millivolts per volt comprises with low apparent resistivity value, below 10 ohm-meter down to nearly 0 ohm-meter. For the background value, the apparent chargeability is about 5 millivolts per volt with comprises of high apparent resistivity, higher than 10 ohm-meter up to 100 ohm-meter. The metal factor of the anomalous zone is strongly higher than background value, its value is very ambiguous. Next, the frequency dependent in the mineralized zone is about 0.35-0.5 whereas the background value is about 0.23. The time constant for a background level is about 5 milliseconds and increases up more higher in the mineralized zone, up to 20 milliseconds and sometime rise up to 150 milliseconds, there is a strong variation for this parameter.

(4) For decay curve plot of those three mineralizations, it can be observed that the non-anomalous decay curve of those minerals are quite similar in their shape and also are not different considerably in their magnitude. While the anomalous decay curve are significantly differ in those three mineralization. Sulphide and graphite have a uniform magnitude of the decay curve whereas clay has a strong variation in its magnitude, range from graphite to sulphide.

(5) In case of survey parameters, it can be concluded that the parameter influence on the decay characteristics is only the time duration of the transmitter. Another survey parameters are less affect on decay curve characteristics.

(6) The time constant of complex resistivity parameter that is assumed to be the parameter which will be used in order to identify type of mineral deposit cannot use in these three study areas.

(6) Meanwhile, the relationship of the apparent chargeability and the apparent resistivity is rather clearly for the purpose of mineral discrimination. Parameter  $a$  and  $b$  are clearly separated in each minerals. Summary of an average value of both parameter,  $a$  and  $b$ , is as follow:

<i>Minerals</i>	<i>Parameter a</i>	<i>Parameter b</i>
Sulphide	4.0 microsiemens	-5.816 millivolts/volt
Graphite	8.0 microsiemens	-1.762 millivolts/volt
Clay	206.0 microsiemens	-7.831 millivolts/volt

The parameter  $a$  of sulphide is averaged about 4.0 microsiemens lower than that of graphite 2 time and lower than that of clay about 50 time. Whereas, the parameter  $b$  of sulphide higher than that of graphite about 3.3 times and lower than that of clay about 1.4 times.